Nonpoint Source Water Pollution Project Grants

CSSR: Collaborative for Sediment Source Reduction
Greater Blue Earth River Basin

Final Report

31 October 2016

Peter Wilcock[1], Se Jong Cho[2], Karen Gran[3], Ben Hobbs[2], Patrick Belmont[1], Martin Bevis[3], Barbara Heitkamp[4], Jeff Marr[4], Sara Mielke[4], Nathaniel Mitchell[3], and Karthik Kumarasamy[1].

[1]Department of Watershed Sciences, Utah State University
[2]Department of Geography & Environmental Engineering, Johns Hopkins University
[3]Department of Earth & Environmental Sciences, University of Minnesota Duluth
[4]St. Anthony Falls Laboratory, University of Minnesota

CSSR was made possible by the combined support of industry, state, and federal programs

1 Contents

2 Executive Summary

Problem: The Minnesota River generates 80-90% of the suspended sediment eventually deposited in Lake Pepin. Up to 50% of that sediment load comes from the 3,540 mi^2 Greater Blue Earth River Basin (GBERB). When the GBERB TMDL was issued in 2012, there were 39 river reaches within the GBERB listed as impaired for turbidity under section 303d of the Clean Water Act. Reduction of sediment loading and turbidity from GBERB will require a large investment in management and conservation actions to reduce sediment inputs as well as peak river flow. The goal of this project is to develop a basis for evaluating and prioritizing different management actions for reducing sediment loading. The resulting product is intended to support watershed-scale prioritization, which we have identified as a gap in the currently available methods.

Waterbody improved: This project focuses on the Greater Blue Earth River Basin (GBERB) in the counties of Blue Earth, Brown, Cottonwood, Faribault, Freeborn, Jackson, Martin, and Watonwan in Southern Minnesota (**HUC** 07020009). The primary water courses in the Greater Blue Earth are the Le Sueur, Cobb, Maple, Watonwan, and Blue Earth Rivers. The Blue Earth is tributary to the Minnesota River at Mankato, MN.

Project highlights: We have developed a sediment budget that quantifies sediment sources in the GBERB. The budget is constrained by measured sediment loads at stream gages and by sediment fingerprinting information that indicates the fraction of sediment that comes from upland fields vs. near-channel sources. We have developed a relation between river discharge and near-channel sediment supply that can be used to relate flow reduction from water conservation measures to reductions in sediment loading. We have developed an innovative, reduced complexity model that links different portfolios of management actions to changes in sediment loading. This model was developed in association with a stakeholder group drawn from state and local agencies, industry groups, and local farmers.

Results: We have identified near-channel sediment sources (primarily eroding bluffs) as the largest source of sediment in the GBERB. Because bluffs are the largest sediment source, the biggest reductions in sediment loading require either bluff stabilization or reductions of peak river flows. The Management Option Simulation Model has been used with project stakeholders to evaluate different portfolios of management actions for reducing sediment loading. Water conservation measures are the most favorable approach because they address the cause of the erosion, rather than the symptom, and because water conservation provides other ecosystem benefits, such as reducing nutrient loading and providing habitat.

2.1 EPA 319 Summary

This project focuses on the Greater Blue Earth River Basin (GBERB) in the counties of Blue Earth, Brown, Cottonwood, Faribault, Freeborn, Jackson, Martin, and Watonwan in Southern Minnesota (**HUC** 07020009). The primary water courses in the Greater Blue Earth are the Le Sueur, Cobb, Maple, Watonwan, and Blue Earth Rivers. The Blue Earth is tributary to the Minnesota River at Mankato, MN.

Mainstem reaches on the Le Sueur, Watonwan, and Blue Earth Rivers have been listed for turbidity since 2002. As of 2012, 39 reaches within the GBERB were listed as impaired under Section 303d of the Clean Water Act (MNSU, 2012). Turbidity has been related to excess sediment loading from agricultural and near-channel erosion sources. A Total Maximum Daily Load (TMDL) was completed for the Greater Blue Earth River Basin in 2012 (MNSU, 2012).

This project is a large, collaborative effort with the goal of identifying strategies for reducing sediment loading at the watershed scale. A wide suite of Management Options (MOs)/activities were evaluated in this study, including practices intended to (i) reduce soil erosion, (ii) retain eroded sediment on the fields and reduce stream sediment loading, (iii) reduce water runoff from fields and reduce peak flows in rivers, and (iv) reduce erosion of near-channel sediment sources, including bluffs, ravines, and streambanks. A major project goal was to examine different portfolios of MOs for the purpose of reducing sediment delivery from the watershed. The project was conducted by researchers from University of Minnesota, Johns Hopkins University, and Utah State University in collaboration with stakeholders from multiple state agencies, industry groups, and individual farmers. A listing of the stakeholder affiliations is given in Table 2.1.

Table 2.1: Active Participants in the CSSR Stakeholder Process

State Agencies and Departments	US Agencies

Minnesota Department of Agriculture
Minnesota Pollution Control Agency
Minnesota Bureau of Water and Soil Resources
Minnesota Department of Natural Resources
University of Minnesota
    Dept. of Soil, Water, and Climate
    Dept. of Bioproducts and Biosystems Engineering
    Minnesota Extension
 	
Local Agencies and Departments
Greater Blue Earth River Basin Association
Blue Earth County Commissioner
Blue Earth County Planning Office
Waseca County Soil & Water Conservation District
Blue Earth County Soil & Water Conservation District
	US Army Corps of Engineers
	US Department of Agriculture, NRCS
	
	Industry and Private Participants
	Minnesota Agricultural Water Resource Center
	Minnesota Corn Growers Association
	Minnesota Soybean Growers Association
	Individual Farmers (4)

3 Work plan review

3.1 Work Plan Modifications

Briefly outline any approved changes from the original work plan, staff, or participating organizations.

See Final Fiscal Report

3.2 Activity Report

Please list and give a brief report on each activity/task identified in your work plan (Attachment A of the 319 Grant Agreement, contract, or work order) or most recently approved work plan amendment. For each task, briefly summarize the activities completed and describe any problems, delays, or difficulties that have occurred in completing the project work. Explain how problems were resolved or list any activities that were not completed.

A summary report on each activity identified in the work plan is given on following pages. The Table identifies any problems, delays, or difficulties for the task and directs the reader to the location in this report where further information on the methods and results from the activity may be found.

Work Plan Objective	Reporting
Objective 1: Fiscal management and planning	
Task 1: Track project grant and matching funds and expenditures	Ongoing throughout project
Task 2: Required reporting	Ongoing throughout project
Objective 2: Sediment fingerprinting for sediment source and sink identification	
Task 1: Collect and analyze fingerprinting samples (Beryllium-10, Lead-210, Cesium-137, or other elements as appropriate) from sediment sources including cultivated uplands, non-cultivated uplands, bluffs, banks, floodplains, and ravines	Completed. Reported in Section 5.
Task 2: Collect and analyze fingerprinting samples (for Beryllium-10, Lead-210, Cesium-137, or other elements as appropriate) from suspended sediment samples.	Completed. Reported in Section 5.
3: Develop sediment budget for GBE watershed	
Task 1: Upscale predictions of sediment source magnitude and location from the Le Sueur to the GBE watershed.	Completed. Reported in Section 5.
Task 2: Establish sediment budget for pre-settlement and current conditions.	Completed. Reported in Section 5.
Task 3: Re-establish ravine monitoring to better constrain erosion rates in ravines. Up to 3 ravines will be monitored with automated samplers. Water samples collected during storm events will be analyzed for TSS	Completed. Reported in Appendix 1.
Objective 4: Establish efficiency and cost of conservation drainage and sediment reduction practices	
Task 1: Compile a database of current conservation drainage and sediment controls practices, including effectiveness, cost, and feasibility based on location.	Completed. Reported in Section 6.5 and 6.6.

Work Plan Objective	Reporting
Task 2: With Stakeholders, develop consensus list of conservation practices to be evaluated in the sediment forecasting and decision analysis models.	Completed. Reported in Section 6.5 and 6.6 and Section 7.
Objective 5: Stakeholder meetings	
Task 1: Establish a collaborative of experts and stakeholders from the Minnesota Pollution Control Agency (MPCA), Board of Water and Soil Resources (BWSR), Minnesota Department of Agriculture (MDA), Minnesota Department of Natural Resources (MN/DNR), National Resource Conservation Service (NRCS), US Army Corps of Engineers (ACoE), Greater Blue Earth River Basin Aliance (GBERBA), Blue Earth County, and Minnesota Agricultural Water Resources Coalition (MAWRC). We will also establish collaboration with researchers at University of Minnesota (UM) working on agricultural BMPs.	Completed. Eight Stakeholder meetings were held.
Task 2: Organize and run seven stakeholder meetings	One-day stakeholder meetings held in Mankato MN: 14 June 2012 17 December 2012 13 June 2013 21 January 2014 8 August 2014 16 January 2015 14 August 2015 12 January 2016 A separate meeting was held 17 October 2016 in St Paul in order to provide information on the project to a different set of stakeholders. Although outside the scope and duration of this project, we plan to hold one more meeting with the Mankato stakeholders in January or February of 2017. We will hold this meeting because we believe that we can make further progress in defining a consensus strategy for sediment reduction.

Work Plan Objective	Reporting
Objective 6: Develop sediment simulation model	
Task 1: Background preparation and stakeholder interaction.	Completed. Eight stakeholder meetings held.
Task 2: Implementation and testing against GBE sediment budget	Completed. Reported in Section 6.
Objective 7: Build a decision-analysis system	
Task 1: In stakeholder meetings, develop methods for quantifying and displaying the performance of different alternatives and characterizing the major uncertainties.	Completed. Reported in Section 7.
Task 2: Develop spreadsheet-based software for displaying tradeoffs and uncertainties, incorporating stakeholder value judgments, and facilitating user control of the assessment process	Completed. Reported in Section 7.
Objective 8: Develop management strategy	
Task 1: Stakeholder evaluation of alternative portfolios.	Performed at January 2016 stakeholder meeting.
Task 2: Develop recommendations for review by management agencies, other stakeholders, and the general public.	Presented at October 2016 Minnesota Water Resources Conference. See Section 7.
Task 3: Develop guidelines for application of the decision tools to other (MRB) locations	Discussed at January 2016 stakeholder meeting and October 2016 meeting in St. Paul.

4 Introduction

4.1 Turbidity and sediment loading in the Greater Blue Earth River Basin

The Minnesota River generates 80-90% of the suspended sediment load eventually deposited in Lake Pepin, a naturally-dammed riverine lake on the upper Mississippi River (Kelley and Nater, 2000). Within the Minnesota River basin, up to 50% of the sediment load comes from the 3,540 mi^2 Greater Blue Earth River basin, which comprises only 20% of the basin area (Wilcock, 2009). When the Greater Blue Earth River basin TMDL was issued in 2012, there were 39 river reaches within the GBERB listed as impaired for turbidity under section 303d of the Clean Water Act (MNSU, 2012).

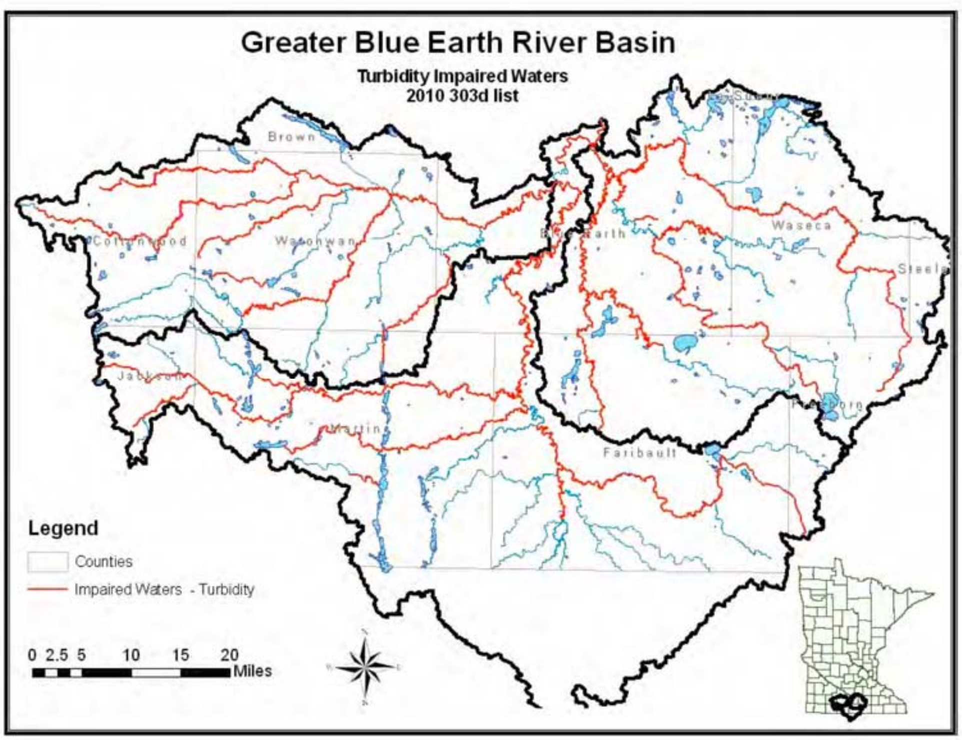

Figure 4.1: List of turbidity-impaired waters within the Greater Blue Earth River basin. From Greater Blue Earth River TMDL (MNSU, 2012).

Prior work within the Le Sueur River basin (Gran et al., 2009; Belmont et al., 2011) and the Blue Earth River basin (Sekely et al., 2002; Thoma et al., 2006), found that near-channel sources contribute the majority of fine sediment load to the mouth of the Blue Earth River. The importance of these near-channel sources arose due to the geomorphic history of the Minnesota River basin.

At the end of the last glaciation, meltwater pooled along the southern margin of the Laurentide Ice Sheet, forming glacial Lake Agassiz. When glacial Lake Agassiz first drained through its southern outlet approximately 13,400 calendar years before present, it formed glacial River Warren, which carved the valley currently occupied by the Minnesota River (Clayton and Moran, 1982; Matsch, 1983; Fenton et al., 1983; Teller and Clayton, 1983). The deep incision associated with this event caused incision to propagate upstream on all major tributaries (Gran et al., 2013). In the GBERB, knickpoints have migrated upstream between 35-65 km, leading to the deeply-incised lower valleys seen today.

Sediment fingerprinting work in Lake Pepin deposits show that before the time of widespread European settlement of the Minnesota River valley, most sediment deposited in the lake came from near-channel sources. In the early to mid-1800s, the deposition rate increased ten-fold and with it came a shift in sediment sources from near-channel to upland sources. Over the past century, deposition rates have remained high, but sediment sources have shifted back to being dominated by near-channel sources (Engstrom et al., 2009; Belmont et al., 2011). This complex history of shifting sediment sources highlights the challenges involved in both identifying erosional hotspots within the basin as well as targeting management options to reduce sediment loading and delivery to the Minnesota River.

4.2 Introduction to the Collaborative for Sediment Source Reduction

Research and monitoring have identified as the Greater Blue Earth River Basin (GBERB) as the largest source of sediment to the Minnesota River and Lake Pepin (Figure 4.12). There is a pressing need to identify the best methods and locations for reducing excess erosion and sediment delivery and to determine the time lag between implementation and reduction of sediment loads at the mouth. The Collaborative for Sediment Source Reduction (CSSR) was launched with the goal of developing a consensus strategy for reducing sediment loading and delivery from the GBERB. At the heart of the project is a collaborative of local, state, and industry stakeholders with whom we developed and applied a simulation model that forecasts changes in sediment loading in response to different portfolios of conservation actions. This model was then used with information on the costs and benefits of management options in order to evaluate different watershed strategies for reducing sediment loading.

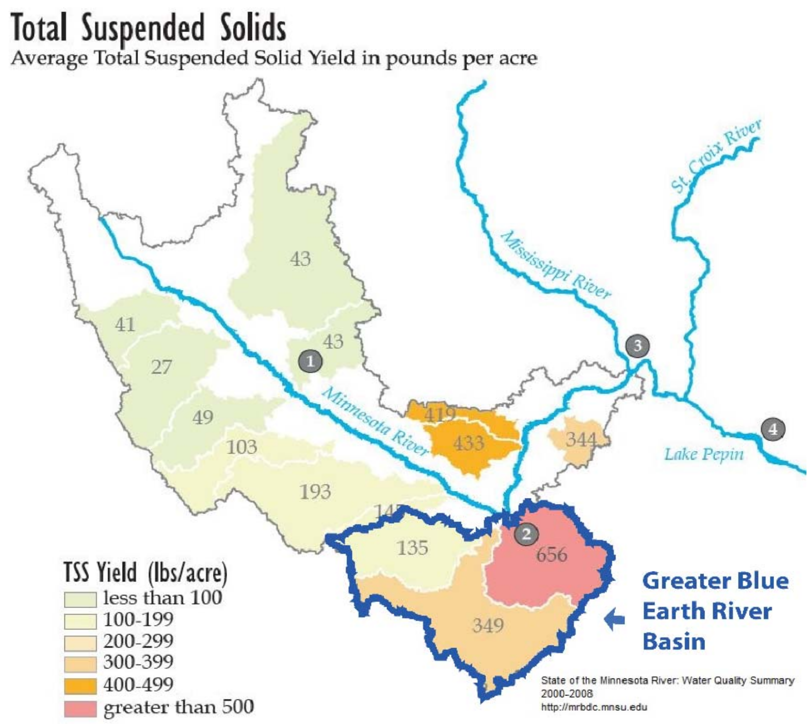

Figure 4.2. Average Total Suspended Solid Yield, Minnesota River Basin

The GBE watershed is naturally primed for high turbidity due to its location, surficial geology, and geomorphic history. Human changes in hydrology and vegetation over the past 150 yrs also play an important role in watershed sediment dynamics and need to be considered in any watershed-wide strategic implementation plan. Using multiple lines of evidence, we have demonstrated that, under current conditions, the largest sediment sources are near-channel (erosion of bluffs, channel widening and incision) within the downstream, incised portions of the watershed. High river flows are an underlying driver of near-channel erosion, and actions to reduce the magnitude and alter the timing of runoff will play a role in reducing sediment loads over the long-term and help mitigate against changes in precipitation. Effective management will require a combination of actions to reduce erosion at its sources and more effectively control the physical drivers of erosion, which will require hydrologic management. If only near-channel sediment sources are addressed, management actions will risk addressing symptoms but not the dominant causes.

In addition to identifying the best methods and locations for reducing excess erosion and sediment delivery, effective implementation also depends on a consensus among the relevant stakeholder groups, including agricultural producer groups, conservation groups, and regulatory agencies. We believe there is a need for groups with different interests to work together to develop a shared understanding of how the watershed responds to different conservation strategies. To that end, we have tried in this project to focus on watershed function without focusing on responsibility for the current watershed condition or for implementing and funding conservation actions. Consensus on strategies for reducing sediment loading has not been easy to reach. A particularly important challenge has been addressing the question of the best balance between reducing sediment sources and controlling runoff. Should management actions focus on soil erosion and drainage modification on agricultural fields or bank and bluff protection along rivers?

***Project Goal**: To identify a consensus strategy for reducing sediment loading in the Greater Blue Earth watershed using a decision framework that incorporates the best available scientific information, accounts for uncertainty, and provides a model for decision making throughout the Minnesota River Basin. We hope that the strategy developed will be effective, cost-efficient, fair, and agreed upon by all stakeholders.*

4.3 A Different Approach to Watershed Sediment Modeling

The grand challenge for identifying a strategy for reducing sediment loading lies in developing a robust, yet accessible sediment prediction model, integrating all lines of evidence and tested at multiple time and space scales, and then using this model to identify and evaluate management strategies that are economically efficient and consistent with the best available monitoring and research results. At the heart of CSSR is a simulation model that forecasts changes in sediment loading such that the costs and benefits of different portfolios of management options can be evaluated consistently and transparently.

Our goal in developing a simulation model for CSSR is to connect management options (type, location, and extent) to reductions in sediment loading at the scale of the Blue Earth Basin. The purpose of the model is to evaluate different portfolios of management options in terms of their cost and the reduction in sediment loading from the Blue Earth River to the Minnesota River. Essential attributes of the model are that it be *reliable, robust, and rapid.* Reliable means that the model provides solutions that are "close enough" and credible at the watershed scale. Robust means that the model is unlikely to produce solutions outside the realm of possibility and that it can operate reliably under a wide range of user input. Rapid means that the model can produce results in seconds, thereby allowing immediate feedback for users, permitting multiple runs that can illustrate change in sediment reduction with extent of management options, and providing a basis for determining uncertainty in the model results by using multiple model runs with plausible variation in the input or parameters.

Our modeling approach differs in important ways from other models used to simulate watershed sediment loads. Other models generally try to represent the physical processes that occur throughout the watershed. Some (like SWAT and HSPF) work at a 'spatially lumped' scale, whereas others (like GSSHA) work at a smaller scale in an attempt to match the local variability in the rates at which different flow and transport processes work. We take a different approach in that we endeavor to distribute the *results* of the physical processes (the sediment loading to rivers) across the watershed. Our starting point is a watershed sediment budget, which is based on years of careful observation of the rates and locations of sediment sources using a wide range of information sources that provide reliable and independent checks on estimated sediment rates. The sediment budget is anchored by the strong constraint of sediment mass conservation (sediment is neither created not destroyed) to estimate the type, magnitude, and location of all sediment sources and sinks. Stated simply, because all of the sources and sinks must add up to match the amount of sediment load measured at gages, our modeling is not likely to go far off the tracks. We do not exclude representation of physical processes where we think we can adequately represent them (e.g. routing of water through the channel network), but we argue that it is generally more reliable, robust, and rapid to operate on well constrained sediment loads than try to predict their occurrence from the driving factors. We focus on the distribution of sediment sources and sinks throughout the watershed and how the magnitude and distribution of sediment sources can be changed via management actions.

There are two sediment processes that existing models do not capture well, or at all. The most important is the supply of sediment from bluffs, the dominant sediment source in the watershed. Bluff supply can be *added to* other models, but it is not predicted. Also missing, crucially, is the ability to predict the *change* in bluff sediment supply with changes in river flow. We have demonstrated that increases in river flows are the cause of the switch in dominant sediment source from fields to bluffs over the 20th Century. We have used measured sediment loads at locations where two gages on the same river bracket large reaches of the incised zone in order to develop a relation between river discharge and sediment supply from near-channel sources in the incised zone. This simple analysis demonstrates that there is a threshold in river discharge above which the rate of sediment additions to the river increases rapidly. This is the link between river flow and bluff sediment supply that we need to forecast the relation between water storage, reductions in high river flow, and sediment supply from bluffs. We call it the “hockey stick” because, to non-Minnesotans anyway, the trend looks like a hockey stick.

Another key process that is not captured in existing watershed models is the deposition and storage of sediment in transport. Only a fraction of soil eroded from fields is delivered to the stream. Only a fraction of the field sediment, or the bluff sediment, delivered into the streams actually makes it all the way to the watershed outlet. This is the *Sediment Delivery* problem. We have developed an approach (which we call TopoFilter) that uses high-resolution topography to link sediment sources to the sediment loads measured at stream gages and informed by sediment fingerprinting. For field sediment supply, we start with USLE soil erosion rates at the scale of soil map units. Rather than define a simple sediment delivery ratio based on drainage area alone, we define sediment delivery ratio based on the distance from each soil map unit to the nearest stream as well as the slope, or drop in elevation from the map unit to the stream. Figure 4.3 shows how this spatially resolved sediment delivery ratio can be used to identify the locations from which most of the field sediment is likely to derive. We apply a similar approach for sediment delivery ratios along the stream, in that we link sediment inputs, from all sources throughout the stream network, to the fraction of the sediment delivered to the watershed outlet, as a function of the distance along the stream and the slope, or drop in elevation from the source to the outlet. The topographic position of a sediment source (distance to outlet, slope between source and outlet) determines the fraction of the sediment source that is actually delivered from the watershed. This represents, in effect, a “discount” that plays an important role in determining the effectiveness of different management options at different locations.

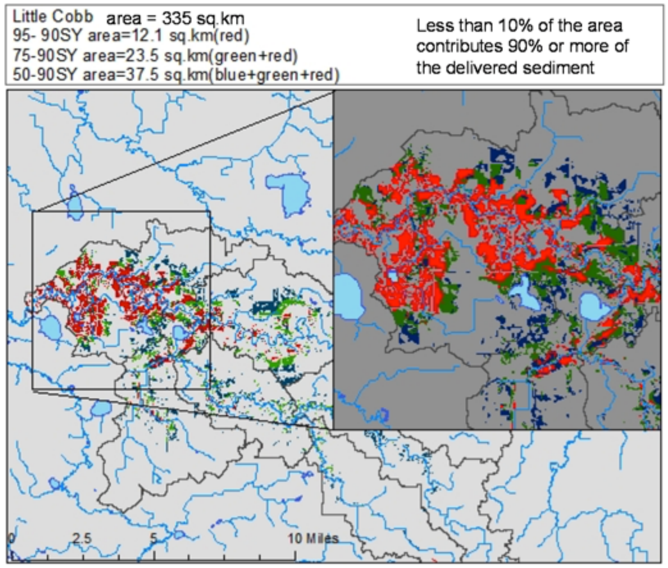

Figure 4.3. Example of detailed Sediment Delivery Ratio determined for a portion of the Little Cobb Watershed. The figure shows the portion of the watershed contributing 90% of the sediment yield in 95% (red), 75% (green and red), and 50% (blue, green, and red) of 10,000 Monte Carlo trials.

Throughout the project, our target has been a model that is well constrained to produce "reasonable" answers. It is designed to provide reliable estimates of the reduction in sediment loading relative to the period over which the sediment budget was developed. Significant features of the model are the ability to characterize sediment delivery ratio as a function of location and topography and the ability to predict the reduction in sediment loading from the largest sediment source, bluffs, as a function of water storage and river flow.

The final key element of the simulation model is that we have reduced the possible conservation actions to a short list based on how the actions change the water flow or sediment erosion and storage in the watershed. There are

(i) Actions to reduce soil erosion, which we call **TLMO**, Tillage Management Options.

(ii) Actions to reduce the amount of eroded soil that gets into the stream. These actions act to reduce the field *sediment delivery ratio* SDR_f that determines the amount of soil erosion that is delivered into streams. These are **AFMO**, Agricultural Field Management Options, **BFMO**, Buffer Strip Management Option, and **WCMO**, Water Conservation Management Options, some of which also store sediment derived from soil erosion.

(iii) Actions to store water and reduce high flows in the rivers as they pass through the incised zone. We connect reductions in high river flows to near-channel sediment sources (mostly bluffs) by the hockey stick relation. Water storage Management options are **WCMO**, Water Conservation Management Options, and **ICMO**, In-Channel Management Options.

(iv) Actions to directly reduce sediment delivery from bluffs, which primarily include stabilizing bluff toes. These are called **NCMO**, Near-Channel Management Options.

(v) Actions to directly reduce sediment delivery from ravines, primarily by reducing or channeling flow through ravines. These are **RAMO**, Ravine Management Options.

Note that all sediment sources, when delivered to the stream channel network, are reduced by a *sediment delivery ratio* for the stream SDR_s, which is determined by the distance from the source to the watershed outlet, as well as the slope, or drop in elevation from source to outlet.

To use the model, the user selects the *extent* of different management options to implement, as well as *location*. Location is grouped into three zones (upland, incised, and transitional areas in between) for only six subwatersheds (Le Sueur, Cobb, Maple, Watonwan, Elm, and Blue Earth). Even with only seven management options and 18 zones, there is an enormous range of choice when considering multiple management options at the same time as well as the extent to which those options are implemented. We believe that this level of detail is about the maximum that can be effectively evaluated when exploring strategies for sediment reduction at the scale of the Blue Earth Basin.

5 Sediment Budget for the Greater Blue Earth River Basin

This goal of this objective was to extend a sediment budget compiled in the Le Sueur watershed to the entire Greater Blue Earth River (GBER) watershed. The sediment budget was developed for fine sediment only (silt and clay) on an annual timescale for modern conditions and pre-settlement conditions. Below we describe the basic framework for the sediment budget; methods used to inventory sediment sources, measure and extrapolate erosion rates, incorporate sediment sinks, and compile the final sediment budget; and then present the budget results. All input files are available as ArcGIS shapefiles and will be included with this report. The sediment budget is in an attached Excel spreadsheet. This sediment budget was used in the construction of a decision analysis model known as MOSM (Management Options Simulation Model). Much of the work here was conducted by Martin Bevis, as part of his Master's degree at the University of Minnesota Duluth. The text presented here on the modern sediment budget is revised directly from his thesis (Bevis, 2015), and the reader is directed there for more details on the modern sediment budget in the GBER watershed (Bevis, 2015; http://hdl.handle.net/11299/170661).

5.1 Sediment Budget Background

Fundamentally, a sediment budget is based on the mass-balance relationship that sediment inputs to a channel must equal sediment outputs, minus any change in storage. The GBER watershed sediment budget builds off of the sediment budget created for the Le Sueur watershed as part of an MPCA-funded project (Gran et al., 2011; Belmont et al., 2011). Work on the Le Sueur River watershed measured erosion and sediment delivery rates from four primary sediment sources. The project converted total sediment load to fine sediment load in order to compare estimated loads against total suspended solids (TSS) loads determined from measurements at gaging stations (Gran et al., 2011; Belmont et al., 2011). Estimated sediment load supplied from bluffs, streambanks, ravines and uplands coupled with deposition in floodplains matched the measured Le Sueur River TSS load for 2000-2010 within 5% (Belmont et al., 2011).

The budget we developed for the GBER watershed takes the same general form as the Le Sueur watershed budget, but includes the potential for sediment to be deposited in lakes, too. Equation 5.1 captures the basic form of the GBER sediment budget, giving the predicted sediment load, Q_s, as

$$Q_s = Bl + Ba + R + U - Fp - L \tag{5.1}$$

where *Bl* is sediment eroded from bluffs, *Ba* is sediment eroded from banks, *R* is sediment eroded from ravines, *U* is net sediment from uplands, and the two sinks, *Fp* and *L*, refer to the sediment mass deposited in floodplains (*Fp*) and in lakes (*L*). Additional sediment sources are assumed to be minor compared to these four sources and are not explicitly considered in the budget. Such sources include sediment from landscape disturbances like fire, urban runoff, construction, road contributions and aeolian deposition.

5.2 Components of the budget

5.2.1 Bluffs

Bluffs are the source of about half the suspended sediment in the Le Sueur River (Belmont et al, 2011; Day et al., 2013). Bluffs here are defined as steep features lining the river channel that exceed the height of a typical bank. In contrast to banks, bluffs are out of reach of typical annual floods and are purely erosional features. Bluffs can be impressive features: the largest have nearly vertical faces up to 70m high and 500m long, and they line about 50% of the channels in the lower reaches of GBER watershed valleys. Bluffs are most often composed of glacial till, although bluffs in former glacial Lake Minnesota deposits are topped by several meters of glaciolacustrine silts and clays, and bluffs on strath terraces are generally capped with

2-3 m of alluvial sediment (Day et al., 2013). Till layers may contain interbedded glaciofluvial sand and gravel deposits. Some bluffs near the mouth of the Blue Earth and Le Sueur Rivers are composed of Paleozoic bedrock.

5.2.2 Streambanks

Streambanks are distinguished from bluffs as being low enough for the river to overtop them during floods. Net sediment loading from banks differs depending on the geomorphic regime. Channels in the GBER watershed are divided by knickpoints into two fundamentally different systems. Above the glacial River Warren-induced knickpoints is a landscape that channel incision has not yet reached. Here, channels are in a state of dynamic equilibrium with the surrounding landscape. These channels may be widening and adjusting to changes in discharge, like Elm and Center Creeks (Lenhart et al, 2011b), but any incision is slow relative to downstream reaches where incision is driven by adjustment to base level fall. In channels that are not incising, bank erosion on the outside of most meander bends can be balanced by deposition on the floodplain, making net sediment flux associated with migration in the reach zero (Lauer and Parker, 2008). Banks above the knickpoint are primarily alluvial in nature, composed of reworked floodplain sediment although there are some places where channels are cutting into till.

Below the knickpoints, channels in the GBER watershed are incising rapidly (Gran et al, 2009; 2013). This has implications for the erosion and deposition in the channel. First, channel incision itself becomes a sediment source. In addition, because the river is downcutting through the landscape below the knickpoints, meander migration is not balanced by floodplain deposition. Incision deepens the channels to the point that floodwaters are not able to access the floodplain, and sediment is transported downstream rather than deposited back onto floodplains.

Channel widening is a further source of channel-derived sediment that has recently become important. Flows have increased in many Minnesota agricultural watersheds in the last-half century (Lins and Slack, 1999; Novotny and Stefan, 2007; Lenhart et al., 2011a; Schottler et al., 2013; Zhang and Schilling, 2006; Foufoula-Georgiou et al., 2015). When annual discharges increase, channels may widen, deepen, straighten or steepen to accommodate higher discharge rates. Minnesota River tributaries have widened substantially to accommodate increased annual discharge from the mid-1900s to the present (Schottler et al., 2013; Lenhart et al. 2011b).

5.2.3 Ravines

Ravines are steep, deep, incised gullies at the tips of the channel network. Ravines connect the uplands to the river valleys, and are usually formed by ephemeral streams with seasonal discharge. Such sites in the GBER watershed display a diverse array of sizes and relief. Erosion in ravines proceeds by a combination of fluvial and hillslope processes. Channel incision and migration leads to oversteepened slopes and mass wasting. Ravines are narrow and deep, and there are often bluffs in ravines. Seeps may occur on steep or near-vertical slopes.

Ravine discharges and sediment loads in the GBER watershed are highly variable. Some ravines connect directly to the channel network, and some discharge onto terraces. When ravines discharge onto terraces, whatever sediment load they carry is dropped as steep ravine slopes transition to nearly flat terrace tops. Ravine discharges also vary seasonally. Since most of the discharge in a ravine comes from the upland above it, flow depends on seasonal variation in precipitation, infiltration and evapotranspiration. Ravines are most active in the spring, when the upland landscape has little or no crop cover and may quickly route precipitation to ravines. Ravines often dry up in mid-summer when crop evapotranspiration is highest and precipitation is low.

Sediment from ravines is a small fraction of the Le Sueur budget, even though they can have very high sediment load concentrations and can locally add a lot of sediment to the system. In dry years ravines were responsible for as little as 2% of the Le Sueur sediment budget (Gran et al., 2011). In the wettest year monitored, ravines were responsible for as much as 15% of the Le Sueur sediment yield.

5.2.4 Uplands

Ove eighty percent of the GBER watershed is composed of low-gradient upland areas in primarily row-crop agriculture. Upland-derived sediment is eroded by wind, precipitation impact, overland flow and concentrated flow in rills and gullies in addition to erosion within the ubiquitous ditch networks. Agricultural uplands in the GBER watershed have low sediment delivery ratios; that is; they deliver just a fraction of eroded soil to channel networks (Quade, 2000; Lenhart, 2008; MPCA et al., 2009). In many watersheds, 5-10 times the amount of upland-sourced sediment that reaches the watershed outlet is stored on fields before it ever reaches a channel (Walling, 1983; Beach 1994; DeVente et al., 2007). A study on the Blue Earth River tributaries Elm and Center Creeks found just 8-13% of eroded field sediment reached the Blue Earth River (Lenhart et al., 2011b). Given the complexity of erosion, in-field deposition, and ditch maintenance, the "upland" term in the sediment budget is a net term that includes both upland erosion and deposition. This approach differs slightly from the MOSM model, in which field erosion rates are calculated directly from RUSLE and then reduced via a sediment delivery ratio.

5.2.5 Storage

Storage on floodplains and in lakes can further decrease the amount of the total eroded sediment that reaches watershed outlets (Trimble, 1999; Verstaeten and Poesen, 2000). Storage estimates in the original Le Sueur budget included an estimate of sediment storage on floodplains. The GBER watershed budget presented here adds estimates of sediment storage in lakes. Previous observation of sediment yields above and below lakes on Elm Creek (a tributary joining the Blue Earth near Winnebago) found that 90% or more of sediment entering a lake is trapped there (Lenhart et al., 2009). Although there are isolated incidents of increased turbidity downstream of lakes with carp present (personal communication, J. Finlay), it is not known how widespread this phenomenon is and thus this process is not included in the sediment budget. Here, we have treated lakes as sinks, and have expanded the budget to include storage in lakes, mediated by a site-specific trapping efficiency. Most of the sediment trapped in lakes was likely generated from upland erosional processes, as most of the lakes with high trapping efficiencies are located high in the watersheds.

5.3 **Methods**

5.3.1 Subwatershed delineations and gaging network

The GBER watershed sediment budget was compiled as a series of three budgets for the Watonwan, Blue Earth, and Le Sueur Rivers. Characteristics of each major HUC-8 watershed are given in Table 5.1. The Le Sueur basin was further subdivided into the Le Sueur, Cobb, and Maple; and the upper Blue Earth was divided into two branches: Elm Creek and the upper Blue Earth subbasin. Other subdivisions were based on geomorphic regime, separating out areas above, within, and below the knickzone (Figure 5.1). Where possible, these divisions were made at the location of stream gages, so that budget predictions of sediment load could be compared with TSS loads determined by the Minnesota Pollution Control Agency (MPCA) and their partners. By separating out subwatersheds based on geomorphic regime, we also ensure that bluff erosion rates, in particular, are only extrapolated to sources in similar geomorphic settings.

Table 5.1: Characteristics of GBER watersheds

	Watonwan	Blue Earth	Le Sueur
knickpoint distance upstream (km)	35	64	35-40
area (km^2)	2,262	4,054	2,878
discharge (mean annual cfs, 1941-2012) [a]	415	1148	583
water yield, cfs/km^2/yr	0.18	0.28	0.20
Land Use			
percent of landscape in row crops [b]	86	85	82
depressional areas lost, % of watershed area [c]	na	17	18
percent of watershed likely tiled [c]	46	46	47
percent of channels ditched [c]	8	28	23
Lakes			
area lakes (km^2) [d]	31.2	49	66.8
number of lakes	463	737	408
lake area as percent of watershed area	1.4	1.2	2.3

sources: a) MPCA et al., 2009; b) Fry et al., 2011; c) Schottler, 2012; d) McKay et al., 2013

Table modified from Bevis (2015)

Estimated sediment budgets on the Le Sueur River are well constrained by a group of seven gages (Table 5.2). TSS loads on the Blue Earth and Watonwan Rivers were monitored by a single long-term gage near the mouth on each river (Figure 5.1, Table 5.2). Additional upstream gages exist, but the record of TSS load data was too short to be used in the current sediment budget. The main gage on the Blue Earth is located just downstream from Rapidan Dam. Downstream of Rapidan, the Blue Earth River has incised into the Paleozoic bedrock (Prk) and flows in a narrow, deep valley. The knickzone on the Blue Earth extends upstream from this gage approximately to the town of Vernon Center. We consider this reach to be below the knickpoint. We further subdivided the area of the Blue Earth basin above the knickpoint at the town of Winnebago, in part because the knickpoint on the Blue Earth River is more diffuse and this part of the channel is different compared to the far upstream reaches. Because of the existing body of work on Elm Creek (Lenhart, 2005; Lenhart et al., 2009; 2011), we separated out calculations for Elm Creek in our sediment budget.

On the Watonwan, the Garden City (GC) gage is fortuitously located near the knickpoint. The knickzone portion of the Watonwan is relatively short, and is captured by the gage at Rapidan on the Blue Earth River. MPCA-published loads for the Blue Earth are determined by subtracting the load at the GC gage from the load at Rapidan and thus loads at Rapidan include sediment from the knickzone of the Watonwan. The Blue Earth reach below the Rapidan gage is ungaged, as is the reach of the Le Sueur below the gage at Red Jacket Park (RJP).

Table 2: Gage locations in Greater Blue Earth River basin with Q and TSS annual loads available

Gage #	Gage Description	TSS annual loads available	Lat	Long
30092001 (05320000)	Blue Earth at Rapidan	2000-2013	44.095556	-94.109167
31051001 (05319500)	Watonwan at Garden City	2000-2013	44.046389	-94.195278
32077002* (05320500)	Le Sueur near Rapidan/Red Jacket	2000-2013	44.109722	-94.041667
32076001	Le Sueur at County Road 8	2006-2013	44.084694	-93.98875
32079001**	Le Sueur at St. Clair	2007-2012	44.083056	-93.854722
32062001	Maple at County Road 18	2006-2013	43.93500	-94.070833
32072001	Maple at CSAH 35	2003-2013		
32071001	Big Cobb at County Road 16	2006-2013	44.04725	-94.000611
32069001** (05320270)	Little Cobb	2000-2012	43.996667	-93.908333
	Additional gages with Q and TSS not used in budget due to limited records			
30025001 (05318270)	Blue Earth at Winnebago	2013	43.769417	-94.19525
31028001	Watonwan at La Salle	2013***	44.05675	-94.503722

**Gage (3207701) moved upstream following major flood*
***Decommissioned in 2012; St. Clair gage was reinstated in 2015.*
**** TSS samples and Q measurements are also available for 2000-2002, but not QA/QC'd TSS loads*

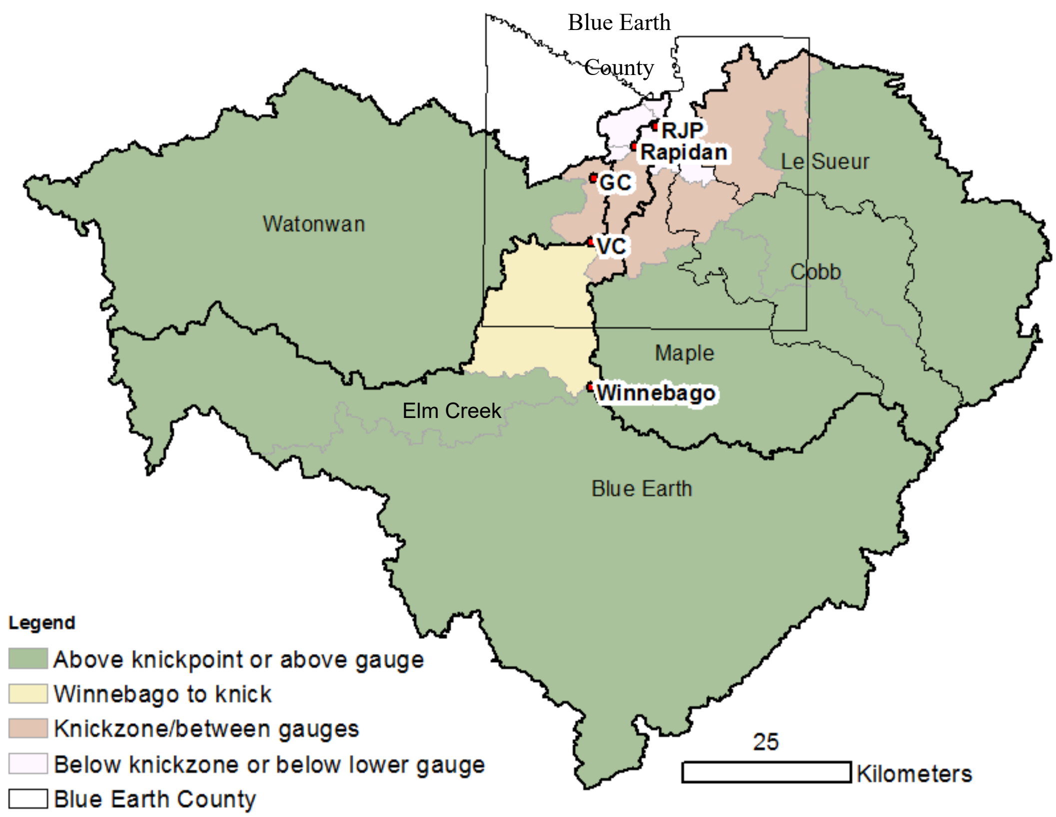

Figure 5.1: Subwatersheds based on geomorphic domain in the GBER watershed. Abbreviations for locations referenced in the text are: RJP: Red Jacket Park, GC: Garden City, VC: Vernon Center. Knickpoints are located at boundary of pink and green subwatersheds. Figure from Bevis (2015).

5.3.2 Sediment source delineations and erosion rate measurements

5.3.2.1 Bluffs

The basic procedure to calculate suspended sediment load eroded from bluffs was to 1) define and measure bluff extents, 2) measure erosion rates where possible, 3) extrapolate measured rates to bluffs on which rates were not measured within a subwatershed, and 4) calculate volume and mass of fine sediment eroded. Because bluffs were the dominant contributor of fine-grained sediment in the Le Sueur budget (Belmont et al., 2011), extra care was taken to evaluate different methods for interpolating and extrapolating measured bluff retreat rates to those bluffs that were not measured directly (see Bevis (2015) for more detail).

To define bluffs in the GBER watershed, lidar-derived three-meter-resolution DEMs from 2005 for Blue Earth County, 2012 for other Minnesota counties, and 2008-2011 in Iowa were used to delineate bluffs. DEMs were obtained from the University of Iowa GIS library and the Minnesota geospatial information office. Vertical accuracy of these DEMs is typically about 15 cm. From a DEM of the basin, features with more than three meters of relief in a nine-by-nine meter square were selected. Following the automated delineation procedure, the bluff inventory was cleaned up to leave only bluffs directly adjacent to channels. Off-channel bluffs were removed by applying a buffer around the active channel. This step removed features that were not within 100m of channels larger than Strahler stream order 3 or within 30m of channels of stream order 3 or lower. A buffer was then used to exclude features for which no part was within 30m of manually-traced channel centerlines. Bluffs along ditches (as defined in the United States Geological Survey National Hydrography Database) were also excluded. Any remaining bluffs not adjacent to a mainstem channel were removed manually. Digitized Minnesota Geological Survey (MGS) data were used to identify bluffs in the watershed composed of bedrock, primarily Oneota Dolomite and St. Peter Sandstone (Steenberg, 2012). Although these bedrock bluffs were not removed from the inventory, they were identified so that users of the sediment budget could choose to include them or not.

Bluff attributes were measured from 1m lidar-derived data including bluff surface area, height and length. Bluff surface area was used to calculate the annual volume of material eroded from bluffs, in keeping with precedent set in previous studies in the basin (Sekeley et al., 2002; Belmont et al., 2011; Day et al., 2013). Bluff stratigraphy, vegetation cover, and bluff material properties were collected from geologic maps and aerial photographs. Surficial geology maps were used in ArcGIS to identify bluffs containing Quaternary alluvium (Jennings, 2010; Jennings et al., 2012). Pleistocene alluvium in the GBER watershed was deposited by meltwater from the final retreat of the Des Moines lobe of the Laurentide ice sheet, and primarily occurs as outwash channels, tunnel valleys, outwash fans, and deltas. The occurrence of Pleistocene alluvium varies systematically across the GBER watershed; it is most common in the northwest and least common in the southeast (Jennings et al., 2012). Holocene alluvium caps terraces formed by the incision of channels in response to late-Pleistocene base level fall (Gran et al., 2009). Terraces are most common in the lower reaches where incision is greatest. We gave these Quaternary alluvial units special consideration when converting volume of sediment eroded to mass because they are the thickest, most widespread alluvial units in the GBER watershed. These units are on average 3m thick in the GBER watershed (Meyer and Lively, 2012).

Bluff crest and toe migration rates were calculated by measuring the difference in location between a feature traced on aerial photos from 1938/9 and 2008. Georeferenced aerial photographs from 1938, 1939 and 2008 were used throughout this project. The 1938/9 airphotos were downloaded from the University of Minnesota Borchert Library website and georeferenced by hand in ArcGIS using a first-order polynomial transformation. At least eight control points were used for each photo, placed on building corners, or roads and property lines if buildings were not available, with points as close to the channels as possible. Of the recent photographs available at the outset of this project, the National Aerial Imaging Program (NAIP) aerial photos from 2008 best suited the needs of this work. This year was chosen over newer photographs because the sun was at a higher angle in the 2008 photos and discharge was within channel banks. Shadows and floodwaters make bank and bluff delineation difficult or inaccurate.

Bluff erosion rates were measured over the longest timescale possible with the photographs available. Retreat rates measured over shorter timeframes are overwhelmed by georeferencing and tracing errors (Day et al., 2013; Belmont et al., 2011). Bluff crest retreat rates were measured wherever it was possible in the watershed. Rate measurements require good resolution of bluff features on aerial photos from both times. It was easier to see bluff crests and toes on large bluffs with sparse vegetation, so our measurements may be biased towards bare bluffs close to the mouth of the watershed.

Toe and crest retreat distances were combined with the time between photos to calculate a long-term average bluff erosion rate for each bluff with measurement of both retreat distances. To do so, we created a conceptual model of how bluff crests and toes retreat over time, then substituted the measured distances into the expression to calculate erosion rates for individual bluffs. We conceptualized bluff erosion occurring in two different ways, discriminating between times when a channel migrates toward and away from a bluff. When a river migrates away from a bluff, only the bluff crest will retreat (Figure 5.2). In this case, we model the volume of bluff sediment eroded as a triangular prism (Equation 5.2).

$$V_{E(away)} = CRR/2 * h * l \quad (5.2)$$

where, $V_{E(away)}$ is volume of bluff sediment eroded, CRR is crest retreat rate, h is bluff height, and l is the length of the modeled bluff.

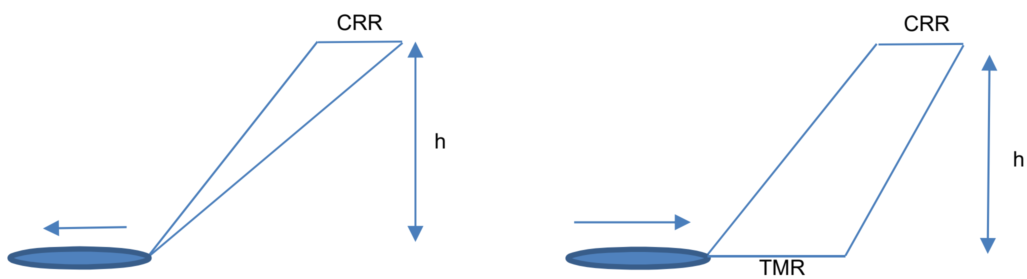

Figure 5.2: Schematic cross sections of eroding bluffs. When a channel is migrating away from a bluff, erosion volume is modeled as a triangle. The crest may retreat, but the toe is pinned. When a channel is migrating toward a bluff, erosion volume is modeled as a trapezoid. The crest and toe may both retreat at different rates. CRR is the crest retreat rate, TMR is the Toe migration rate and h is the height of the bluff. Figure from Bevis (2015).

Because the volume eroded is the erosion rate multiplied by bluff surface area, Equation 5.3 describes the erosion rate when the river is migrating away from a bluff (E_{away}) as:

$$E_{away} = CRR/2 \quad (5.3)$$

When a channel migrates towards a bluff, the base of the bluff may retreat as well as the crest. This situation can be modeled like a trapezoid, where:

$$V_{Etoward} = (CRR+TMR)/2*h*l \quad (5.4)$$

and

$$E_{toward} = (CRR+TMR)/2 \quad (5.5)$$

To combine Equations 5.3 and 5.5 into an average bluff retreat rate, we assume the river spends equal amounts of time migrating into and away from a bluff over long timescales, so the long-term erosion rate, E is taken as:

$$E = E_{away}/2 + E_{toward}/2 \tag{5.6}$$

Substituting Equations 5.3 and 5.5 into 5.6 and simplifying gives:

$$E = (2CRR + TMR)/4 \tag{5.7}$$

And thus, the volume eroded (V_E) from one bluff with measured crest and toe retreat rates is

$$V_E = SA*(2CRR + TMR)/4 \tag{5.8}$$

Measured bluff erosion rates are applied to bluffs on which it was not possible to measure crest and toe retreat distances via interpolation and extrapolation. To interpolate erosion rates, we used locally-measured bluff erosion rates. The ArcGIS tool *focal statistics* was used to measure the surface area (SA) and volume eroded (V_E) for all bluffs within a 3 km radius of each bluff with measured E (Equation 5.9).

$$E_{interpolate} = \Sigma V_E/\Sigma SA \tag{5.9}$$

For bluffs that are too far away from bluffs with measured E, rates were extrapolated based on the measured subwatershed E rate.

We measured erosion rates on just 408 of the nearly 3,500 bluffs in the final GBER budget. This small number of bluffs accounts for about 1/3 of the surface area of bluffs and about 40% of the annual volume of sediment eroded from bluffs in the GBER watershed. More bluffs, and a larger proportion of bluffs, were measured in the Le Sueur watershed than the Blue Earth or Watonwan. Of the bluffs on which we were not able to measure erosion rates, about 700 were within 3 km of measured bluffs, which makes up about 1/3 of the surface area and accounts for 40% of the annual volume of sediment eroded. The final group of bluffs contains extrapolation bluffs, which are greater than 3 km from bluffs with measured rates. About 2/3 of the bluffs were in this group by count, but they are responsible for only 20% of the annual volume of sediment eroded from bluffs in the watershed. Extrapolation bluffs account for the final 1/3 of bluff surface area.

To calculate the volume of sediment eroded from a bluff, the erosion rate (measured, interpolated, or extrapolated) was multiplied by bluff surface area. The volume of sediment eroded was converted to mass of silt and clay-size sediment (i.e., that which becomes suspended sediment) based on sediment bulk density and texture of till, outwash and Holocene alluvium (Table 5.3).

Table 5.3: Sediment texture and bulk density data

	bulk density	percent fines*	mass mud/volume sediment
Till	1.8 Mg/m^3	0.65	1.17 Mg mud/m^3 till
Holocene alluvium (Hal)	1.3 Mg/m^3	0.5	0.65 Mg mud/m^3 Hal
Pleistocene alluvium (Pal)	1.3 Mg/m^3	0.31	0.40 Mg mud/m^3 Pal

*silt and clay. Bulk density from Thoma et al., 2005; textures from Jennings, 2010 and Belmont et al., 2011.
Table from Bevis (2015).

Bluffs capped by Quaternary alluvium had a portion of their thickness treated as alluvium in terms of bulk density and texture and the rest was considered to be till. Surficial units in the GBER watershed were identified in ArcGIS using surficial geology maps of Blue Earth County and the middle Minnesota River watershed (Jennings, 2010; Jennings et al., 2012). These maps were constructed from 1:90,000 and

1:250,000 aerial photos. Alluvial units selected included surficial and shallowly-buried sediments from streams, fans, deltas and beaches, which are Pleistocene alluvium; and terrace deposits, which are Holocene alluvium. Sand depth was determined using data from the sand distribution model in the Blue Earth County geologic atlas (Meyer and Lively, 2012). We averaged the sand depth of the units selected above, and applied this mean depth (3m) to surficial sand units throughout the GBER watershed. Where Quaternary alluvium was mapped on bluffs, we altered the bulk density and texture of a three-meter-high band of bluff sediment in our calculations according to published sediment density and texture in the GBER watershed (Table 5.3).

Vegetation can play a role in stabilizing river banks (e.g. Hupp and Simon, 1991; Millar, 2000; Erskine et al., 2012; Lenhart et al., 2013; Gurnell, 2013), but bluffs in the GBER watershed are generally too tall for root strength to influence erosional processes near the toe. Inactive bluffs may have significant vegetative cover on their slopes, however, but it is more a sign of recent inactivity than a predictor of future stability. Day et al. (2013) found no correlation between modern (2005) vegetation cover and long-term decadal-scale bluff retreat rates from 1938-2005 on bluffs lining the Le Sueur River. There is the potential for bias, however, towards measurement of bluff retreat rates on unvegetated bluffs as they are easier to delineate. To account for this possibility, vegetative cover was noted on all bluffs where it could be determined from recent aerial photographs, and a method was developed for determining differential erosion rates for vegetated vs. unvegetated bluffs within a given subwatershed. The methodology for this is covered in detail in Appendix 2 of Bevis (2015). The sediment budget spreadsheet was constructed with a function that allows the user to extrapolate bluff retreat rates considering vegetation cover.

5.3.2.2 Banks

Sediment supply from stream banks was split into three components: 1) bank sediment derived from meander migration, 2) sediment derived from channel widening, and 3) sediment sourced from channel incision. Sediment supply rate from meander migration was determined using the method of Lauer and Parker (2008). The method is based on the assumption that on a stream in dynamic equilibrium, cutbank erosion is balanced by floodplain deposition. If a channel is incising, it is reflected in the difference in elevation between the eroding and depositing banks. Sediment export due to meander migration on incising channels is therefore equal to the volume of sediment eroded on the part of the cutbank that is higher than the opposite bank. The ArcGIS plugin *Planform Statistics* was used to determine channel migration rate from 1938 to 2008 on the Blue Earth and Watonwan Rivers (Lauer and Parker, 2008), following the same procedure used on the Le Sueur River (Belmont et al., 2011). Channel banks were traced on 2008 and 1938/9 aerial photographs extending as far upstream as possible. Traced channels adjacent to bluffs were not considered as they are part of the bluff portion of the sediment budget. From traced banklines, *Planform Statistics* interpolates a channel centerline based on nodes spaced every 20m. The tool then compares the 1938 and 2008 centerlines in order to calculate mean annual migration rate at each node. *Planform Statistics* was also used to create 5m buffers outside of the banklines. The tool splits the buffers into boxes with lines normal to the channel centerline at each node. The *zonal statistics as table* tool in ArcGIS was used to extract mean bank height in each buffer box from the one meter resolution DEM.

When a channel is migrating towards the higher bank, the annual volume of eroded sediment is the product of the difference in bank height, reach length on the 2008 centerline, and migration rate. Sediment volumes were converted to mass using a bulk density of 1.3 Mg/m^3 and a silt and clay composition of 50% (Belmont et al., 2011) (Table 5.3). Above the knickpoint, where incision is not occurring, channels were assumed to be in dynamic equilibrium with cutbank erosion balanced by floodplain deposition over time.

Widening rates were calculated from the traced banklines around a series of bends throughout tributaries to the lower Minnesota River. Channel surface areas in 1938 and 2008 were divided by the associated reach length to obtain average widths, which were divided by 70 years to obtain annual widening rates (Gran et al., 2011). For calculations involving modern channel width in the greater Le Sueur watershed, we used a flow accumulation layer and the hydraulic geometry relationship $w = 1.02A^{0.50}$ (width (w) in meters, upstream basin area (A) in square kilometers; Gran et al., 2013). Channel widening rates were only applied to channels order 4 and higher. Air photo resolution limited the measurement of channel widening to these larger channels, and lacking direct evidence of systematic widening in the smaller channels, we did not include it in the sediment budget.

The incision rate calculated for the Le Sueur is based on a record of incision preserved in fluvial terraces and kinematic modeling (Gran et al., 2009, 2011, 2013). Channel incision rate is unlikely to vary much between GBER channels, because the channels have incised the same depth over the same time period to create a network of channels similar in long profile elevation, so the Le Sueur rate was used (2.6 mm/a below knickpoints, no incision above knickpoints; Gran et al., 2013).

5.3.2.3 Ravines

Ravine sediment source extents were digitized manually, based on break in slope on 3-meter lidar-derived DEMs. For this study, as in the Le Sueur River sediment budget, only ravines with area > 10,000 m^2 are included in the budget. We estimated that this threshold selects at least 85% of all ravine area based off of a comparison with all ravine areas in the lower Le Sueur watershed. To calculate the sediment supply rate from ravines to GBER channels, we used erosion rates based on monitoring season TSS yields measured on 4 ravines in the lower Le Sueur (Belmont et al., 2011). TSS loads were calculated and compared with TSS loads on the Le Sueur over the same monitoring period. A positive relationship was found between TSS load and incised ravine area (Belmont et al., 2011). As part of this project, an additional two years of data were collected from a subset of the original ravines, but the data were not complete enough to be used for additional annual load calculations. The Le Sueur yield (0.00022 Mg/yr/m^2 of incised ravine area (Gran et al., 2011; Belmont et al., 2011)) was applied to other ravines in the GBER watershed based on incised area.

5.3.2.4 Uplands

Upland sources cover all of the area that is not a near-channel sediment source or a lake. In the Le Sueur, upland supply rates were determined using sediment fingerprinting paired with loads at upstream gages. Sediment fingerprinting uses meteoric Beryllium-10 (^{10}Be) and Lead-210 (^{210}Pb) isotopes produced in the atmosphere to differentiate between sediment derived from near channel sources and upland-sourced sediment (Schottler et al., 2010; Belmont et al., 2011; Belmont et al., 2014). Sediment fingerprinting for the Le Sueur budget was conducted at the upper gages where load is less affected by near-channel sources. Because samples were collected on mainstem channels, the upland erosion rates in the Le Sueur budget already account for deposition on fields prior to sediment delivery to channels as well as erosion, deposition and dredging in ditch networks or lakes. Thus, the upland erosion rate determined from sediment fingerprinting should be considered a measure of net sediment delivery to channels from exposed upland surfaces. Calculated yield was applied to upland sediment supply areas throughout the watershed. Sediment fingerprinting data were used in conjunction with TSS loads from the upper gages on the Maple River and the Le Sueur River to determine upland yields as part of the Le Sueur River sediment budget (Belmont et al., 2011), with the upland yield derived from the Maple applied to the Cobb River basin as well given their similar surficial geology.

Beryllium-10 and ^{210}Pb are both naturally-occurring tracers that are delivered to soil surfaces via atmospheric deposition (Willenbring and Von Blanckenburg, 2010; Belmont et al., 2014). Specifically, ^{10}Be is produced when high-energy cosmic rays interact with oxygen atoms in the atmosphere and is subsequently delivered to Earth’s surface, where it adsorbs to soil particles within the top meter of the soil profile. Lead-210 is part of the decay chain of naturally-occurring Uranium-238 and is delivered to Earth’s surface via rainfall or dry deposition and adsorbs to soil particles within the top few centimeters of the soil profile. These specific tracers were selected because they have significantly different half-lives, 1.4 million and 22.3 years for ^{10}Be and ^{210}Pb, respectively. Generally, upland sediment contains high concentrations of both tracers. Bluff sediment exhibits very low concentrations of both tracers. Sediment that is eroded from uplands and temporarily deposited in floodplains, which is subsequently re-mobilized by bank erosion, is deficient in ^{210}Pb after 50-60 years because of its short half-life, but ^{10}Be concentration remains essentially unchanged.

Upland yield data from the Le Sueur and Maple Rivers were augmented with additional fingerprinting samples from the Beauford Ditch, Blue Earth River near Rapidan and the Watonwan River at Garden City. The sediment fingerprinting data were used in conjunction with TSS loads at these two gage sites to determine upland yields. Additional samples were collected from upland, bluff and bank source areas to constrain the geochemical signature of each source. Suspended sediment samples were collected by a combination of staff from the Belmont Lab at Utah State University, the Water Resources Center at Minnesota State University, Mankato, and the Triplett Lab at Gustavus Adolphus College. Samples were dried and split for analysis of grain size, ^{10}Be concentration at Purdue University PRIME Lab, and ^{210}Pb activity at the St. Croix Watershed Research Station.

5.3.3 Sediment Storage

5.3.3.1 Storage on floodplains

The amount of floodplain storage in the Le Sueur budget was calculated differently for reaches above, within and below knickzones. Above the knickzone, where banks are in dynamic equilibrium, deposition rates were set accommodate the sediment eroded from banks via channel migration, thus maintaining dynamic equilibrium. Within the knickzone, floodplain extent is very limited (Belmont, 2011) since channels are actively incising, so the budget included no floodplain storage. Below the knickzone, floodplain deposition rates were calculated based on observations that the summed loads from gages at the downstream end of the Le Sueur knickzone (Maple, Big Cobb, and Le Sueur) were equal to the gaged load at Red Jacket Park near the mouth of the Le Sueur, in spite of sediment supply in the intervening reach. The estimated load from bluffs in the reach between the lower gages and Red Jacket must therefore be stored on floodplains in this reach (Belmont et al., 2011). This gives a rate of mass storage below the knickzone estimated at 530 Mg of mud stored per channel kilometer per year. To estimate storage from aggradation on the Blue Earth below the knickzone (i.e., below the confluence with the Watonwan) this "storage yield" below the knickzone of the Le Sueur was applied to the Blue Earth reaches below the knickzone.

To determine where bluff and bank sediment could be stored on Blue Earth and Watonwan floodplains, we compared cross-sections of the Blue Earth and Le Sueur floodplains (Belmont, 2011). While floodplains within the knickzone are very small or non-existent on the Le Sueur and its tributaries, floodplains in the knickzone of the Blue Earth are similar to Le Sueur floodplains above the knickzone, so we included storage of bluff sediment within the Blue Earth knickzone. Cross sections of Watonwan floodplains were not included in the study as most of the Watonwan lies above the knickzone. We assume that the floodplain geometry on the Watonwan within the knickzone behaves like that of the Blue Earth. We therefore estimated the amount of sediment trapped on floodplains in all subwatersheds except for reaches in the Le Sueur knickzone. To do so, our spreadsheets "stored" a 2m-high band of eroded bluff sediment on floodplains in the same way bank sediment above knickpoints is stored on floodplains.

5.3.3.2 *Storage in lakes*

The ability of a waterbody to trap sediment (i.e., trap efficiency, TE) depends on characteristics of the inflowing sediment and the retention time of the waterbody, functions of lake geometry and watershed runoff characteristics (Verstaeten and Poesen, 2000). This project estimated storage in lakes based on the ratio of waterbody capacity and watershed area (Brown, 1943). In this relationship (Equation 5.10), trap efficiency is defined as a function of reservoir storage capacity (C, in m^3); watershed area (W, in km^2); and an empirical form factor (D, ranging from 0.046 –1). Curves demonstrating the effect of the form factor are shown in Figure 5.3. Though simple, when compared with more complex methods, Brown's curve has provided accurate results when used on watersheds of similar size to the GBER watershed (Butcher et al., 1992).

$$TE = 100*(1-\frac{1}{1+0.0021D\frac{C}{W}}) \quad (5.10)$$

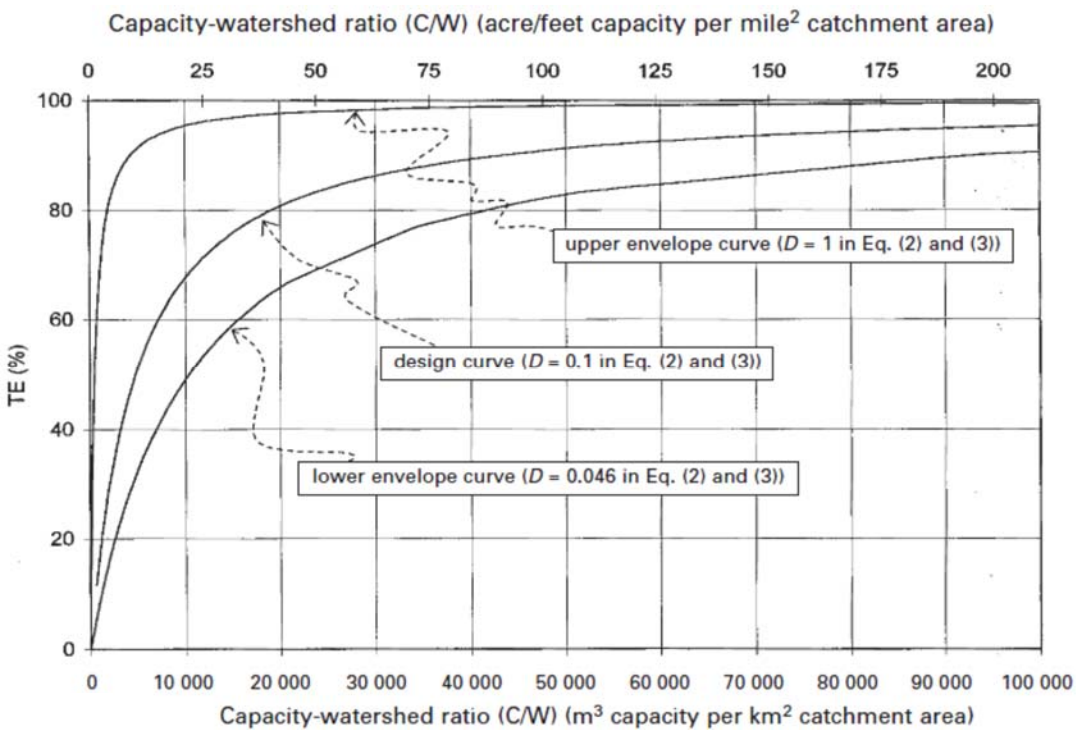

Figure 5.3: Relationship between C/W ratio and trapping efficiency. The median estimated C/W of the largest lake basins in the GBER watershed is 75,000 m^3/km^2. Figure from Brown, 1943.

We automated estimates of lake trapping efficiency in ArcGIS to estimate unique TE for all lakes in the GBER watershed. This was done with a 10m resolution DEM. The automated method used *zonal statistics* to identify the largest flow accumulation value within National Hydrography Dataset waterbodies, then a raster algebra statement using a threshold to select the raster cell with the highest flow accumulation value within the lake. These cells were used as pourpoints to delineate "lakesheds" with the *watershed* tool. Lakeshed areas were paired with lake volumes, and trapping efficiency was calculated using the relationship between lake volume and watershed area described in Equation 5.10. We used the middle curve in Figure 5.3, where D = 0.1. Lake capacity was estimated using a linear regression between lake volumes from Minnesota Department of Natural Resources bathymetry data and lake surface area. Average lake depth in the GBER watershed is about 2m. The sediment budget draws on these data to include sediment storage in every lake. While Rapidan Dam on the Blue Earth River might be expected to trap sediment, its reservoir is already full of sediment. The reservoir currently has little storage capacity even for water, and thus the impoundment has a trapping efficiency near zero.

5.3.4 Holocene Sediment Budget

A Holocene sediment budget was constructed to apportion sediment based on pre-settlement conditions. The estimated Holocene budget in the Blue Earth and Watonwan Rivers was heavily based on extensive research in the Le Sueur basin (Gran et al., 2013). There, terrace ages were used to constrain a numerical model of valley growth over the last 13,500 years. The model showed that in the absence of large-scale changes in climate and land use such as were experienced in the last 200 years, the mass of sediment derived from valley excavation (bluff and bank erosion) was 47,000 Mg/yr of silt and clay, which is slightly less (within 5%) than the mean export rate based solely on total valley volume removed in 13,500 years and 3 times lower than the predicted modern fine sediment load associated with bank and bluff erosion.

To determine valley excavation rates in the Blue Earth River, the valley volume was measured using lidar data. A polygon was fit to 5km-long valley reaches, and the missing mass determined between the upland surface and the modern valley bottom. Volumes from all of the valley reaches were summed and converted to mass of fine sediment using bulk density and grain size distributions for till (Table 5.3). The Blue Earth River pre-settlement rate was taken to be 95% of the mean, assuming the pattern of erosion in the Blue Earth River was the same as in the Le Sueur River over the past 13,500 years.

Pre-settlement ravine erosion rates are less constrained. The total volume of material removed from ravines in the Blue Earth River watershed was summed, converted to Mg of fine sediment, and divided by 13,500. These pre-settlement loading rates were then compared with modern estimates of ravine loads and found to be ~50% of modern loads. Upland contributions were assumed to be negligible given the prairie vegetation and low-relief or zero relief over much of the upland area. Streambank meandering and incision components were considered with bluff erosion as part of the valley excavation portion of the budget. River widening was assumed to be zero. Floodplain and lake deposition is relatively unconstrained and thus reductions in depositional sinks were made commensurate with reductions in primary erosional sources contributing to them.

5.4 **Results**

5.4.1 Bluff extents, migration rates, and erosion rates

Bluffs are primarily found below the knickpoint, with bluffs increasing in size near river mouths. To normalize bluff extent data to different basin areas, we calculated bluff frequency (bluff surface area per channel length). Bluff frequency has consistent trends in the basin: On each GBER channel, bluff surface area is near zero above the knickpoint, but increases rapidly below the knickpoint (Figure 5.4).

Retreat and migration rates are highly variable along channels in the GBER watershed (Figure 5.5), but follow similar trends on each river. Where channels flow in bedrock reaches they often migrate more slowly than channels bounded by till or alluvium. For example, channel migration rates on the Blue Earth River below the Rapidan Dam are much lower than rates above the dam (Figure 5.6). On the Le Sueur, channel migration rates rise near confluences with the Cobb and Maple Rivers, then decrease below the Maple River, where bedrock is more prevalent. Migration rates rise near the confluence with the Blue Earth. Channel migration rates on the Blue Earth River follow a similar trend: directly below Rapidan Dam, where the channel is primarily bedrock, migration rate is very low, but as confluences with the Le Sueur and then Minnesota Rivers near, migration rate increases. Below the knickpoint on the Watonwan, channel migration rates may be slowed by bedrock. We normalized channel migration rates to channel width as a surrogate for discharge, because channel width on major rivers in the Le Sueur basin changes with the square root of basin area (Gran et al., 2013). Normalized migration rates remain highest on the Blue Earth River (Figure 5.6).

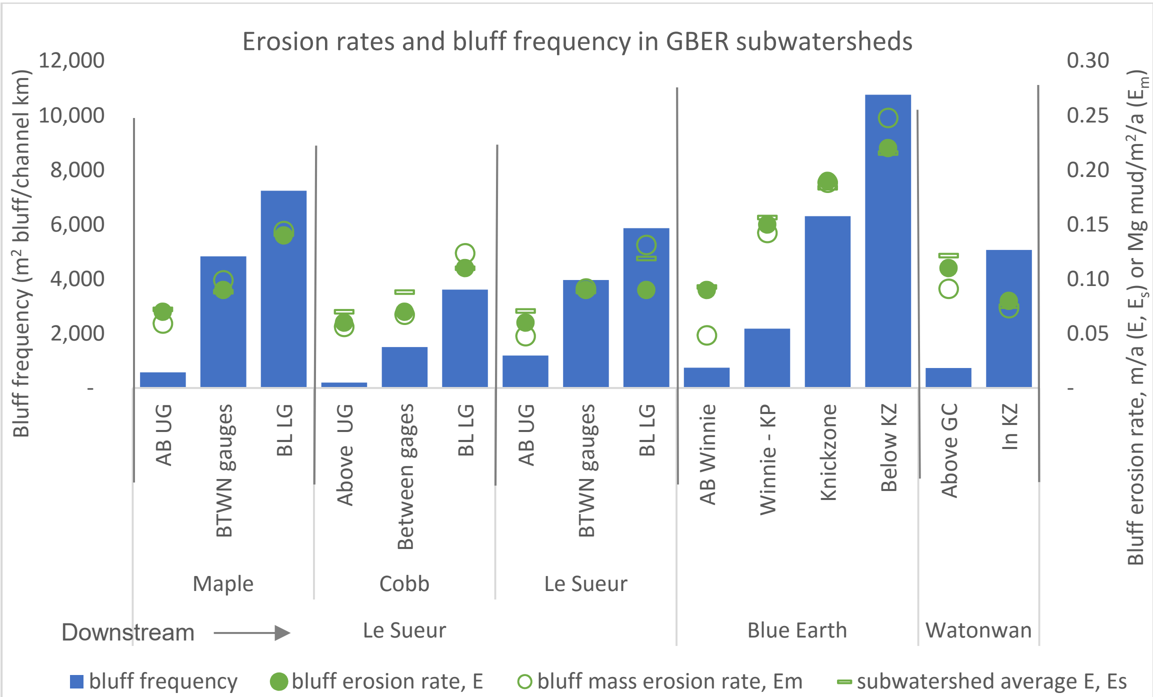

Figure 5.4: Bluff frequency (blue bars) and erosion rates (orange dots) follow remarkably similar trends in the GBER watershed. Bluff frequency is bluff surface area per channel length (m^2/km). Average measured erosion rate (E m/a), the average of all measured and extrapolated rates in a subwatershed (E_s, m/a), and mass erosion rate (E_m, Mg mud/m^2/a) are similar in each subwatershed. Upstream is to the left, bedrock bluffs are included in bluff frequency. Figure from Bevis (2015).

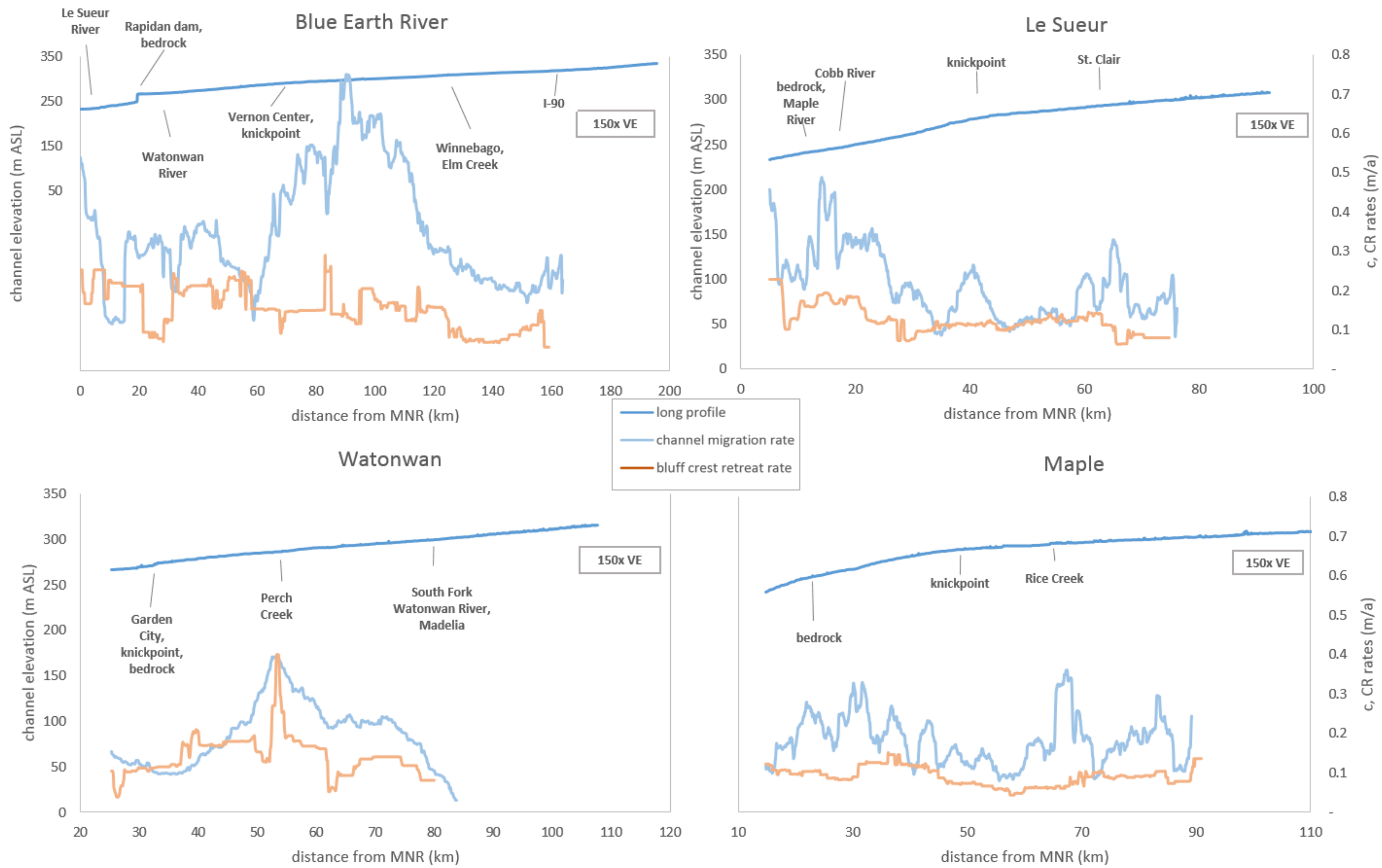

Figure 5.5: Bluff crest retreat and channel migration rates, smoothed over a 3 km radius. Channel migration rates include bluffs, banks and bedrock reaches, but not reaches that avulsed or were shortened from 1938 to 2008. Long profiles have 150x vertical exaggeration. Figure from Bevis (2015).

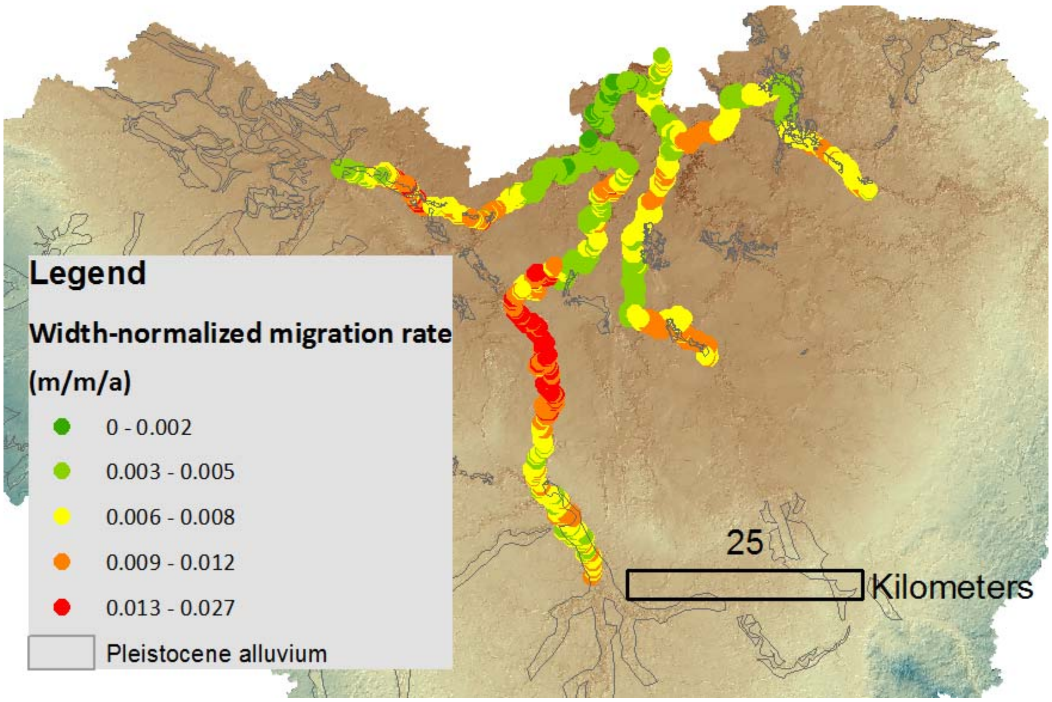

Figure 5.6: GBER watershed annual channel migration rates normalized to channel width for comparison across watersheds. High channel migration rates often occur in Pleistocene tunnel valleys and outwash channels (outlined in grey; not shown but believed to exist on the reach of the Blue Earth with the highest migration rates). Figure from Bevis (2015).

Bluff extent and retreat rates were used to calculate volumetric (E) and mass erosion rates (E_m) (Figure 5.4). A mass erosion rate is simply the mass of mud (silt and clay) eroded from each bluff or subwatershed divided by surface area to account for different bluff surface areas in each subwatershed. Subwatershed E_m rates include adjustments for bulk density and texture. Mass erosion rates in this figure also include the effect of lake and floodplain storage. Like E, mass erosion rates (E_m) increase downstream in GBER watersheds. On the Blue Earth, E_m rates near the mouth are about twice as high as rates higher in the watershed (Figure 5.4). Average E_m rates on the Blue Earth River are just under twice the average E_m rates on the Le Sueur and Watonwan. Note also that E_m rates closely follow E rates, but are reduced by storage on lakes high in watersheds, and changed by interpolation downstream. In Figure 5.4, subwatershed-averaged mass erosion rates are plotted alongside bluff frequency. The product of E_m and extent is load. When load is normalized to stream length, the along-channel trend in each subwatershed is even stronger (Figure 5.7).

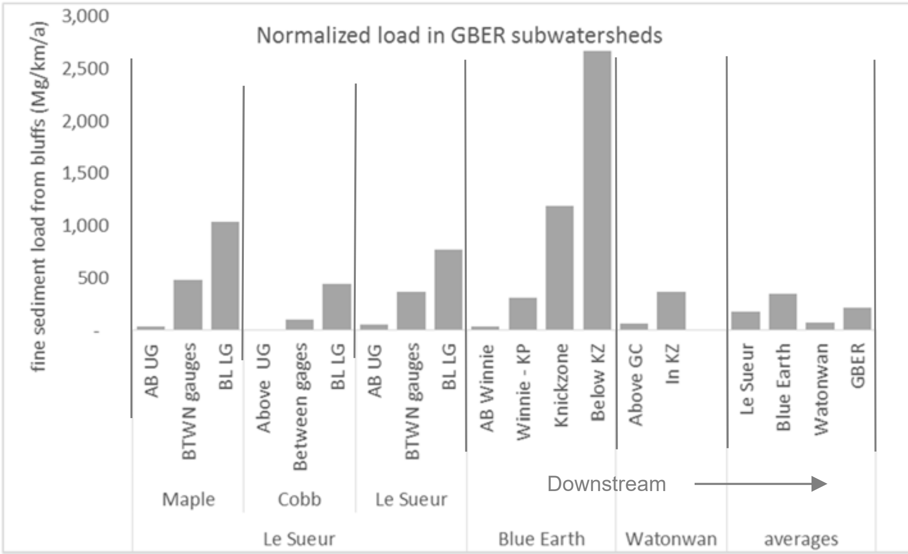

Figure 5.7: Bluff load normalized to channel length for subwatersheds in the GBER watershed. Load accentuates the trends seen in its components, rates and extents. Here load includes erosion from bedrock bluffs and the effects of storage. Figure from Bevis (2015).

5.4.2 Upland Sediment Fingerprinting

Our fingerprinting sampling strategy sought to expand existing datasets for sediment sources and gages in the Le Sueur watershed, while also expanding to additional sites within the Le Sueur, Blue Earth and Watonwan watershed. Samples collected in locations where we had existing data showed generally consistent concentrations for both ^{10}Be and ^{210}Pb. Adequately constraining source area fingerprints is challenging due to the spatial variability in tracer delivery rate, potential for mixing of sediment spatially and vertically within the soil profile, differences in grain size and carbon content. Nevertheless, source area concentrations were found to be fairly consistent. Bluff samples analyzed as part of this and previous studies fall within a relatively narrow range from 6.65 x 10^6 to 3.14 x 10^7 with an average 0.12 x 10^8 atoms/g for ^{10}Be and were consistently found to be devoid of ^{210}Pb. Banks, which are alluvial deposits that consist of a mixture of upland and bluff sediments, averaged 0.80 x 10^8 atoms/g for ^{10}Be and were also consistently found to be devoid of ^{210}Pb. Uplands were found to be more variable, as is expected from the wide range of land use and erosional histories throughout the study area, but on average exhibited concentrations that were approximately 20 times higher than bluffs. Including previous upland ^{10}Be samples as well as new samples collected as part of this study and as part of a complementary study conducted by St. Croix Watershed Research Station, upland ^{10}Be concentrations ranged from 2.02 x 10^8 to 2.91 x 10^8 at/g and averaged 2.7 x 10^8 at/g for ^{10}Be. Excluding samples collected in a separate study by St. Croix Watershed Research Station due to potential discrepancies in grain size distributions, the average ^{10}Be concentration of upland sources is 2.4 x 10^8 atoms/g. Excess Lead-210 activities were measured for two samples collected from Beauford Ditch (2.28 and 2.58 pCi/g) and were otherwise assumed to be equivalent to the upland source area fingerprint constrained by St. Croix Watershed Research Station (2.3 ± 0.66 pCi/g).

Figure 5.8 shows average concentrations of each of the tracers for suspended sediment samples. Measured values follow a predictable pattern, with Beauford Ditch (dark yellow) plotting near the upland fingerprints (high in both ^{10}Be and ^{210}Pb). Samples from St. Clair (tan) plot half way between upland and bluff source area fingerprints and suspended sediment samples collected from the Highway 8 gage (dark orange, gage located further downstream in the knick zone of the Le Sueur River) plot at progressively lower concentrations, shifted in the direction toward banks and bluffs, as expected. There is a considerable shift in ^{10}Be concentrations from Upper Maple (darker purple) to Lower Maple (brighter purple) watershed and samples collected from Red Jacket (red) at the mouth of the Le Sueur watershed plot essentially between the Highway 8 and Lower Maple samples. Samples from the Watonwan (green) demonstrate considerably higher concentrations of ^{10}Be and ^{210}Pb, suggesting that uplands are a relatively more important sediment source in the Watonwan watershed. This finding is consistent with early findings of the sediment budget for the Watonwan watershed, which initially indicated significant over-prediction of bluff erosion when we assumed that bluff erosion rates were the same in the Watonwan as they were in the Le Sueur watershed. Suspended sediment samples collected near the mouth of the Blue Earth River (blue) plot lowest in terms of ^{10}Be, but higher than samples collected from knick zones of other tributaries with respect to ^{210}Pb. Table 5.4 shows average results interpreted for source apportionment. Percent upland plus bank are computed from ^{10}Be samples using a simple unmixing model between upland and bluff concentrations. Percent upland minus bank are computed from ^{210}Pb results using a simple unmixing model between upland and bank sources. These numbers should be viewed as preliminary until related projects at Utah State University and St. Croix Watershed Research Station are completed and upland fingerprints have been better constrained.

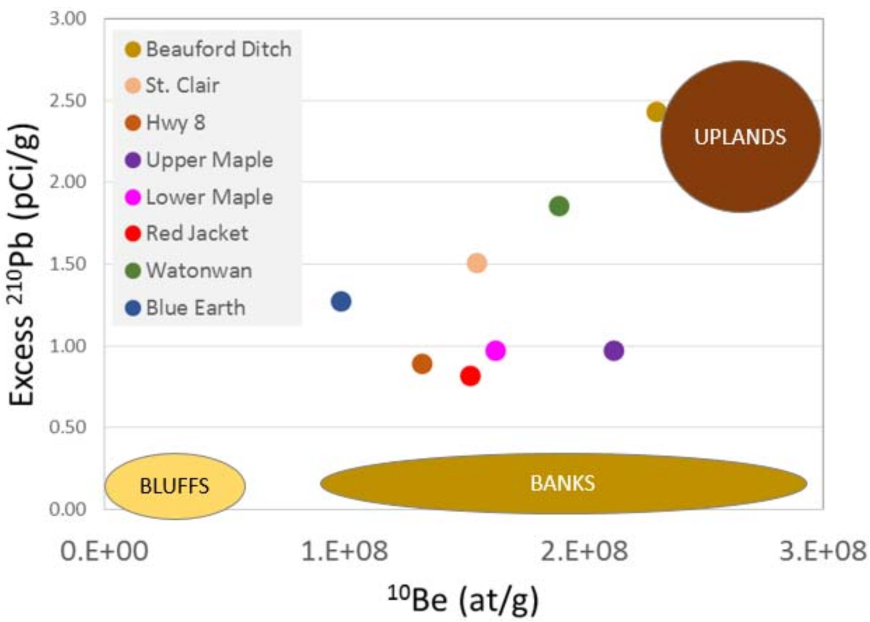

Figure 5.8. Results from sediment fingerprinting analyses. Large circles indicate the range of tracer concentrations found in source areas. Small dots indicate the average concentration of each tracer measured in suspended sediment samples.

Table 5.4. Average sediment fingerprinting samples from source areas and suspended sediment samples. These values are preliminary pending completion of related projects.

Summary Table	Avg ^{10}Be (at/g)	Avg ^{210}Pb (pCi/g)	%upland +bank	%upland-bank
Uplands	2.39E+08	2.30		
Bluffs	1.19E+07	0.00		
Banks	8.03E+07	0.00		
Beauford	2.30E+08	2.43	101	106
St. Clair	1.55E+08	1.51	68	66
Hwy 8	1.32E+08	0.89	58	39
Red Jacket	1.52E+08	0.82	67	36
Upper Maple	2.12E+08	0.97	93	42
Lower Maple	1.63E+08	0.97	72	42
Watonwan	1.89E+08	1.86	83	81
Blue Earth	9.88E+07	1.27	43	55

5.4.3 Ravines

Ravine loads were taken directly from loads measured in a series of 4 ravines in the Le Sueur River basin. Differences in the relative importance of ravine loads were therefore driven primarily by ravine area. The Le Sueur watershed has a greater density of ravines compared to the rest of the GBER watershed; the incised ravine area in the Le Sueur watershed was approximately the same as in the Blue Earth and Watonwan watersheds combined. The Watonwan watershed had quite a large area of ravines found in the far upper basin, associated with high relief in that region and not associated with the knickzone. It is possible that these ravines erode at a significantly different rate than the ones monitored in the lower Le Sueur River, but we currently have no data on the rates of erosion there. We consider this to be a source of uncertainty in our Watonwan ravine load estimates and could be one reason why sediment loads predicted in the Watonwan are consistently higher than loads measured at the Garden City gage.

5.4.4 Streambanks and Floodplain Deposition

Under the sediment budget for the Greater Blue Earth River basin, streambanks appear to be a much more important source of sediment compared with the earlier Le Sueur River sediment budget (Gran et al., 2011; Belmont et al., 2011). The main reason has to do with how sediment loads are reported in the GBER watershed budget. Here, we separate out sources and sinks. Thus, although streambanks account for approximately 20-30% of the total budget in terms of source contributions, much of that sediment is deposited in floodplains. Estimated floodplain deposits in the Watonwan almost completely match streambank contributions (70-80%), whereas on the Blue Earth River, floodplain deposition accounts for approximately 40% of the total streambank-sourced loads. On the Le Sueur River, floodplain deposition accounts for approximately half of the total streambank-sourced loads, with most of the floodplain capacity coming in below the knickzone. When net streambank contributions are considered (streambank erosion minus floodplain deposition), the fraction of sediment derived from streambanks is only 15% of the total sediment budget for the GBER watershed.

5.5 **GBER watershed sediment budgets**

The GBER sediment budget shows similar results to the Le Sueur sediment budget with a predominance of near-channel sediment sources in the total fine sediment load. Detailed sediment accounting is included on an accompanying Excel spreadsheet and general results are presented here. The spreadsheet allows the user to include or exclude bluffs in bedrock reaches. In addition, the user can consider vegetation cover as a factor in extrapolating bluff retreat rates or not. Although work by Day et al. (2013) in the Le Sueur watershed found no correlation between long-term decadal-scale erosion rates and vegetation cover, it is frequently discussed as a potential control on bluff erosion and may be more important in other watersheds. Thus, the user is able to consider vegetation cover as a factor in erosion rates or not. Upland yields are set by fingerprinting data that are still considered preliminary pending completion of a related project. Because of this, ranges of upland % determined from fingerprinting data are included on the budget front page and the user is able to adjust the percent within the specified range. The median values are used in the results shown in Table 5.5 and Figure 5.9.

For comparison with observed TSS loads, the user can compare the predicted loads from the budget to observed loads from a range of timescales (2000-2013, 2000-2010, and 2007-2012). The benefit of the shorter timescale (2007-2012) is that all gages were operating during the entire time period, so all loads are based on FLUX calculations made from direct sampling. In the Le Sueur subwatersheds, 2007-2012 had noticeably lower TSS loads (72-88% of longer time periods), although TSS loads are more comparable in the Blue Earth and Watonwan (96-105%). For longer time periods, data had to be adjusted for some of the gages (data were adjusted based on the relative loads from a mouth gage (Red Jacket on Le Sueur subwatersheds and Rapidan for Blue Earth and Watonwan Rivers) between the time period of actual gaging vs. the time period of averaging. The time period of 2000-2010 was used in the original Le Sueur budget, and the time period 2000-2013 represents the most up-to-date TSS load data available as of June 2016.

Comparing predicted loads with 2000-2013 data, the total fine sediment load on the Watonwan and Blue Earth Rivers is best predicted when vegetation cover is considered (see Table 5.5). In general, bare bluffs composed a larger proportion of the measured bluffs than extrapolated bluffs, and when this is the case, erosion rates that considered vegetation cover were lower. The best fit scenario for the Le Sueur was the scenario in which all bluffs were included and vegetation cover was not included as a factor. Under all scenarios, the majority of the fine sediment was derived from near-channel erosion of bluffs and streambanks (60-78% over all different bluff scenarios).

Bluffs in the Blue Earth watershed contribute more sediment to the river than Le Sueur bluffs, primarily because there is more bluff surface area in the Blue Earth watershed, but also because erosion rates are higher. Figure 5.7 shows channel migration rates throughout the GBER, with the highest migration rates present on the Blue Earth River. The Watonwan has a relatively higher proportion of sediment derived from banks than other GBER watershed rivers, primarily because the other major sources (bluffs and uplands) are not as high. The rate of channel sediment supply from the Watonwan is not significantly different than on other GBER watershed channels. The Watonwan has little incised channel length, and meander migration rates are only a little higher than rates on the Le Sueur. Widening is in line with widening measured on other GBER watershed channels.

Upland sediment yields as determined from preliminary sediment fingerprinting data give yields of 1.4×10^{-5} $Mg/m^2/yr$ (124 lbs/acre) on the upper Le Sueur watershed, 1.3×10^{-5} $Mg/m^2/yr$ (113 lbs/acre) on the Watonwan watershed, and 2.2×10^{-5} $Mg/m^2/yr$ (218 lbs/acre) in the Blue Earth watershed. Although the range in sediment fingerprinting data can appear quite large (for ex. Upper Maple is 0.4 – 0.93 % upland with preliminary fingerprinting data), the impact on the overall sediment budget is not large. Varying the upland fingerprints from the lowest to the highest resulted in a variability in the total sediment load at the mouth gage of ± 4% on the Le Sueur, ± 3% on the Blue Earth, and ± 1% on the Watonwan. Changes in upland yields to the channel are mediated in part by commensurate changes in lake storage in the uplands.

Storage is a significant portion of the budget. Values listed above for each source are gross contributions. Storage then removes fine sediment from the river prior to the gage at the mouth. On the Blue Earth and Le Sueur Rivers, the fraction stored varied between 23-26%. On the Watonwan, the fraction stored was much higher: 44-48%. The Watonwan gage is located near the knickpoint, so the geomorphic regimes where source contributions are high and sinks less abundant (i.e. the knickzone) are not as extensive on the Watonwan above the gage.

The budget is set up to display sources relative to each other in a series of pie charts (Figure 5.9A). Magnitudes of sediment contributions are displayed in a bar graph for each major watershed, broken down by geomorphic regime (above vs. below knickpoint) (Figure 10). It is important to note that the pie charts in the GBER sediment budget show a comparison of sediment sources only, without including depositional volumes. To illustrate the difference between source comparisons and net (source – sink) comparisons, Figure 5.9B has net sediment loads plotted for each source. Since most of the sediment deposited in lakes is derived from upland sources, lake depositional volumes were removed from upland source loads. Similar to the original Le Sueur River budget, we also removed floodplain deposits from streambank erosional volumes.

Table 5.5: Example sediment budget predictions and observations for major HUC-8 watersheds

	Predicted via sediment budget, Le Sueur River (Mg/yr silt and clay)			
	Scenario 1 Exclude bedrock bluffs	Scenario 2 Include bedrock; Do not consider vegetation cover	Scenario 3 Exclude bedrock; Consider vegetation cover	Scenario 4 Include bedrock; Consider vegetation cover
Uplands	41,016	41,016	41,016	41,016
Ravines	20,009	20,009	20,009	20,009
Bluffs	110,843	117,286	67,835	74,278
Streambanks	46,592	46,592	46,592	46,592
(Lakes)*	(16,002)	(16,059)	(10,792)	(10,849)
(Floodplains)*	(26,367)	(26,367)	(25,260)	(25,260)
Total Predicted	176,091	182,477	139,401	145,787
	Observed at Red Jacket gage (Average TSS load, Mg/yr)			
2000-2013	211,860	211,860	211,860	211,860
2000-2010	229,762	229,762	229,762	229,762
2007-2012	186,553	186,553	186,553	186,553

	Predicted via sediment budget, Watonwan River (Mg/yr silt and clay)			
	Scenario 1 Exclude bedrock bluffs	Scenario 2 Include bedrock; Do not consider vegetation cover	Scenario 3 Exclude bedrock; Consider vegetation cover	Scenario 4 Include bedrock; Consider vegetation cover
Uplands	27,612	27,612	27,612	27,612
Ravines	9,886	9,886	9,886	9,886
Bluffs	55,043	55,043	27,662	27,662
Streambanks	29,221	29,221	29,221	29,221
(Lakes)*	(13,802)	(13,802)	(12,842)	(9,552)
(Floodplains)*	(23,463)	(23,463)	(21,132)	(21,132)
Total Predicted	84,497	84,497	63,697	63,697
	Observed at Garden City gage (Average TSS load, Mg/yr)			
2000-2013	34,515	34,515	34,515	34,515
2000-2010	34,842	34,842	34,842	34,842
2007-2012	35,696	35,696	35,696	35,696

	Predicted via sediment budget, Blue Earth River (Mg/yr silt and clay)			
	Scenario 1 Exclude bedrock bluffs	Scenario 2 Include bedrock; Do not consider vegetation cover	Scenario 3 Exclude bedrock; Consider vegetation cover	Scenario 4 Include bedrock; Consider vegetation cover
Uplands	98,531	98,531	98,531	98,531
Ravines	9,342	9,342	9,342	9,342
Bluffs	152,997	152,997	130,088	130,088
Streambanks	107,352	107,352	107,352	107,352
(Lakes)*	(29,066)	(29,066)	(25,572)	(25,572)
(Floodplains)*	(44,497)	(44,497)	(43,147)	(43,147)
Total Predicted	294,659	294,659	276,593	276,593
	Observed at Rapidan gage minus Watonwan contributions (Average TSS load, Mg/yr)			
2000-2013	205,994	205,994	205,994	205,994
2000-2010	224,732	224,732	224,732	224,732
2007-2012	215,932	215,932	215,932	215,932

**Lakes and Floodplains are sinks and are subtracted from the 4 source contributions.*

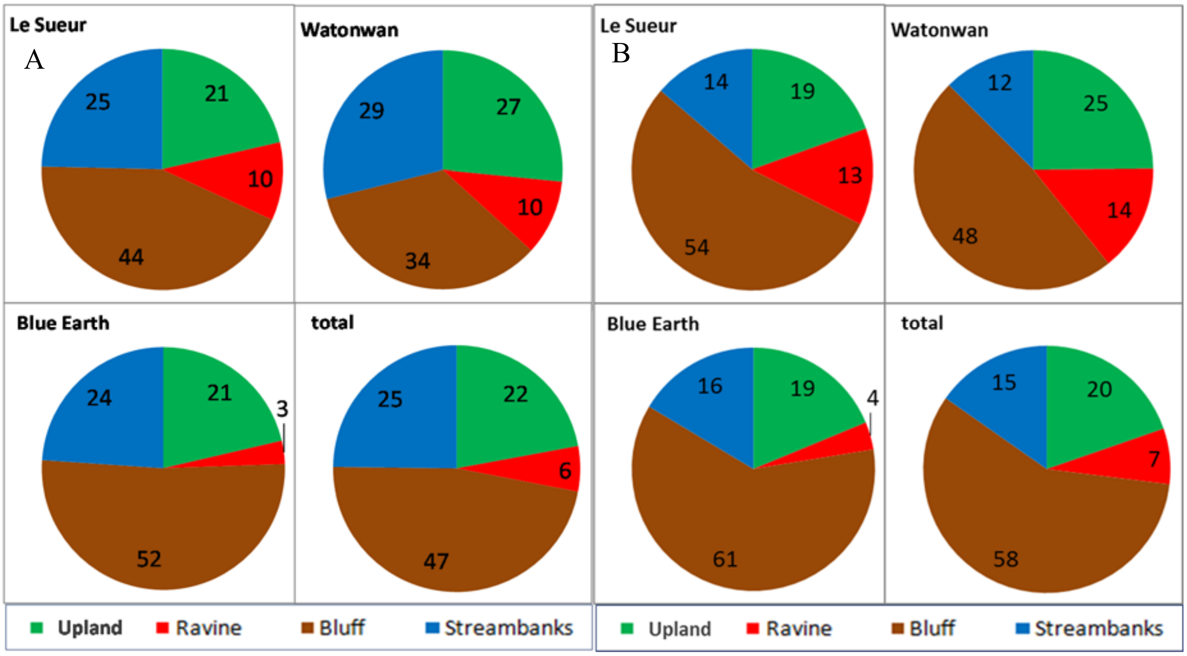

Figure 5.9: Pie charts from Scenario 4. On the left (A) are four pie charts showing the break-down of sediment sources in each major watershed, without considering sediment sinks. On the right (B) are four charts illustrating the effects of including both sources and sinks. Here, lake deposition was removed from upland source contributions and floodplain deposition was removed from streambank contributions.

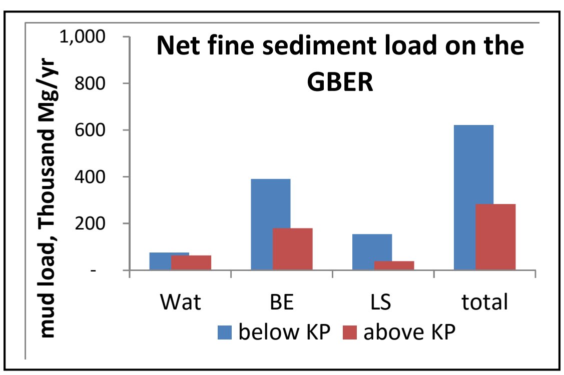

Figure 5.10: A chart illustrating the relative net sediment contribution from each major watershed, broken down into sediment derived from different geomorphic regimes (above vs. below knickpoint). Data shown are from Scenario 4.

5.5.1 Pre-settlement (Holocene) sediment budgets

Much of the Le Sueur and Blue Earth River watersheds were covered by glacial Lake Minnesota which drained shortly before the incision of the Minnesota River valley by glacial River Warren. Because of this, the modern river valleys and ravines carved are into what was once a flat-lying glacial lake bed, now covered by rich agricultural lands. In the Le Sueur River, we were able to measure the volume of material eroded from the valleys of the Le Sueur, Cobb, and Maple Rivers and convert that into fine sediment volumes using bulk density and grain size analyses (Gran et al., 2013). Here, we extended this analysis to the Blue Earth River, where we measured 1.76 x 10^9 Mg of fine sediment removed over the past 13,500, for a mean annual erosion rate of 130,000 Mg/yr of silt and clay.

In the Le Sueur River valley, Gran et al. (2013) used terrace ages coupled with hydraulic geometry and surface grain size data from the modern channel to construct a best-fit incision model for the mainstem Le

Sueur. This model was then used to investigate how sediment loads varied through time as the knickpoint migrated upstream and channels incised and migrated laterally, expanding the valley size. The results from the best-fit model indicate that erosion rates increase initially, then slowly decline over time. Interestingly, long-term pre-settlement erosion rates determined from the incisional model indicate that erosion rates today should be quite similar to the mean average annual erosion rate. We assume for now that the Blue Earth River likely eroded in a similar pattern to the Le Sueur River and use the mean average erosion rate as the pre-settlement long-term erosion rate.

The mean annual valley erosion rate in the Blue Earth River over past 13,500 years was 130,000 Mg/yr of silt and clay. Valley erosion is a combination of bluff erosion, bank erosion, and channel incision. Combining the streambank and bluff portions of the sediment budget gives 237,000 – 260,000 Mg/yr under different scenarios for modern conditions. Neither of these calculations includes the effects of deposition. Valley excavation rates have thus increased by only a factor of two on the Blue Earth, compared to a factor of 3 on the Le Sueur.

To compile a Holocene-scale sediment budget for the Blue Earth River, we used the valley excavation data to constrain bluff erosion rates at half of the present rates. Ravine erosion rates were estimated by taking the total volume of sediment removed via ravine erosion, converting it to mass, and taking an average over 13,500 years. The resulting ravine yield is 50% of the modern yield on the Blue Earth and Watonwan, so ravine yields were set to 50% modern rates. Streambank rates are less constrained and were set the same as the Le Sueur River pre-settlement rates (modern rates above the knickzone, 50% modern within the knickzone, and 33% modern below knickzone). Upland erosion rates are assumed to be essentially zero (set to 1% of modern rates) given pre-settlement prairie vegetation and low gradient relief found in most of the Blue Earth watershed uplands. Relative erosion rates, depicted as a fraction of the modern, were set the same in the Watonwan watershed as the Blue Earth watershed. The Holocene sediment budget can be accessed on the "GBER budget" page by toggling the "time frame flag" in cell A55. We used the best-fit bluff scenario for each major tributary (scenario 2 for Le Sueur and 3 for Blue Earth and Watonwan) to compare predictions for Holocene loads vs. modern loads. Comparing predictions of loads at the mouth of the Greater Blue Earth watershed, the predicted Holocene load is 290,000 Mg/yr or 53% of the modern predicted load of 542,000 Mg/yr. At the three gages (Le Sueur, Blue Earth, and Watonwan), the predicted Holocene average load was 238,000 Mg/yr, or 45% of the averaged measured TSS load (2000-2013) of 533,000 Mg/yr.

5.6 Sediment Budget Summary

The sediment budget presented here was motivated by the need to understand sediment sources causing high turbidity in the Minnesota River. Work in Lake Pepin by Engstrom et al. (2009) shows that fine sediment deposition rates have increased ten-fold since the early 1800s. Most of the fine sediment deposited in Lake Pepin now comes from near-channel sediment sources (Belmont et al., 2011), primarily the high bluffs that line the incised lower valleys of major tributaries (Sekely et al., 2002; Gran et al., 2009; Belmont et al., 2011). The sediment budget developed here for the GBER watershed has comparable results to these earlier studies.

Bluffs are the dominant source of sediment in the GBER watershed. Uplands and streambanks are the next largest source of sediment, with ravines making up the smallest share of the 4 major sources. It is important to note that the GBER budget presented here separates sources and sinks. Much of the sediment derived from streambanks is balanced by deposition in the floodplain, particularly in the upper watersheds. Most of the sediment deposited in lakes comes from upland erosion, although lake deposition rates are not high enough to trap the majority of the upland sediment.

Most of the work presented here from Bevis (2015) focuses on bluffs because they are such an important source. Bluff contributions are a function of both bluff extent and erosion rate. Because bluff extents are more variable across watersheds than bluff erosion rates, careful work is required to accurately delineate extents for a budget. Bluffs are largest and most frequent below GBER watershed knickpoints; they are smaller and less common upstream. Bluff erosion rates, a function of channel migration and bluff crest retreat rates, are also highest below knickpoints. Channel migration rates were slower (but not zero) where bedrock outcropped along the channel, and faster in locations where higher inputs of bedload material are expected. Bedload is concentrated in GBE river channels by erosion of till, at channel confluences, and where glacio-fluvial sediments are present, all of which are common below knickpoints.

We explored sediment budget sensitivity to many potential improvements and adjustments. We found that fine sediment load from bluffs is primarily a function of bluff extent and erosion rate; other factors, like the extent of Pleistocene alluvial deposits, have minor effects only. Even though coarse bedload may affect channel migration rates, adjustments for differences in sediment texture and bulk density from terraces vs. valley bluffs or from glaciofluvial sediments more present in the Watonwan River had little effect on total fine sediment load estimates. Vegetation cover was not an important predictive element: the current bluff vegetation state has little correlation with long-term bluff erosion rates and thus time spent mapping vegetation cover on bluffs was not useful. Different methods of bluff erosion rate interpolation and extrapolation resulted in similar fine sediment load from GBER watershed bluffs, suggesting that elaborate extrapolation techniques are not as useful as detailed work in delineating bluff extent. We advocate extrapolating subwatershed-scale bluff erosion rates. Sediment fingerprinting was useful in obtaining basin-integrated upland sediment yields, and there are differences in upland yields across the GBER watershed. Storage is an important part of the budget, with 20% of the sediment eroded in the GBER watershed is stored on floodplains and in lakes, and should be included in a sediment budget format.

The original Le Sueur sediment budget came within 10% of the average TSS loads at the Red Jacket gage from 2000-2010. In this version of the Le Sueur budget, the total predicted loads declined. More care was taken in this budget to delineate only bluff extents actively along the channel, and bluff trimming to not include portions that were disconnected by floodplains was more aggressive. This budget also extended lidar data analysis into the entire watershed (not just Blue Earth County), and thus some bluff and ravine sources higher up in morainal complexes were included that might not have been in the original budget. Likewise, lake deposition was included. The net effect of all of these changes was to lower the predicted sediment loads on the Le Sueur.

The Blue Earth and Watonwan sediment budgets tended to overpredict sediment loads, with the problem more pronounced in the Watonwan watershed. With the Watonwan River, there are a significant number of ravines and bluffs that lie in the far upper basin. They tend to be much smaller and more vegetated than bluffs further downstream. By using bluff air photo analysis and ravine load monitoring from sites well within the knickzone to determine rates to extrapolate into the far upper watershed, it is likely that these rates were over-estimated. Given that fingerprinting data indicate uplands comprise 77-83% of the total load at Garden City, that leaves very little load left to account for with bluffs and ravines (<7,000 Mg). Most of the streambank contributions are balanced by deposition.

By developing a budget for all three major watersheds in the GBER, we can also examine commonalities and differences between the three basins. Upland rates varied some across the watershed, with the Blue Earth River having higher upland yields than the Watonwan, Cobb, Maple, and Le Sueur Rivers. The Watonwan overall had lower sediment loading than the other two watersheds. In part, this is due to the location of the mouth of Watonwan, far upstream and near the top of the knickzone, leading to a much shorter incised valley length and less sediment derived from bluffs and streambanks.

The sediment budget produced here was intended to both provide information on the dominant sources, sinks, and pathways for fine sediment moving through the Greater Blue Earth River basin, allow for comparisons of some of the differences between the Le Sueur, Blue Earth, and Watonwan Rivers, and provide information to help constrain the Management Options Simulation Model (MOSM). It both provides the framework for MOSM and acts as a check on MOSM results to determine if they are reasonable and scientifically-sound.

6 Simulation Model

6.1 Introduction

In this section, we present the management option simulation model (MOSM). In addition, we describe a number of supporting research actions for the development of MOSM: evaluation of sediment delivery and loading from various sources, simulation of stream flow for different water conservation scenarios, and development of the management options (MOs) database.

MOSM is a reduced-complexity simulation model that evaluates both river discharge and sediment loading, and predicts changes in the watershed-wide sediment load as result of implementation of different MOs. The intention of the model is to understand the effects of various environmental intervention strategies at the watershed scale to guide planning and investment to address the water quality degradation due to excess sediment.

In the following subsections, we describe the development of Topofilter to estimate sediment delivery ratios and loads (6.2), evaluation of sediment loading from near-channel sources in the incised zone as a function of peak river discharge (6.3), utilizing SWAT outputs in the river routing algorithm (6.4), development of MO database (6.5-6.7), structure and function of MOSM (6.8), and deliverable associated with MOSM (6.9). The text presented in this section is revised directly from Se Jong Cho's PhD thesis, and the reader is directed there for more detail on the development of MOSM and the supporting research actions.

6.2 Sediment sources and routing through Topofilter simulation

Topographic filter simulation model (Topofilter) presents a robust analytical framework to predict sediment loading from agricultural nonpoint sources (NPSs), and to identify the dominant source areas in a watershed. The analysis includes NPS sediment loading from agricultural fields and near-channel sources (NCSs) including ravines, streambanks, and bluffs. Model outputs include spatially-explicit and stochastic sediment delivery ratios (SDR) on fields (SDRf) and in streams (SDRs) that provide a foundation for MOSM's sediment loading algorithm.

Topofilter takes advantage of two exceptional data sources: soil production rates mapped at the field-scale and high-resolution digital topography. Combined with sediment loading records at stream gages and spatial analysis computational tools, these data sources present an opportunity to evaluate the topographic influences on the fate and transport of NPS sediment. Specifically, Topofilter evaluates the transit of sediment on fields and in streams to the watershed outlet, linking the sediment erosion rates (SE) at the agricultural field scale and NCSs to the observed sediment loading (SL) at various gage locations in the watershed.

We explain here how Topofilter works in the Le Sueur River basin. Five gage locations define Topofilter subwatersheds (Toposhed) as illustrated by the map in Figure 6.1(a): Upper Maple (UM), Main Cobb (MC), Little Cobb (LC), Upper Le Sueur (UL), and Le Sueur River Basin (LSRB) outlet (LO); and Figure 6.1(b): Above Winnebago (AW), Upper Watonwan (UW), Winnebago to Knick (WK), Knick to BE Outlet (KO). In the following discussion, we use the LSRB to illustrate model algorithms and outputs.

Topofilter evaluates sediment delivery within each subbasin through a simple model structure intended to capture the effect of topography (i.e., flow length and gradient) on sediment delivery. Consequently, Topofilter connects the enormous data availability on soil loss from agricultural fields using USLE (>11,000 plot-years of data across the US (Wischmeier and Smith, 1978)) and sediment production rates from NCSs quantified using the integrated sediment budget (Gran et al., 2011) to the surface topography to evaluate sediment delivery and consequent annual SL rate at each of the Toposhed outlets.

A stochastic simulation approach is used according to the general concept of equifinality and model conditioning (Beven, 2001). The model conditioning process identifies a whole set of plausible parameter values and the interaction among parameters at each Toposhed. As a result, we can assess how different ranges of parameter values on the corresponding topographic variable impact the simulation outputs. Because we include a range of plausible parameter values in the analysis given the probability distribution of the observed data, the model conditioning process yields more robust solutions accounting for multiple sources of uncertainty (e.g., assumptions made about model structure, observational error, and natural variability).

Figure 6.1(a) illustrates the conceptual approach of Topofilter (upper left figure) to condition model parameters in order to determine all plausible SDRf and SDRs values (right top and bottom figures) in each of the Topofilter modeling unit, sediment subbasin (SEDSB, shown in bottom left figure).

As illustrated in Figure 6.1 (a), model outputs include sets of plausible SDRf values and corresponding probability distribution parameters and sets of plausible SDRs values and corresponding parameter space over all SEDSBs. These outputs are used in MOSM to calculate stochastic SDR parameters and corresponding SLs for every iteration in a Monte Carlo (MC) simulation.

The distribution of plausible SDRf values is calculated by conditioning the parameters $a1$ and $b1$. The model parameter is conditioned by comparing the estimated sediment loading against the observed data. SDRf is calculated for all field raster cells *i* of a SEDSB *j*:

$$SDRf_{ij} = \exp(a1 \left(\frac{dE}{dL}\right)_{ij}^{b1} L_{ij}) \quad (6.1)$$

Mean annual sediment input from the agricultural field source to stream network of the SEDSB j ($SI_{F\,j}$) is calculated by summing the product of SE and SDRf over all field cells *i*. Then the average SDRf over the SEDSB *j* is calculated:

$$SI_{F\,j} = \sum_{i=1}^{I_j} SDRf_{ij} * SE_{ij} \ \forall j \quad (6.2)$$

$$SDRf_j = \frac{SI_{F\,j}}{\sum_{i=1}^{I_j} SE_{ij}} \ \ \forall j \quad (6.3)$$

Consequently, Topofilter provides a population of SDRf values at each SEDSB. For instance, in the UM Toposhed, we illustrate the SDRf outputs for select SEDSBs shown in Figure 6.2, highlighted in yellow. Figure 6.3 shows the cumulative density function (CDF) of all plausible SDRf values in these SEDSBs. The population of SDRf values varies from one SEDSB to another based on its areal extent, location in relation to the Toposhed outlet, and gradient. The plot of CDFs reveals that the SDRf is generally smaller for larger SEDSBs where flow length to stream network is generally longer (e.g., SEDSB 1084) and is greater for smaller SEDSB where flow length is generally shorter (e.g., SEDSB 890). However, the distribution of SDRf in the SEDSBs near the Toposhed outlets, where gradient is steeper due to the presence of the knickpoints marking the incised zone, areal extent of the SEDSB is less important than the gradient in determining the SDRf values.

(a)

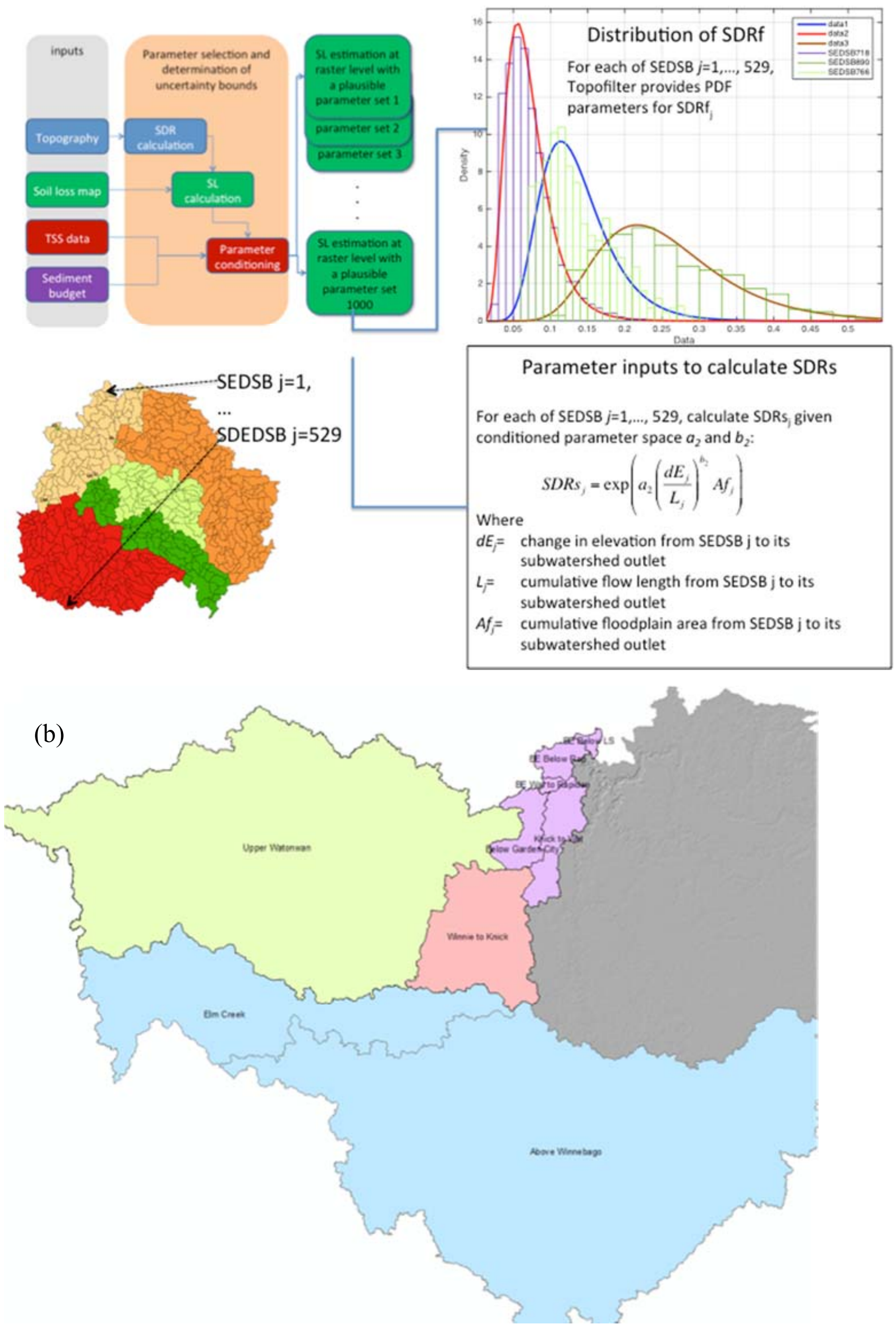

Figure 6.1 (a): Topofilter model consists of 529 sediment subbasins (SEDSBs) over five Toposheds in the LSRB, UM (red), MC (green), LC (light green), UL (orange), and LO (tan). Plausible SDRf and SDRs values are calculated according to observed sediment loading at gage located at the outlet of each topographic subwatershed (Toposhed) of the Le Sueur River Basin (LSRB). (b): Toposhed delineation for the entire GBERB consists of AB (blue), UW (green), WK (red), and KO (purple), in which plausible SDRf and SDRs are calculated or all SEDSBs. There are total of 1,096 SEDSBs in AB, UW, WK, and KO.

Topofilter analysis revealed that field raster cells near the stream network generally have larger SDRf values because they have smaller flow lengths and steeper gradient created from the stream network compared to the further upland areas. It is important to recognize that the areas proximal to the stream network (A_p) have larger SDRf values than the areas further away (A_f) when evaluating different management options. For example, buffer strip management options (BFMO) would treat the sediment loading from A_p compared to other field management options such as agricultural field management options (AFMO) that would be implemented further inland. Thus, we use the Topofilter to calculate SDRf in A_p (SDR_{fp}) and in A_f (SDR_{ff}), and their distribution parameters to be implemented in MOSM.

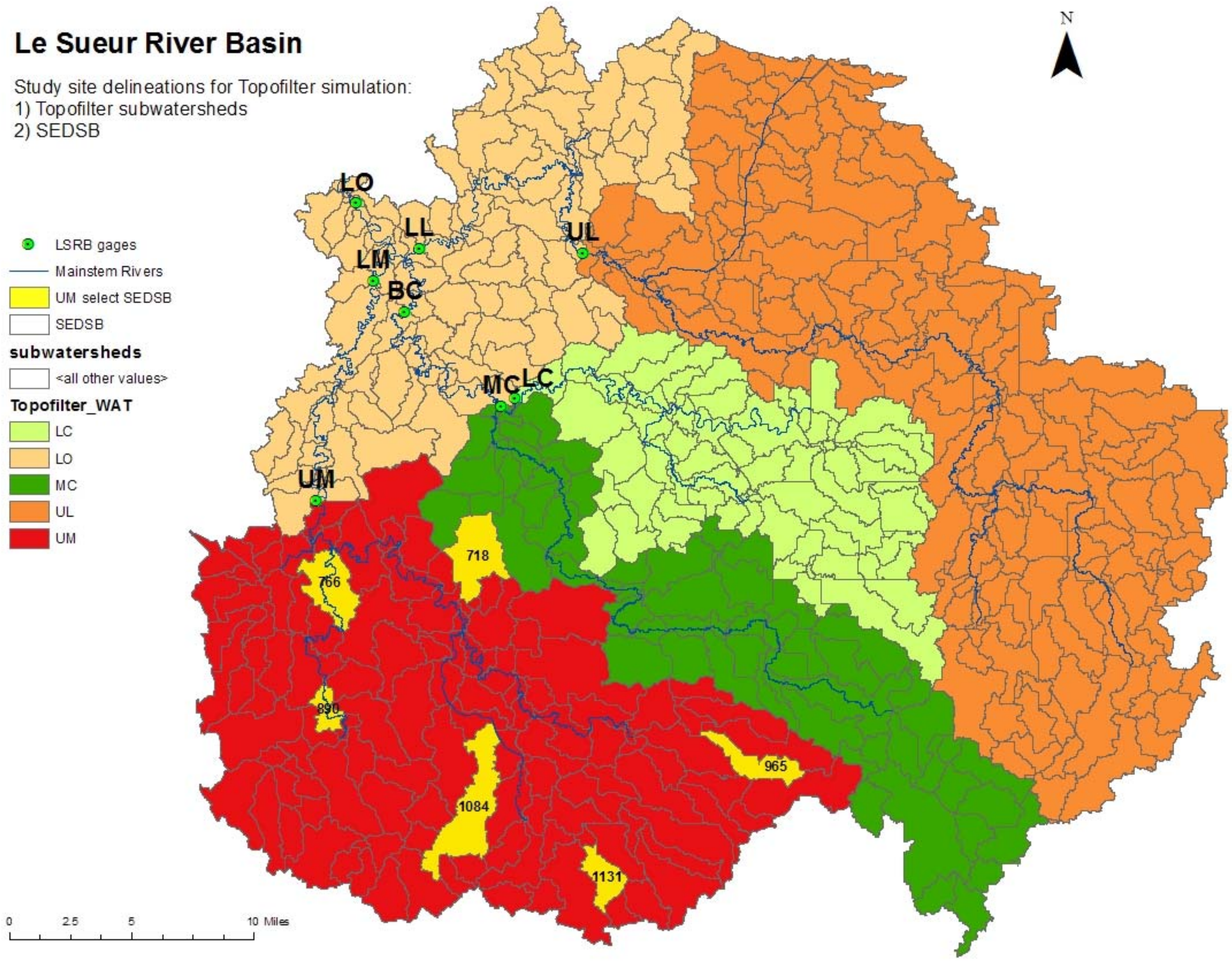

Figure 6.2: LSRB study site delineation for Topofilter simulation including five Toposheds defined by the five gage locations and SEDSBs defined by reach extent. Gages consists of upper gages at Upper Maple (UM), Main Cobb (MC), Little Cobb (LC), and Upper Le Sueur (UL), lower gages at Lower Maple (LM), Big Cobb (BC), and Lower Le Sueur (LL), and gage at the outlet of Le Sueur (LO). This figure also shows the selected SEDSBs in the UM to illustrate selected model results.

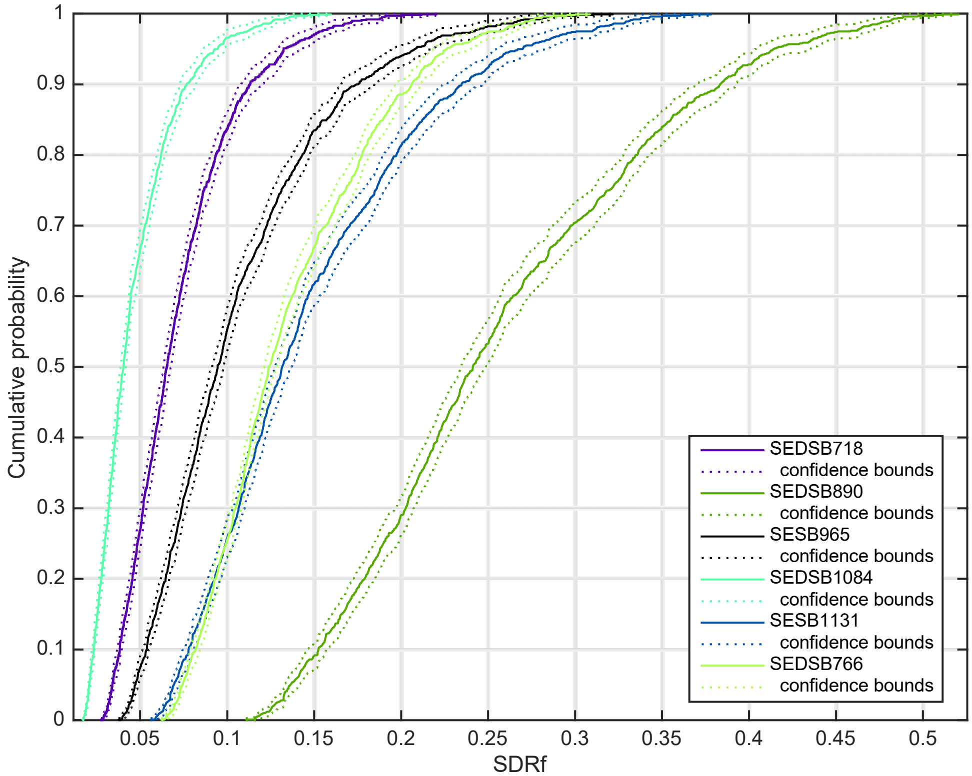

Figure 6.3: Cumulative probability distribution of SDRf for SEDSBs shown in Figure 6.2

In addition to the mean annual sediment input rate from the field (SI_F), we quantified the mean annual sediment input rate from streambanks (SI_S), ravines (SI_R), and bluffs (SI_B) by summing over the mean annual sediment production rates from these NCSs from each individual SEDSB. Mean annual sediment production rates from the NCSs are allocated using the integrated sediment budget for the LSRB and GBERB (Gran et al., 2011; Chapter 5).

The reach network of the SEDSBs is a conduit of sediment inputs from field, stream, ravines, and bluffs. SDRs expresses the proportion of the sediment inputs from these sources that arrives at the Toposhed outlets: UM, MC, LC, UL, and LO. SDRs is a function of flow length in the stream (L_j), gradient $\left(dE_j\right)$, and floodplain area (Af_j) from any given SEDSB j to the Toposhed outlets:

$$SDRs_j = \exp\left(a2\left(\frac{dE_j}{L_j}\right)^{b2} Af_j\right) \quad (6.4)$$

The probability distribution of SDRs values depends strongly on the location of the SEDSB. For example, the Monte Carlo realizations of SDRs values in SEDSB 766, located very near the Toposhed outlet, are larger than other sampled SEDSBs as shown in Figure 6.4. In fact, the population of SDRs values recedes as we move further away from the mouth of the Toposhed, from SEDSB766, 890, 718, 1084, 1131, then 965.

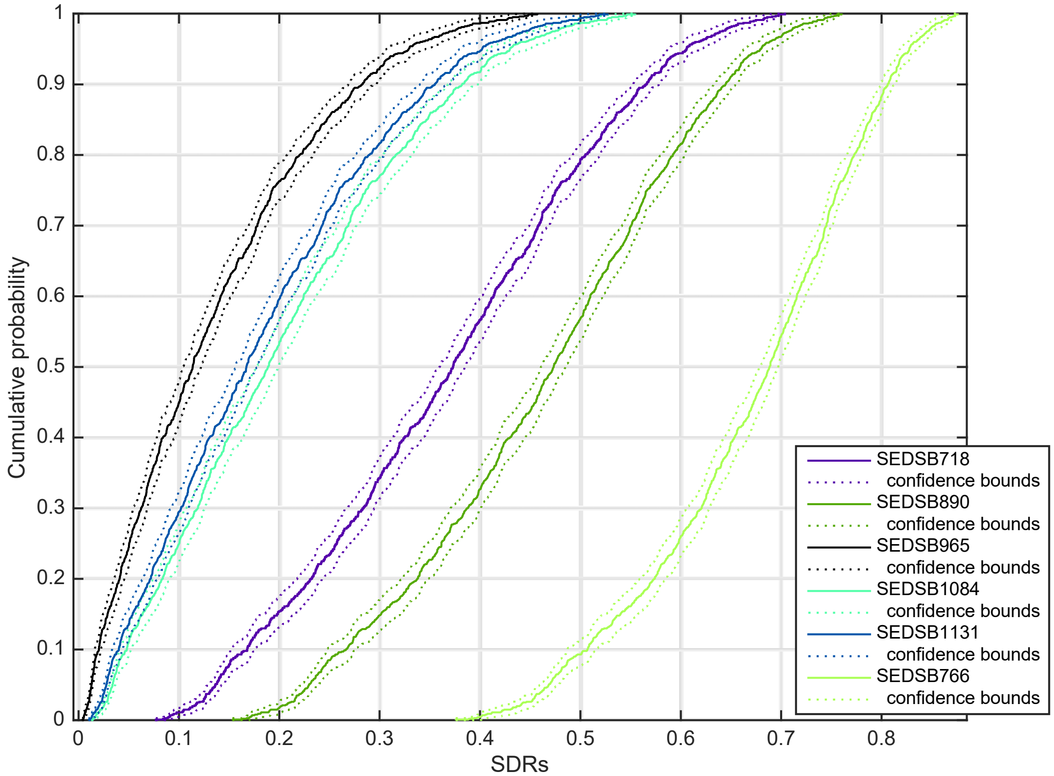

Figure 6.4: Cumulative probability distributions of SDRs for SEDSBs show in Figure 6.2

The outputs from this analysis inform the MOSM in the sediment loading simulation: SDRf and SDRs distribution outputs for each SEDSB are used in the MOSM to simulate stochastic sediment loading and effects of MOs using MC simulation over all SEDSBs in the LSRB.

6.3 Near channel source sediment loading and peak river discharge

Bluffs have been identified in the sediment budget as the largest source of sediment in the GBERB. River discharge has been increasing in the watershed (Novotny and Stefan, 2007), suggesting that an important management option for reducing sediment loading is a reduction in river discharge. This, a key element of MOSM is a relation between river discharge and the rate of sediment supply from near-channel sources, such that it is possible to evaluate the tradeoff between management options that store water in the uplands to reduce peak river discharge versus direct stabilization of streambanks and bluffs.

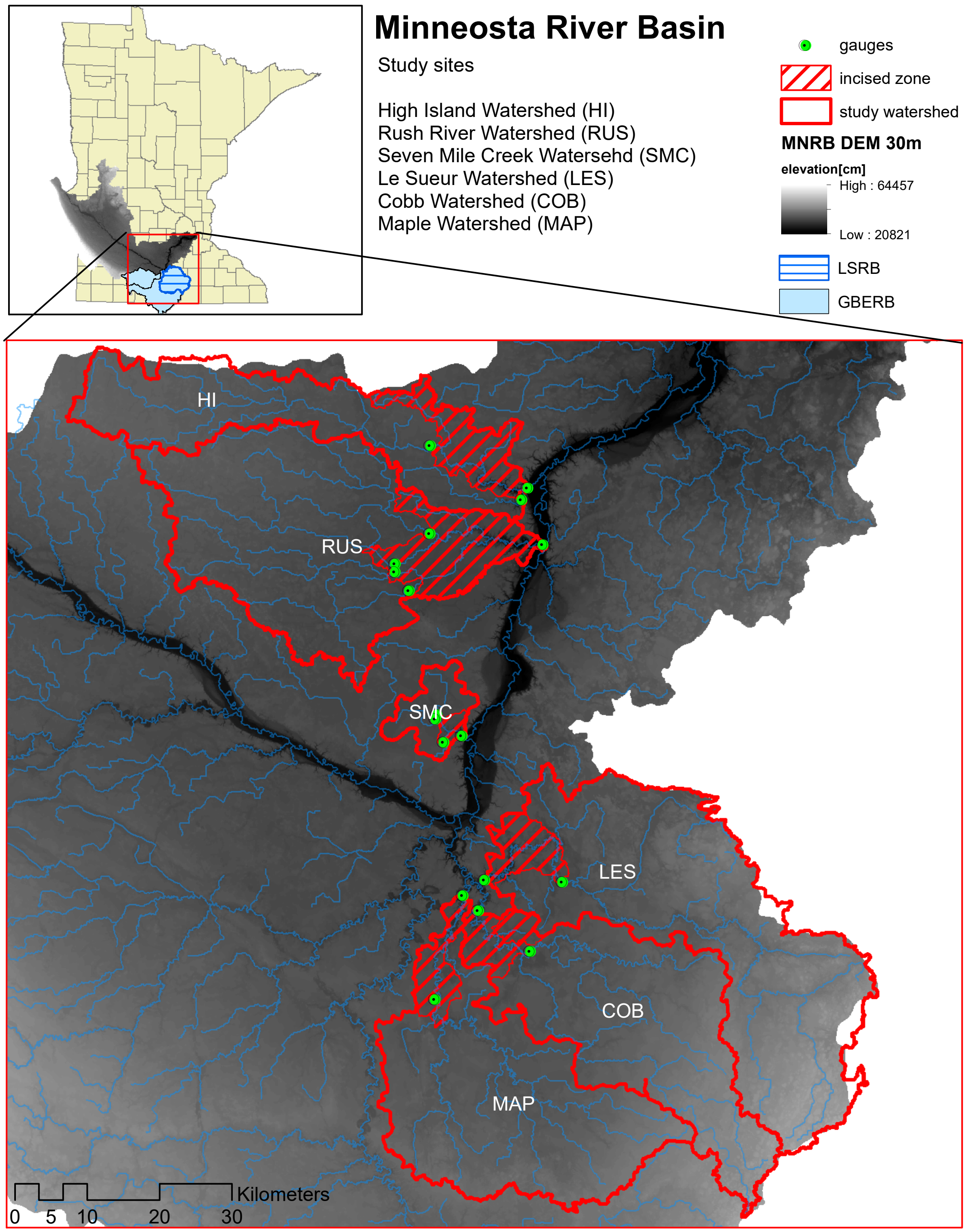

Figure 6.5: Study sites and their locations with indications of the incised zones and the gage locations

In order to develop an estimate for sediment contributions from near-channel sources, we took advantage of the presence of two gages bracketing most or all of the incised zone on each of six streams. Maple (MAP), Cobb (COB), and Le Sueur (LES), subwatersheds of the LSRB, have definable incised zone created from the base level drop to the Minnesota River valley. High Island (HI), Rush (RUS), and Seven Mile Creek (SMC) drain to the Minnesota River northeast of the LSRB (Figure 6.5). These subwatersheds have similarly developed incised zones. Thus multiple subwatersheds, within and outside of the GBERB, are included in the analysis to develop a general relationship between peak river discharge and sediment loading from the incised zones; however, the analysis is focused on quantifying and verifying the sediment loading in the LSRB.

We used water quality data from gages that bracket the incised zones of the study subwatersheds. The water quality data are collected during various storm events from 2005 to 2012, and include measurements of total suspended solid (TSS) and river discharge. We extracted these instantaneous sediment loading and river discharge readings for all monitored storm events and compiled the upper and lower gage data by date and time of data collection. The length of the streambanks and bluffs in the incised zone is used to normalize the sediment loading observations, and the upstream drainage area is used to normalize the river discharge observations in order to compare these multiple subwatersheds. Although the amount of water discharge and sediment loading varies among the watershed, Figure 6.6 shows that the scaled values of sediment loading vs. river discharge collapse to a common trend.

In general, sediment loading from NCS is negligible for low to moderate flow events. Negative sediment loading indicates that there is more sediment entering the incised zone than leaving. In other words, sediment is being stored in the incised zone. There are 175 observations of negative sediment loading in the study period (i.e., 25% occurrences). However, as the river discharge increases, sediment loading dramatically increases for all rivers (we refer to this as “hockey stick relation”). The red dotted line in Figure 6.6 uses a threshold river discharge (Qthreshold) of 0.01 $m^3/s\text{-}km^2$ at which sediment loading begins to increase dramatically with the river discharge. The flow duration analysis indicates that Maple, Cobb, and Le Sueur rivers have 30% exceedance probabilities at the Qthreshold of 0.01 $m^3/s\text{-}km^2$ (about 30% chance that Qthreshold is equaled or exceeded).

Consequently, we developed a predictive model of sediment loading from streambanks and bluffs in the incised zone as a function of river discharge exceeding the Qthreshold (i.e., Q>Qthreshold). Figure 6.7 shows the power function regression model (“hockey stick model”) derived from the compiled water quality data.

Subsequently, applying continuous river discharge data (i.e., 15 minute interval river discharge data collected from 2003 to 2011 at the lower gages) to the hockey stick model, we estimated the mean annual sediment loading from near-channel sources in the incised zone. The estimated mean annual sediment loading using the hockey stick model is compared to the sediment budget results in Figure 6.8.

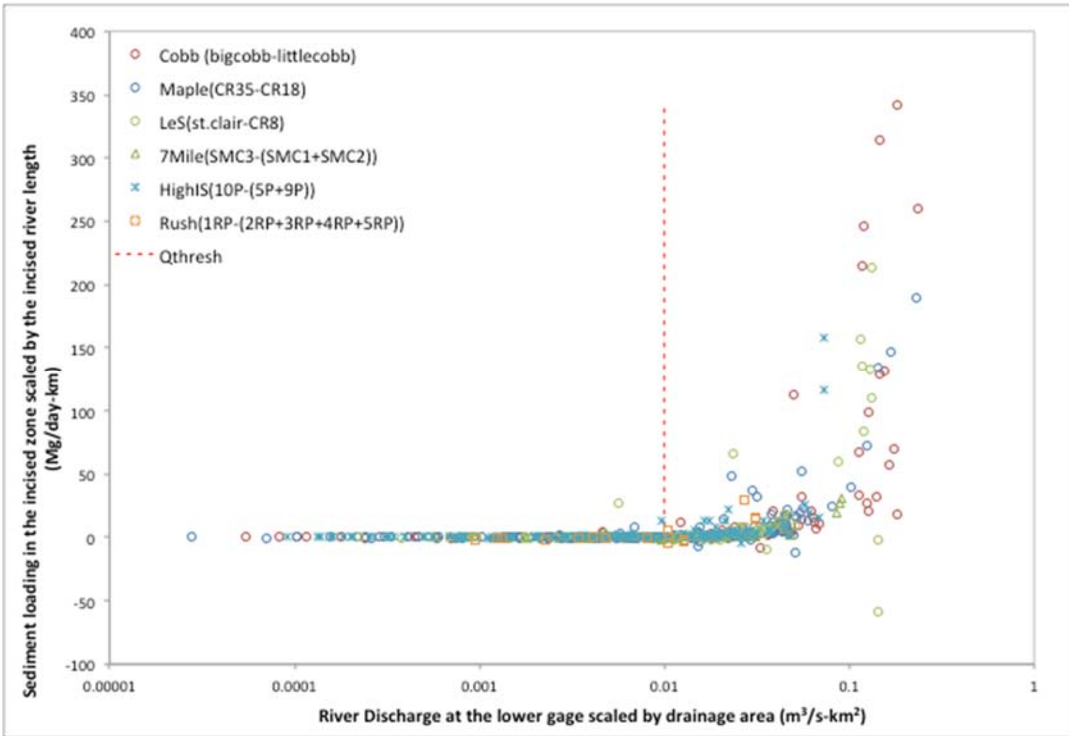

Figure 6.6: Sediment loading from NCSs in the incised zone normalized by the mainstem river length as a function of river discharge normalized by the upstream drainage area shows that sediment loading responds to peak river discharge, particularly when the river discharge exceed the threshold point marked by the red dotted line.

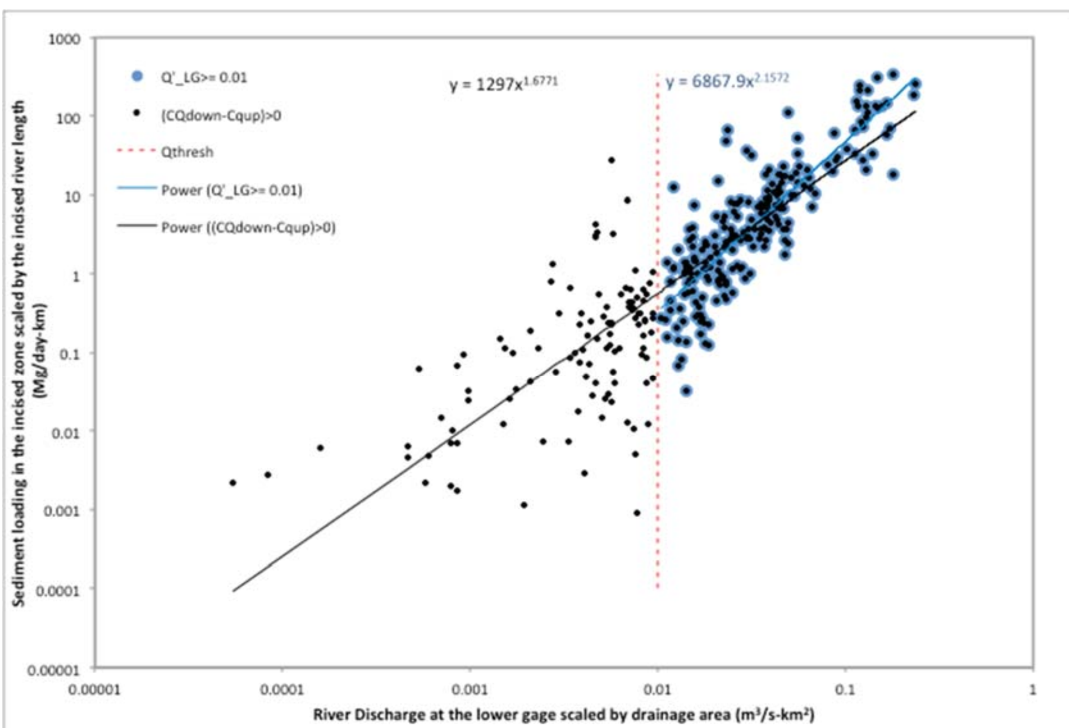

Figure 6.7: River discharge and sediment loading on log-log scale with fitted power regression

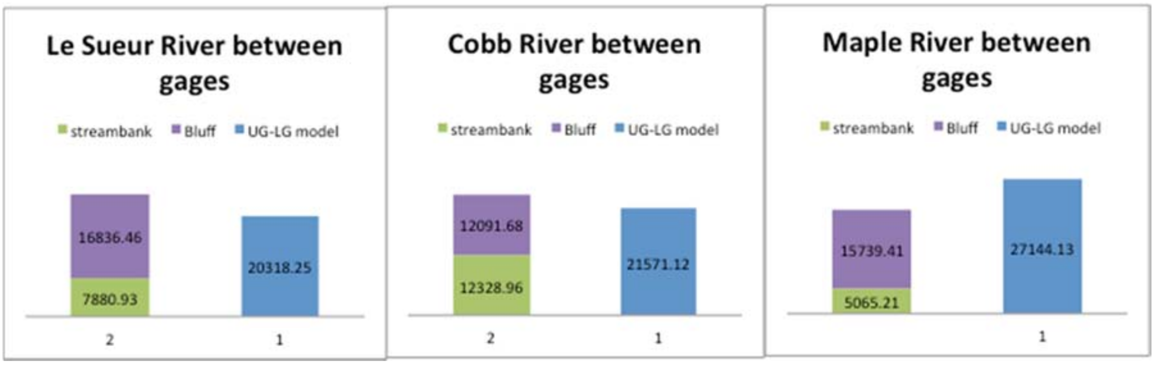

Figure 6.8: Model estimate (blue column on right) vs. sediment budget estimates (purple and green column on left) of sediment loading from bluffs in the incised zone

The hockey stick relation indicates that sediment loading from streambanks and bluffs may be reduced if the duration of flows larger than Qthreshold can be reduced. Thus, the results of this analysis can be used to evaluate the effects of water conservation management options (e.g., wetland restoration, water retention ponds, etc.) on sediment loading from streambanks and bluffs. For example, Soil and Water Assessment Tool (SWAT) simulation analysis demonstrated that wetland restoration with its capacity to store water in the uplands can mitigate peak river discharge (Liu et al., 2008; Mitchell, 2015).

Therefore, the hockey stick model coupled with a stream flow routing model can be used to predict the sediment loading reduction from streambanks and bluffs by implementing water conservation management options. In section 6.4, we describe the stream flow routing algorithm built in MOSM, then in section 6.8.3, we describe the application of hockey stick model with the stream flow routing algorithm to quantify the overall sediment loading reduction from water conservation measures.

6.4 Streamflow routing

We developed a hydrologic routing algorithm in MOSM to simulate the daily hydrographs before and after water conservation management. Then, we apply the hockey stick model to estimate the sediment loading reduction from NCSs

MOSM accesses the output of water yield data at each hydro subbasin (HYDSB) at a daily time step from 1/1/1985 to 12/31/2009 from a calibrated 30-subbasin SWAT model. HYDSB uses the same spatial delineation as the SWAT model's 30 subbasins in the LSRBS. Water yield data represents the net amount of water that leaves the HYDSB and contributes to stream flow in the reach during each time step (Arnold et al., 2011).

The water routing algorithm simulates the changes in time and magnitude of peak river discharge as a result of implementing water conservation management options (water conservation MO (WCMO) and in-channel MO (ICMO), see section 6.5) in the watershed. In this section, we describe the *level pool routing method* to estimate the effects of water storage on the daily water yield values at each HYDSB, and the *Muskingum-Cunge method* to route the water from each HYDSB to downstream HYDSBs all the way to the watershed outlet.

6.4.1 Storage-outflow calculation: level pool routing

The inflow hydrograph of an average water storage structure is calculated from a calibrated SWAT model's water yield data. Consistent with the lumped approach used in SWAT, the water yield is uniformly distributed over the HYDSB; hence, the inflow to the water storage structure consists of the water yield occurring in its drainage area, calculated as a proportion of the structure's drainage area over the total area of the HYDSB. Drainage area of WCMO is calculated from a linear regression defining water storage site's drainage area as a function of its surface area (Mitchell, 2015). Here, the drainage area is calculated from flow accumulation values sampled at the farthest downstream outlets of the sampled candidate water storage sites. Drainage area of ICMO is calculated in a similar manner but the coefficient for the linear relationship is a user input in MOSM where the drainage area is calculated as some multiple of its surface area.

The outflow from a water storage structure depends on the length of crest (L) and the total head over the crest (*H*). For WCMO, we use the spillway discharge equation: $Q = CLH^{3/2}$ where C is a variable coefficient of discharge that the user can specify in MOSM for different outflow structures. Effective length, L, will depend on wetland spillway design. Thus, we assigned a user-input parameter α in MOSM that determines the fraction of WCMO's circumference where water would spill out. Head over the storage structure, H, is calculated from the inflow of current time step and outflow of the previous time step and the user-inputted dimensions of the water storage structure. Water loss from seepage and evaporation is allowed given the user-inputted hydraulic conductivity and evapotranspiration rate.

For ICMO, the outflow depends on the user-specified design weir width (WW) and design depth over which water will flow out during significant flow events. During low to moderate flow days; the water flows out through a notch (smaller opening in the weir). Notch design can be specified in the MOSM including the design notch width (NW) and notch height (NH).

6.4.2 River routing: Muskingum-Cunge method

After calculating the water yield from each HYDSB, the water is routed downstream. Lumped hydrologic routing method is used to route water through the river network to the watershed outlet.

Muskingum-Cunge (Mg-Cg) method is used to estimate the routing parameters (Chow et al., 1988). *K* expresses the travel time of a flood wave through the length of reach (Δx) in a HYDSB. *X* is a weighting factor ranging [0, 0.5] where *X*=0 indicates reservoir-type storage with no wedge and no backwater, and *X*=0.5 indicates a full wedge storage.

$$K = \frac{\Delta x}{c_k} = \frac{\Delta x}{\frac{dQ}{dA}} \qquad (6.5)$$

$$X = \frac{1}{2}\left(1 - \frac{Q}{Bc_k S_o \Delta x}\right) \qquad (6.6)$$

To express the celerity (c_k) in [6.5] and [6.7] and the weighting factor in [6.6] in terms of quantifiable hydraulic geometric measures of the river system, we substitute the expression for river discharge (Q) with the Manning's formula [S.I.] in [6.8] given the hydraulic geometry inputs (*n*= Manning's n; *A*= cross section area; *h*= depth of water; *P*= wetted perimeter; S_o= slope of the channel; *B*=channel width) at each HYDSB, sampled and extrapolated from the surveyed river cross sections of the Maple and Le Sueur Rivers (Belmont, 2011). Subsequently, [6.9] expresses the unit river discharge in terms of hydraulic geometry of the channels:

$$c_k = \frac{dQ}{dA} = \frac{d}{dA}(Q) \qquad (6.7)$$

$$Q = \frac{S_o^{\frac{1}{2}}}{n} A R^{\frac{2}{3}} = \frac{S_o^{\frac{1}{2}}}{nP^{\frac{2}{3}}} A^{\frac{5}{3}} \text{ where } R = \frac{A}{P} \qquad (6.8)$$

$$\frac{d}{dA}(Q) = \frac{5}{3}\left(\frac{S_o^{\frac{1}{2}}}{nP^{\frac{2}{3}}}\right)A^{\frac{2}{3}} \approx \frac{5}{3}\left(\frac{S_o^{\frac{1}{2}}h^{\frac{2}{3}}}{n}\right) \text{for a wide channel} \quad (6.9)$$

Substituting c_k expressed in terms of hydraulic geometry:

$$K = \frac{\Delta x}{c_k} = \frac{\Delta x}{\frac{5}{3}\left(\frac{S_o^{\frac{1}{2}}h^{\frac{2}{3}}}{n}\right)} \quad (6.10)$$

$$X = \frac{1}{2}\left(1 - \frac{A^{\frac{5}{3}}}{nP^{\frac{2}{3}}Bc_kS_o^{\frac{1}{2}}\Delta x}\right) \quad (6.11)$$

Subsequently, the outflow in the one time-step forward, Q_{j+1} is expressed with the Muskingum coefficients, *C1, C2*, and *C3*:

$$Q_{j+1} = C_1 I_{j+1} + C_2 I_j + C_3 Q_j \quad (6.12)$$

where the Muskingum coefficients are calculated using the terms in [6.10] and [6.11] for time step, Δt:

$$C_1 = \frac{\Delta t - 2KX}{2K(1-X)+\Delta t} \quad (6.13)$$

$$C_2 = \frac{\Delta t + 2KX}{2K(1-X)+\Delta t} \quad (6.14)$$

$$C_3 = \frac{2KX(1-X) - \Delta t}{2K(1-X)+\Delta t} \quad (6.15)$$

6.4.3 River routing map

Water yield from each HYDSB is routed to its downstream HYDSB using the Muskingum-Cunge method along the river network until reaching the watershed outlet. For instance, along the Maple River before the confluence with the Le Sueur River, there are nine HYDSBs as shown in Figure 6.9. The model begins the water routing from the uppermost HYDSBs (e.g., HYDSB 30, 28, 29, and 23 in Figure 6.6), and the downstream HYDSBs (e.g., HYDSB 25) collect inflow from all upstream HYDSBs (e.g., HYDSBs 30 and 28) and route the water yield downstream all the way to the watershed outlet.

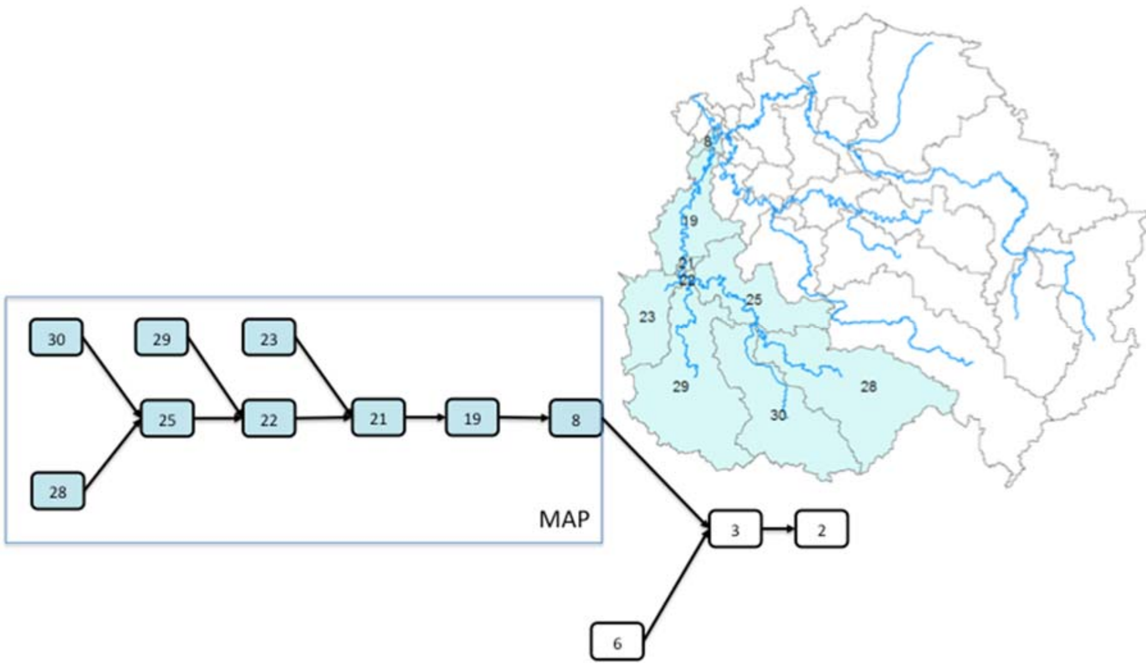

Figure 6.9: Water routing along the Maple River HYDSB before the confluence with the Le Sueur River in HYDSB 3

6.5 Management options

The management option (MO) database was developed through a collaborative process. We assembled an initial list for a wide array of options; then, through discussions with stakeholders this list was filtered to contain only the relevant management options for the study site. For modeling purposes, these filtered MOs were sorted into management types based on how they physically reduce erosion and/or trap sediment. The final MO types used in the MOSM are defined in Table 6.1, along with the primary mechanism through which they reduce erosion.

Subsequently, we conducted spatial analysis to determine the available spatial extent of MOs (section 6.6), and conducted research, interviews, and literature review to determine the MO effectiveness and cost (section 6.7). MOSM accesses the MO database to allocate MOs based on user inputs and evaluate their impacts on the overall sediment loading (section 6.8).

The goal of this objective was to collect data on management options, cost, effectiveness, and potential spatial extent within the Greater Blue Earth River watershed. The process was iterative in that data were assembled for a wide array of management options, and this list was then reduced based on conversations with stakeholders at semi-annual meetings. For modelling purposes, management options were sorted into categories based on how they physically prevent erosion and/or trap sediment. The final management option (MO) categories used in MOSM are defined in Table 6.5, along with the primary mechanism through which they reduce erosion. For each of these general categories, installation costs, maintenance costs, and estimated lifespan are noted in Table 6.6. It was very difficult to find robust data on effectiveness, so we utilize a sliding scale in the MOSM model that allows users to input estimated effectiveness for each management option. Likewise, many MOs, particularly the newer techniques, lacked information on estimated lifespans, and the lifespan will affect annualized costs. We carried out additional research on the effectiveness of water control management options (WCMOs) through detailed simulations using the Soil and Water Assessment Tool (SWAT) model. These are summarized in Mitchell (2015) and Mitchell et al. (*in prep.*).

Table 6.1: Description of the MO categories used in the MOSM and the primary function in reducing sediment loading evaluated by the model

MO Types	Definition	Location of implementation	Example MO	Primary Function in Sediment Reduction
TLMO	Tillage MO	Field	Conservation tillage, reduced tillage	-Reduce erosion on fields
AFMO	Agricultural field erosion MO	Field	Grassed water ways	-Trap sediment on fields (reduce sediment delivery ratio)
WCMO	Water control MO	Field	Water Retention ponds, wetland restoration	-Reduce flow to reduce near-channel erosion -Trap sediment on fields
ICMO	In-channel storage MO	Channel	Temporary water storage in ditches	-Reduce flow to reduce near-channel erosion
BFMO	Buffer MO	Field near channel	Buffer strips along channels	-Trap sediment (reduce sediment delivery ratio)
RAMO	Ravine MO	Ravines	Ravine tip stabilization to reduce branch growth	-Reduce erosion from ravines
NCMO	Near-channel MO	Bluffs	Bluff stabilization, toe protection	-Reduce erosion from bluffs

6.5.1 TLMO – Sediment conservation measure

Tillage management options are generally based on leaving some crop residue on the field in order to reduce erosion and trap sediment. Tillage as a management option is classified and studied in many ways throughout the country, including moldboard plowing, sweep tillage, chisel plowing, ridge tillage, strip tillage, mulch tillage, minimum tillage, disk tillage, and no till (Zhou et al., 2009; Moncrief et al., 1997; Penn State, 2016;Uri, 2000). In MOSM, we provide three different types of tillage management: conventional, reduced, and conservation tillage, explained in more detail below.

6.5.1.1 Conventional Tillage

The practice of fully overturning the fields in the spring and fall to the iconic appearance of uninterrupted black dirt describes the classic practice of conventional till. When remaining residue is less than 15%, the practice is considered conventional or intensive tillage.

6.5.1.2 Conservation tillage

Conservation tillage aims to prevent erosion of topsoil by leaving a portion of the crop residue on the field for stability. This includes practices known as no-till or zone tillage, among other methods and nomenclature. As defined by the EPA, conservation tillage is any planting system that maintains at least 30 percent of the soil surface covered by residue after planting to reduce soil erosion by water; or, where soil erosion by wind is the primary concern, maintains at least 1,000 pounds of flat, small-grain residue equivalent on the surface during the critical erosion period. When the soil is covered by residue, there is also a decrease in soil sealing from compaction due to raindrops, which increases infiltration (US EPA, 1993). Increasing fuel costs originally jump-started the practice in the late 1970s, and now the focus is on reducing soil erosion (Penn State, 2016). Conservation tillage can reduce gross field erosion by 50 – 65%

according to Moncrief et al. (1997), as high as 75%, as gathered from a 1993 literature review done by the EPA, and up to 90% according to MWPS.

6.5.1.3 Reduced tillage

Between conventional and conservation tillage is a group of practices that reduces soil exposure by a moderate amount. Practices known as mulch or ridge tillage, or chisel plowing would be classified as reduced till. As a general rule of thumb, tillage is considered reduced when 15-30 % of crop residue is left remaining on the land. Most studies classify tillage as either conventional or conservation and opt instead to categorize by method; few studies explore this zone in between the two by percentage.

Reduced and conservation tillage is more effective on well-drained soils and may raise challenges related to delayed field access to poorly-drained glacial till soils (Moncrief et al., 1997). As far as crop productivity, there are mixed results. According to Penn State (2016), less tillage introduces greater variability in crop yield, and Zhou et al. (2009) determined that there are no statistical yield differences among tillage systems. Uri (2000) claims that crop yields depend more on weather conditions during the growing season than on the tillage system, and the EPA backs this up claiming that conservation tillage is more effective in humid regions (US EPA, 1993).

6.5.2 AFMO – Sediment conservation measure

AFMOs are agricultural field management options with a primary function of trapping sediment and reducing the sediment delivery ratio. AFMOs included in the MOSM are grassed waterways and terraces, two options that are commonly used in tandem.

A grassed waterway is a natural or constructed channel lined with grass or other groundcover to supply stability to a sloped area that is exposed to concentrated flow and might otherwise be at risk of becoming a gully. The vegetation acts to trap sediments and reduce the concentrations conveyed to the waterway. An EPA literature review reports a 35% sediment reduction with installation of grassed waterways (US EPA, 1993). The roughness of the grass and the reduction in velocity prolongs residence time providing a high sedimentation rate (Fiener and Auerswald, 2003). According to Arora et al. (2003), the average sediment retention was 90% for 15:1 area ratio and 87% for 30:1 area ratio.

Geographically, grassed waterways are installed in the fields on steeper slopes, where concentrated flows occur. Zhou et al. (2009) estimate that an average of 1.2% of land is taken out of production to accommodate the waterways.

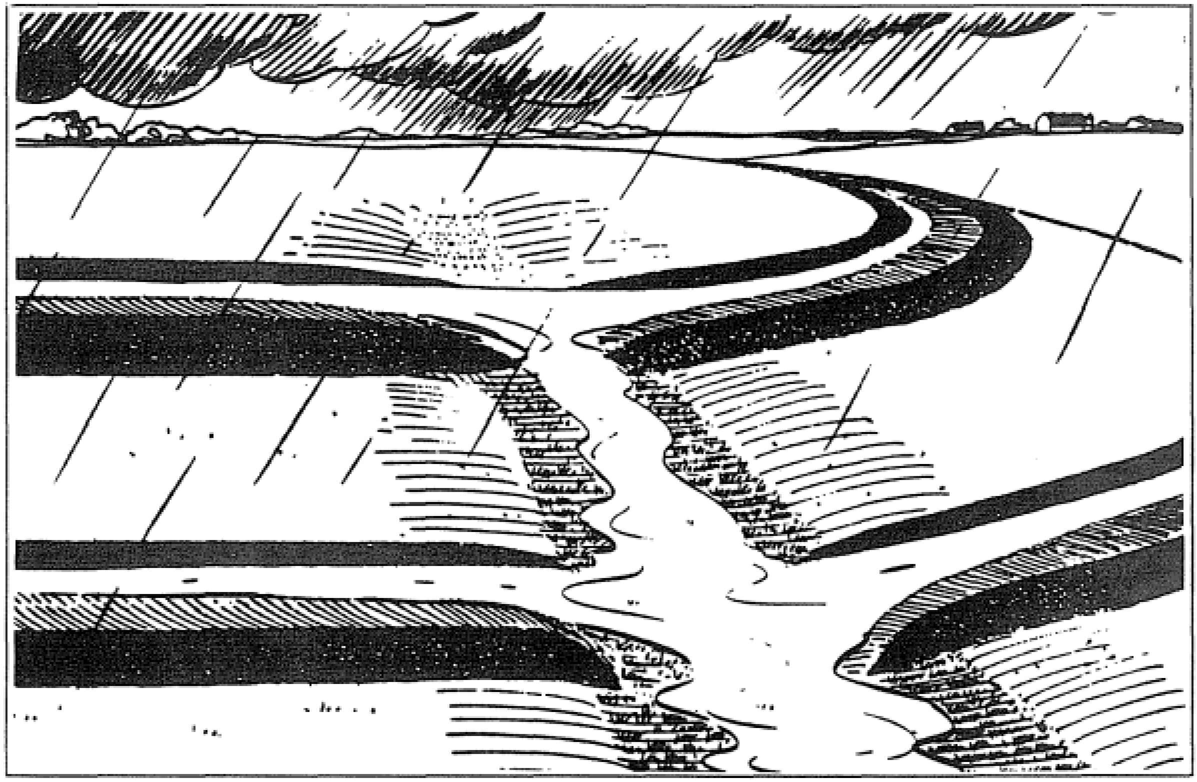

Figure 6.10. Gradient terraces with grassed waterway outlet. From US EPA Doc. EPA-840-B-92-002, January 1993

Terraces are ridges or earthen embankments that run perpendicular to the slope and are sometimes combined with a channel or grassed waterway (Figure 6.10). Water runs off an individual terrace and funnels into a channel instead of transferring to the next terrace below, thereby reducing the erosive effect of the cumulative flow. Terraces reduce the erosion rate and production of sediment within the terrace interval while also trapping sediment and passing surface runoff at a lower velocities, increasing infiltration (US EPA, 1993).

Terraces are useful on steep slopes and generally only require about 5% of land taken out of production (Zhou et al., 2009). Upon reviewing the literature, the EPA found that sediment reduction from terrace farming was around 85% (US EPA, 1993).

Maintenance of AFMOs could include mowing grassed waterways twice per year to maintain the efficiency of the grass, and inspecting and seeding after any degradation from heavy rains. Controlling weeds and vermin may be necessary for both grassed waterways and terraces.

6.5.3 WCMO – Hydrologic conservation measure

Water Conservation Management Options (WCMOs) include measures such as Wetland Restoration, sediment basins, and WASCOBs. These features primarily reduce flow and trap sediment, and have secondary/tertiary functions of reducing erosion and creating and enhancing habitat and reducing nutrients.

Wetland restoration is recognized as an important management option for its ability to improve local water storage capacity and water quality by removing sediment and nutrients from the water passing through (Galatowitsch and van der Valk, 1994). Wetland restoration is a complex management option, incorporating components of many disciplines including soil science, ecology, hydrology, etc. It can be very difficult to get right – high nutrient loads in agricultural areas can create a challenge in establishing biodiversity (Lewandowski et al., 2015). Wetland restoration can have varying goals and a large range of associated costs.

A less rigorous and more compact option is a constructed wetland. Whereas wetland restoration attempts to reestablish ecological processes in a location that a wetland previously existed, the goal of wetland construction is to initiate wetland processes at a new site and mimic the benefits of a natural wetland (Argonne National Lab). A retention structure is placed at the outlet of a small watershed or in a location convenient for a farmer. The water level is maintained to reduce peak flows and trap sediment. Maintenance requires periodic removal of sediment accumulation (Lewandowski et al., 2015).

In a more basic function, sediment basins are constructed to intercept sediment and other debris moving downstream, removing it from the runoff.

A WASCOB is an earthen berm build perpendicular to a moderate to steep slope in order to back up and detain water and trap sediment (Figure 6.11). The effectiveness of trapping sediment and phosphorous can be exceed 90% in silt loam soils (US EPA, 1993). One potential challenge associated with WASCOBs is that water temperatures may increase slightly due to the longer exposure of the surface water to warming during its impoundment.

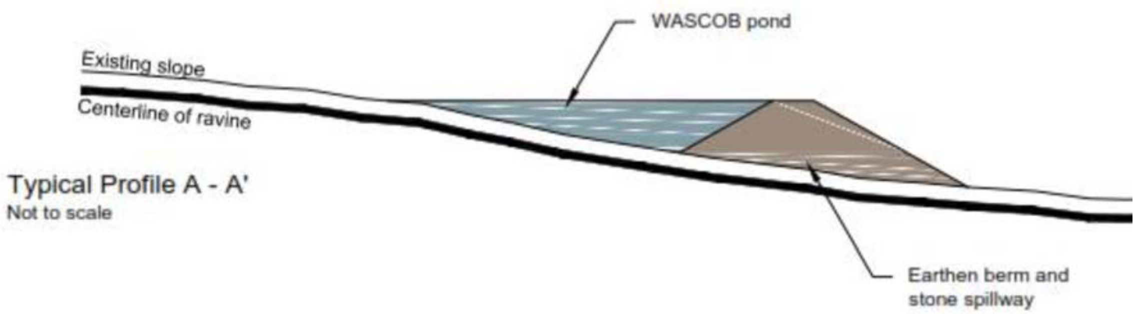

Figure 6.11. Conceptualized drawing of a WASCOB pond. From Inter-fluve, 2015.

6.5.4 BFMO – Sediment conservation measure

Buffer strip management options include filter strips, field borders, contour buffer strips, and alternative tile inlets. These practices are intended to trap sediment and reduce flow and erosion.

Contour buffer strips, filter strips, and field borders are used in different geomorphic settings but are all essentially swaths of single or multi-species grasses, legumes, or forbs planted adjacent to the crops in order to filter water running off of the crop land and intercept sediment and other nutrients coming off the fields. Contour buffer strips are used on sloping surfaces and run in between neighboring rows of crops, filter strips are used when the crop land is adjacent to a stream or other surface waters, and field borders are located at the edge of or around the perimeter of a field, and are sometimes used to connect various types of buffers.

6.5.4.1 Contour buffer strips

Contour buffer strips are installed on sloped fields subject to sheet and rill erosion (Figure 6.12). These permanent swaths of vegetation are planted parallel to the crop rows in narrower widths to filter sediment and nutrients running off of the cropland above. In a 1996 study, Arora et al. found contour buffer strips installed on 0.41 ha to reduce total sediment by a minimum of 75.9% for 6 strips.

Figure 6.12. Contour buffer strips. From USDA, 2011.

Operation and maintenance of buffers strips includes maintaining the original length and width of the strips and harvesting, mowing, reseeding, and fertilizing as necessary to maintain plant density and vigorous plant growth. Inspection and removal trapped sediment after large storms will keep the strips in proper working condition.

6.5.4.2 Filter strips and Field borders

Filter strips and field borders intercept sediment and contaminants running across a field under sheet flow and prevent them from entering an adjacent surface water. These types of filter require thorough maintenance and have a relatively short service life; if not properly maintained, floods may overload filter strips and field borders and may release a pulse of pollutants into the surface water. According to Zhou et al. (2009), filter strips can take 10% of land out of production, and can reduce sediment up to 76% according to Arora et al. (2003) and 65% according to an EPA literature review (US EPA, 1993).

6.5.5 RAMO – Sediment conservation measure

Ravine tip stabilization is undertaken to prevent a ravine's upstream migration during storm events. Ravines are characterized by steep, often entrenched channels within a narrow valley with steep valley walls. They develop at the edge of the uplands as runoff encounters the change in slope. They initiate in a swale or small gully, and then rapidly incise or degrade. Incision can occur at multiple nick points or headcuts along the profile and migrates its way upstream during runoff events until bank heights become unstable. The sediment travels down the channel until eventually hits the bottom of the ravine and the material is deposited.

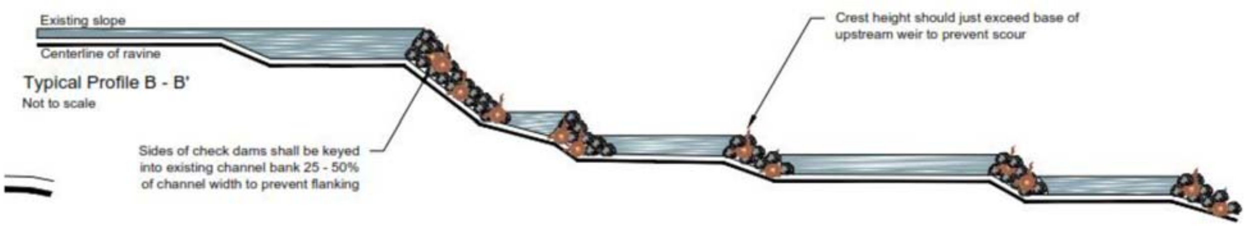

Figure 6.13. Conceptualized drawing of rock and wood check dams for use in limiting sediment transport and production in ravines. From Inter-fluve, 2015.

Ravine development is unsteady and the features are often difficult to stabilize as they are usually actively adjusting in both the vertical and horizontal directions. A ravine stabilization design charrette was held in October of 2010 with the goal of producing a deliverable to address ravine management challenges that could be used by stakeholders to identify solutions and designs to be used in the Minnesota River basin (Emmons and Olivier, 2011). One outcome of the workshop was a proposed two-pronged approach to ravine stabilization, targeting both the hydrology through rate and volume control in the upper watershed, and the physical erosion through grade control within the ravines. This involves small check dams and stream bank stabilization measures to be employed along the channel within the ravine. Rate and volume control and smaller grade control reduces slopes over short reaches and stores water to lessen the impact of larger flows (Figure 6.13, Inter-fluve, 2015). The structures needed to stabilize a ravine are highly variable in size and construction based on the dimensions and hydrology of the particular site, leading to a wide range in scope and costs.

6.5.6 ICMO – Hydrologic conservation measure

In-channel WCMOs perform the same functions as WCMOs, but are installed within a channel – namely the practice of in-ditch storage. Among many types of structures that can be used to back up water, a common installation for this management option is a flap gate structure that is installed in a ditch to back up water for a slower release. The extended detention time reduces downstream peak flows and allows time for sediment and nutrients to settle out. Rate control weirs can be installed to automatically control the discharge, but at a significant cost.

Several variations of flap gate design exist. The one shown in figure 6.14 (a), consists of a steel plate pivoting about a horizontal axis with a counterweight on top to control the rate at which water can exert pressure on and displace the plate and flow out of the ditch/channel (Ambrosini, 2014). Figure 6.14(b) shows an in-ditch storage consisting of a weir with a notch opening design to reduce peak flow while allowing water to flow through the notch during low flow condition.

Figure 6.14. (a) Flap gate structure. From http://www.itrc.org/projects/images/flapgate.jpg; (b) In-ditch retention structure from https://www.extension.umn.edu/environment/water/publications/docs/fields-to-streams2-sec.pdf

6.5.7 NCMO – Sediment conservation measure

Near channel management options target locations in which a stream is eroding streambanks or bluffs. Bluff and streambank stabilization projects primarily reduce erosion by armoring the bank or deflecting the river flow. Depending on site specifics, these project have a wide range of scopes and costs.

Bluffs form where a stream channel abuts a valley or terrace wall at the edge of its floodplain. As the flow interacts with the adjacent wall it erodes material at the toe, which leads to slumping of the land above and further migration of the bluff face (see figure 6.15). The GBE contains high, unvegetated bluffs of unconsolidated glacial till and the erosion of these surfaces accounts for a large percentage of the sediment budget of the watershed (Day et al., 2013; Bevis, 2015).

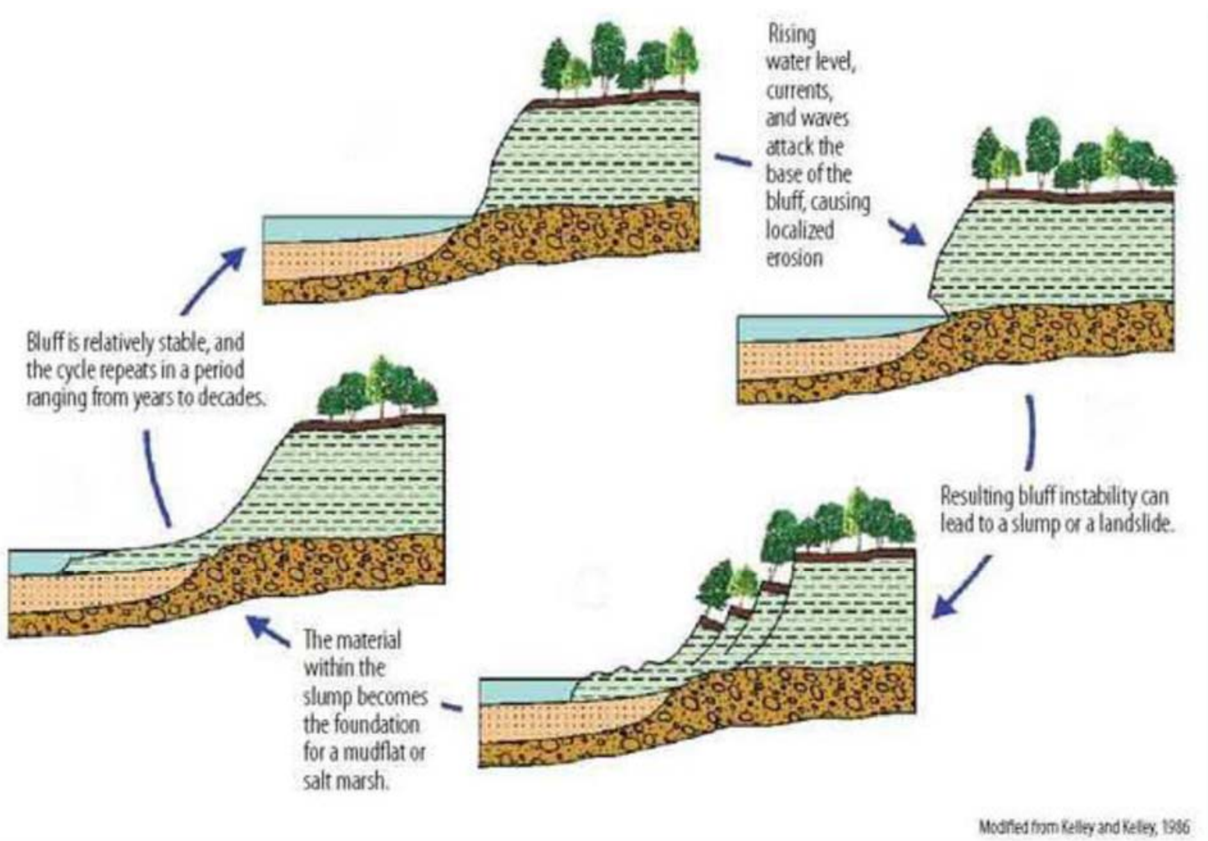

Figure 6.15. Bluff erosion cycle showing bluff toe erosion, followed by rotational failure/slumping, bar formation and transport, and back to bluff toe erosion. From Inter-fluve 2015.

Bluff stabilization measures are generally taken to stabilize the toe of the bluff and eliminate erosion there, followed by a natural or mechanical adjustment of the bluff face and upper bluff. If left to happen naturally, material eroding from the face falls and accumulates near the base of the bluff and works to lower the overall slope passively, and as vegetation is able to take root, it will work to reinforce the process.

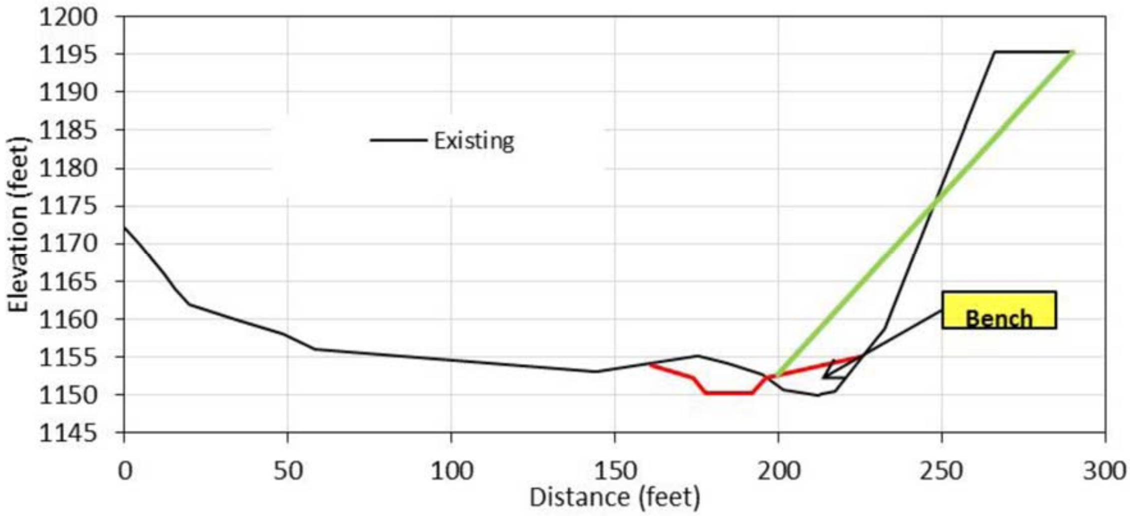

Figure 6.16. Existing, proposed, and expected typical cross section at a typical bluff stabilization site. The existing ground (black line) shows the channel scouring at the toe of the bluff on the right side of the valley. The proposed channel (red line) will be excavated away from the bluff toe to allow room for placement of the treatment (riprap or cribwall) and to provide room for the upper bank material to slump over (green line).From Inter-fluve, 2015.

Engineered wood toes are a design element often included in bluff stabilization projects, involving the placement of regularly or strategically spaced clusters or log jams along the bluff toe to intercept circulating cross currents, thereby minimizing toe erosion and instead creating depositional features (Figure 6.17).

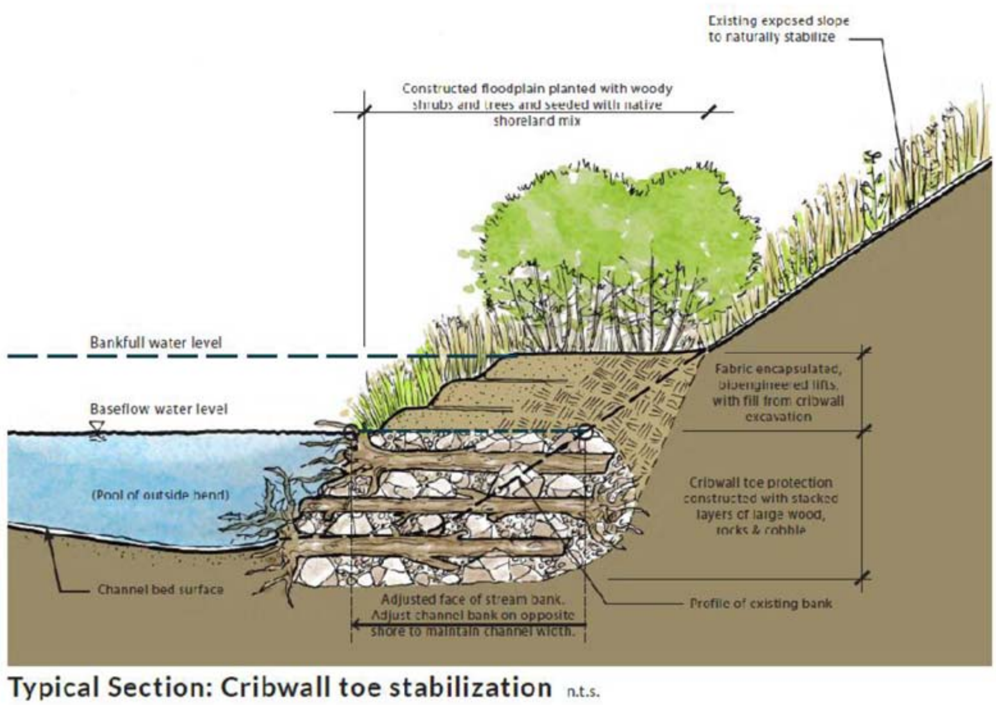

Figure 6.17. Toe-wood stabilization technique for bluffs. From Inter-fluve, 2015.

6.6 Cost and effectiveness of management options

The costs associated with the various management options and the best management practices within each option can vary quite substantially. Both installation and maintenance costs are specified by the user of MOSM. The model provides a default starting cost for each of the management options (Table 6.2). For the purpose of comparison among different management options, costs are annualized (C_{ann}) for each MO, using end-of-year payout and including installation and maintenance costs over the lifetime of the MO with default interest rate (i) of 5%:

$$C_{ann} = \left[\left(\frac{P_{inst} + P_{land}}{1+i}\right)\left(\frac{(1+i)^n \cdot i}{(1+i)^n - 1}\right) + P_{mntn}\right] * A \quad [7.1]$$

Where P_{inst}, P_{land}, and P_{mntn} are installation, land acquisition, and annual maintenance costs per extent for each MO.

Table 6.2: Install and maintenance costs summarized for major MO categories used in MOSM.

Tillage Management Option (TLMO) ALLOCATION				Install range	Install assumptions	Maintenance details
Extent of all farm land (ac)	Install. ($/ac)	Mntnc [$/(ac*yr)]	(yr)			
Conventional till (%)	26	8	1		Costs from 2016 Iowa custom rate survey w/ cost breakdown[9]	
Reduced till (%)	28	11	1			
Conservation till (%)	14	6	1			
Agricultural Field Management Option (AFMO) ALLOCATION						
Extent of all MOs (ft)	Install. ($/ac)	Mntnc [$/(ac*yr)]	Life Span			
Input extent (ft)	3,200	64[7]	10	1,900-4500/acre[3] 2000-3000/acre[4]	35' width	Mow 2x per year. Inspect/seed after heavy rain. Control weeds. Control vermin.
Buffer Strip Management Option (BFMO) ALLOCATION						
Extent of all MOs (ft)	Install. ($/ac)	Mntnc [$/(ac*yr)]	Life Span			
Input extent (ft)	1,000	45[7]	10	500-2000/acre[4] 750-1150/acre[3]		Mowing 2x per year.Remove sediment at upper end of gradient every 2 years.
Water Conservation Management Option (WCMO) ALLOCATION						
Extent of all MOs (ac)	Install. ($/ac)	Mntnc [$/(ac*yr)]	Life Span			
Input extent (ac)	3,000	574[5,7]		6000 (ea)[2] 300-5,300/acre[3] 100-150/ln ft, 12,000-17,000/acre[4]		Inspect embankment/ridge and repair if necessary after heavy rain. Control weeds. Control vermin. Periodically clean channel with heavy equipment.
In-Channel Management Option (ICMO) ALLOCATION						
Extent of all MOs (ft)	Install. ($/ft)	Mntnc [$/(ft*yr)]	Life Span			
Input extent (ft)	250	1.4[7]		1000-3000 (ea) for structure[3] 15,000-20,000 (ea) for rate control weir[4]	cost based on flap gate structure	Grease gate annually. Paint every few years.
Ravine Management Option (RAMO) ALLOCATION						
number of ravine tips	Install. ($/TIP)	Mntnc [$/(tip*yr)]	Life Span			
Input number of tips	6,000	35[7]		1,000-11,500 (ea)[2] 571-2,100/ft; 3,750-60,000 (ea)[1] 1,000-21,000 (ea)[3]		Check for pipe blockage
Near-Channel Source Management Option (NCMO) ALLOCATION						
Extent of all MOs (ft)	Install. ($/ft)	Mntnc [$/(ft*yr)]	Life Span			
Input extent (ft)	200	0.7[7]		11-77/ft[3] 500-1000/ft[4] 26-208/ft[6] 62-226/ft[2]		Inspection, planting shrubs

[1]*Miller, T.P., J.R.Peterson, C.F. Lenhart, and Y. Nomura. 2012. The Agricultural BMP Handbook for Minnesota. Minnesota Department of Agriculture.*
[2]*Nelson, Paul. July 26, 2016. Personal Communication.*
[3]*USDA-NRCS MN-WI-MI Regional Rates for Environmental Quality Incentive Program (EQIP). 2016. Accessed at http://www.nrcs.usda.gov/wps/portal/nrcs/detail/mn/programs/financial/eqip/*
[4]*Lewandowski, A., Everett, L., Lenhart, C., Terry, K., Origer, M., & Moore, R. (2015). Fields to Streams: Managing Water in Rural Landscapes. Part Two, Managing Sediment and Water.*
[5]*Iowa State University. 2016 Iowa Farm Custom Rate Survey. March 2016. Accessed at https://www.extension.iastate.edu/agdm/crops/pdf/a3-10.pdf*
[6]*Melchoir, Marty. Jan 19, 2014. Personal Communication.*
[7]*Center for Watershed Protection (2004). Stormwater Pond and Wetland Maintenance Guidebook. Accessed at http://www.stormwatercenter.net/Manual_Builder/Maintenance_Manual/pondwetlandguidebookdraft.pdf*
[8]*Ambrosini, K. (2014). Analysis Of Flap Gate Design and Implementations for Water Delivery Systems in California and Nevada. Accessed at http://digitalcommons.calpoly.edu/cgi/viewcontent.cgi?article=1125&context=braesp*
[9]*Uri, Noel D. "An evaluation of the economic benefits and costs of conservation tillage." Environmental Geology 39.3-4 (2000): 238-248.*

6.7 **Spatial extent of management options**

The spatial extent of areas appropriate for each management option was determined in ArcGIS. We identified locations and quantified available extents of the MOs in Table 6.1 using spatial analysis. Factors considered in the analysis include geographic location, landcover and landuse, soil properties, and crop productivity. Thus, we define the maximum extent of available MO sites that constraints the MO extent input in the MOSM. We also collected the geophysical characteristics, such as soil type, landuse, distance to waterways and existing conservation sites, to inform the site allocation algorithm

The datasets used to delineate spatial extents are listed here, with source information at the bottom of the page:

- 3-m and 30-m Digital Elevation Model (DEM)[1]
- National Conservation Easements Database (NCED)[2]
- Soil Survey Geographic database (SSURGO)[3]
- Identification and classification of wetlands and deep-water habitats of the Contiguous US (CONUS wet polygons) [4].
- National land cover database 2011 (NLCD)[5]
- National hydrography dataset (NHD) blue lines[6]
- University of Minnesota Water Resource Center (WRC) ditch shape file[7]

TILMO: Area available for Tillage Management Options were identified as cultivated crops in NLCD data, excluding areas in conservation easement as shown in NCED data or wet polygons in CONUS data. TILMO act on the landscape by reducing the initial erosion rate on fields through reduced tillage or other conservation tillage practice.

AFMO: Agricultural Field Management Options include treatments designed to trap sediment already eroded from fields and includes practices such as installation of grassed waterways, water and sediment conservation basins (WASCOBs), or terraces. Areas available for AFMOs were delineated by using a stream power index (SPI) calculated as

$$SPI = \ln(\alpha * tan\beta) \quad (6.16)$$

where (α) is upstream contributing area and (β) is slope. Areas with $SPI \geq 7$ were identified as areas susceptible to water erosion on fields. Areas with $SPI \geq 11$ often had existing ditches or channels already in them. Thus, areas with $7 \geq SPI \geq 11$ were used for potential AFMO treatment. Within this range, only areas available for cultivated crops as determined from NLCD data were used, and wet polygons in CONUS

---

1 USGS The National Map Viewer, http://viewer.nationalmap.gov/viewer/
2 National public conservation easement map layer is obtained from the National Conservation Easement Database (NCED) https://s3.amazonaws.com/nced/20130911/NCED_metadata_7_01_2012.htm. Phase I completed on July 31, 2011 and predict a nearly complete (>90%) mapping of publicly held easement in Minnesota.
3 USDA web soil survey, http://websoilsurvey.sc.egov.usda.gov/App/HomePage.htm
4 U.S. Fish and wildlife Service and National wetlands Inventory, http://www.fws.gov/wetlands/
5 National land cover product created by Multi-Resolution Land Characteristics (MRLC) Consortium obtained from http://www.mrlc.gov/nlcd2011.php
6 USGS The National Map Viewer, http://viewer.nationalmap.gov/viewer/
7 WRC ditch shape file received from Paul Davis of the Minnesota Pollution Control Agency on June 24, 2013

were removed. Additional area was removed if it was within an existing channel or ditch or if the line length was below a minimum threshold (100 m).

BFMO: Buffer management options were added after the January 2016 stakeholder meeting at the request of stakeholders following a Minnesota state-wide buffer initiative. The official map of affected waterways was not yet available at that time and we created an estimate of buffer extent for use in MOSM. NHD blue line data were used to identify all natural streams and rivers and manmade streams and ditches. All streams were given a 50 foot buffer, and all NHD blue lines identified as artificial waterways were given a 16.5 foot buffer.

WCMO and ICMO: Water control management options include any MO designed to hold water back. ICMOs specifically refer to in-channel water control MOs and WCMOs broadly refer to any wetland restoration or temporary water storage basin not in a ditch or channel. Candidate sites for ICMOs included all "public open ditch" lines from the WRC ditch shape file. WCMOs were identified as topographic depressions on 3-m DEM (filled DEM minus raw DEM). Only topographic depressions with high topographic index (TI) values were used

$$TI = \ln\left(\frac{\alpha}{tan\beta}\right) \quad (6.17)$$

Developed land, forest, water, and existing wetlands as determined by NLCD data were removed as were sites on existing wet area polygons in CONUS and sites where existing conservation easements already exist. Finally, WCMO sites < 0.74 acres (3000 m^2) were removed to avoid having numerous sites that would cause significant challenge for producers to work around in fields.

RAMO: Ravine management options were modeled as MOs that provide additional stability to ravine tips, preventing ravine growth. Examples include berms or WASCOBs placed around ravine tips. All ravines were mapped by hand from lidar data, noting the sharp slope break between the low-gradient uplands and the steep ravine walls. Tips were counted and recorded per mapped ravine.

NCMO: Near-channel management options specifically refer to actions that directly stabilize a bank or bluff. In MOSM, only bluffs are considered as these are the primary sources of sediment to the stream. For the sediment budget, bluffs were mapped as areas with > 3m of relief in a 9m x 9m area and then trimmed to only include bluffs immediately adjacent to streams. The area available for NCMO was the same bluff area determined by the sediment budget.

The determination of MO extent allowed the model to have realistic potential area from which to select treatment areas in different scenarios. These areas were initially mapped in ArcGIS and summarized in a series of tables, noting the available MO area in each sediment subbasin within the GBER watershed. It is important to note that these maps do not specify which sites should be used first. In many cases, the user of MOSM can specify which prioritization scheme should be used in selecting various sites (i.e. largest WCMO sites first or sites closest to existing wetlands first), but the model does not provide guidance in terms of placement at scales finer than the subbasin level. There are several new tools in existence now that can be used to look at specific sites at the scale of an individual landowner's property (for example ACPF (Tomer et al., 2013)), and these can be used in conjunction with MOSM if specific site locations are desired. The strength of MOSM is the ability to integrate all of the different management actions together at the scale of a 9200 km^2 watershed, in real-time, to compare different portfolios of actions across a wide range of possibilities (water retention to buffers to bluff stabilization).

6.8 **Management option simulation model**

6.8.1 Database inputs

MOSM simulates movement of water and sediment in a watershed, and evaluates the effects of various management option scenarios on sediment loading. The model algorithms consist of (1) MO allocation; (2) water routing; and (3) sediment routing algorithms as illustrated in Figure 6.18. Algorithm (1) accesses the MO database described in section 3.6; algorithm (2) accesses the water yield data from SWAT to route water and evaluate the impacts on sediment loading from streambanks and bluffs as described section 3.4; and algorithm (3) accesses sediment delivery ratio values simulated by Topofilter as described in section 3.2. In the following sections, we describe these algorithms and the model outputs.

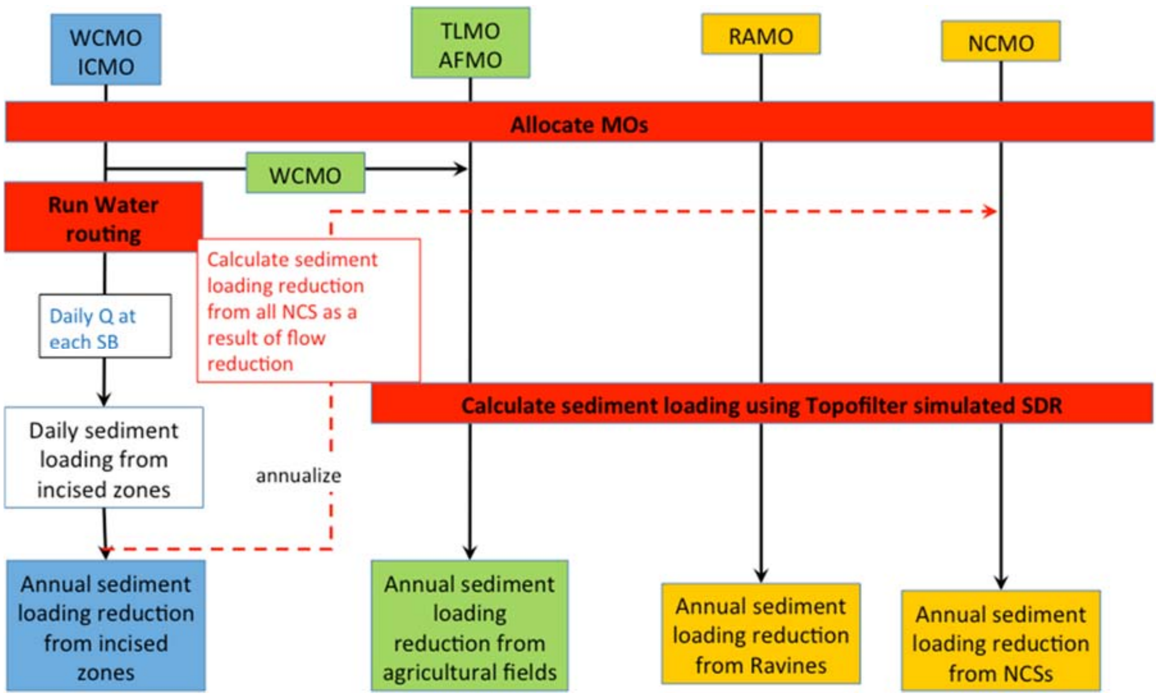

Figure 10: Illustration of overall MOSM structure with subroutines in red box (allocation, water routing, and sediment loading)

6.8.2 MO allocation algorithm

The MO database defines the total available MO extents in the 1) watershed's geomorphic zones for MO allocation, 2) HYDSBs for water routing, and 3) SEDSBs for sediment loading calculations.

In MOSM, a user can specify the different MOs and their input extents for implementation in different zones of the three subwatersheds: Maple, Cobb, and Le Sueur (i.e., nine extent inputs for each MO). Figure 6.19 shows the subwatershed, zone, HYDSB, and SEDSB delineation in the LSRB. In the GBERB, the user will specify MO inputs in three zones of five subwatersheds including Blue Earth and Watonwan in addition to three subwatersheds in the LSRB (i.e., 15 extent inputs for each MO). In the following discussion, we use the LSRB model to demonstrate model algorithm and outputs.

The user can also specify MO site selection criteria that would prioritize individual MO sites according to its geophysical characteristics. For example, if crop productivity index (an index developed in Minnesota based on past crop yields where higher value indicates larger observed crop yields (Schaetzl et al., 2012)) is specified as the site selection criteria for WCMO, then the model allocates WCMO sites with lowest CPI values first.

MO allocation algorithm uses the *greedy adding heuristics* (Cohon, 2004) to prioritize candidate site selection by sorting the MO database according to the user-specified selection criteria. Then, the model adds up the candidate sites discretely starting from the most prioritized sites until right after reaching the user-specified extents for implementation in each zone of the subwatersheds.

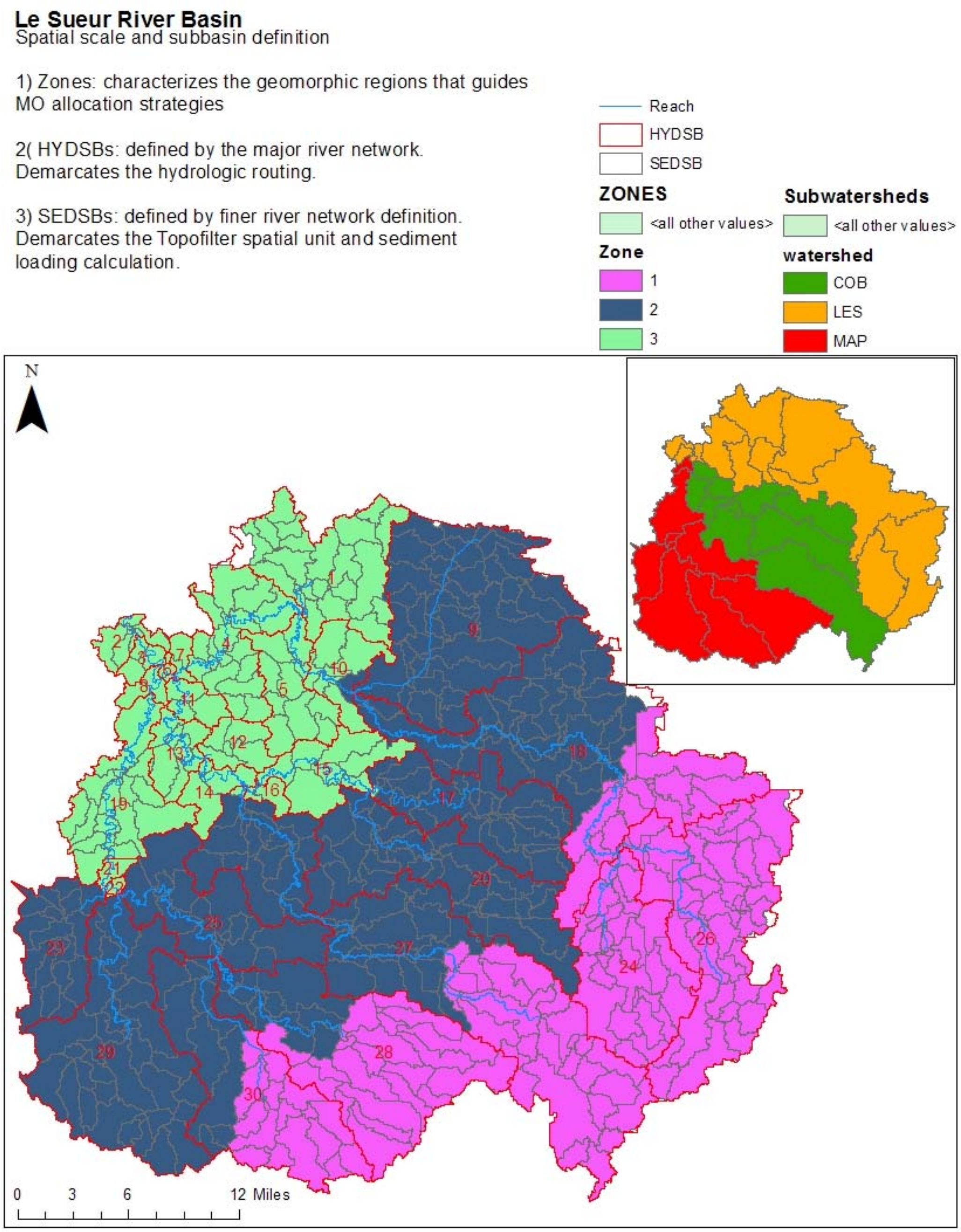

Figure 6.19: LSRB zones, HYDSBs, and SEDSBs with subwatersheds in the insert

After the allocation is completed, the model calculates the total extents of allocated MOs in each HYDSB and SEDSB. Subsequently, the water routing algorithm evaluates the effects of water storage achieved by WCMO and ICMO in each HYDSB and consequent sediment loading reduction from NCS using the hockey stick model. Then, the sediment loading algorithm calculates reduction in soil erosion and sediment loading from each SEDSB as a result of implementing TLMO, AFMO, WCMO, BFMO, RAMO, and NCMO.

6.8.3 Water routing and evaluation of water conservation

Stream flow routing described in section 6.4 sets the basis for predicting the effects of water conservation measures with WCMO and ICMO as illustrated in Figure 6.20. To summarize, the model evaluates the impacts on water yield at each HYDSB as a result of implementing water storage using the storage-outflow method. Then, using Muskingum-Cunge routing, we estimate the time and magnitude of peak flow attenuation in the river stream as result of water storage. Finally, using the hockey stick model, we evaluate the sediment loading reduction from streambanks and bluffs as a result of peak flow attenuation.

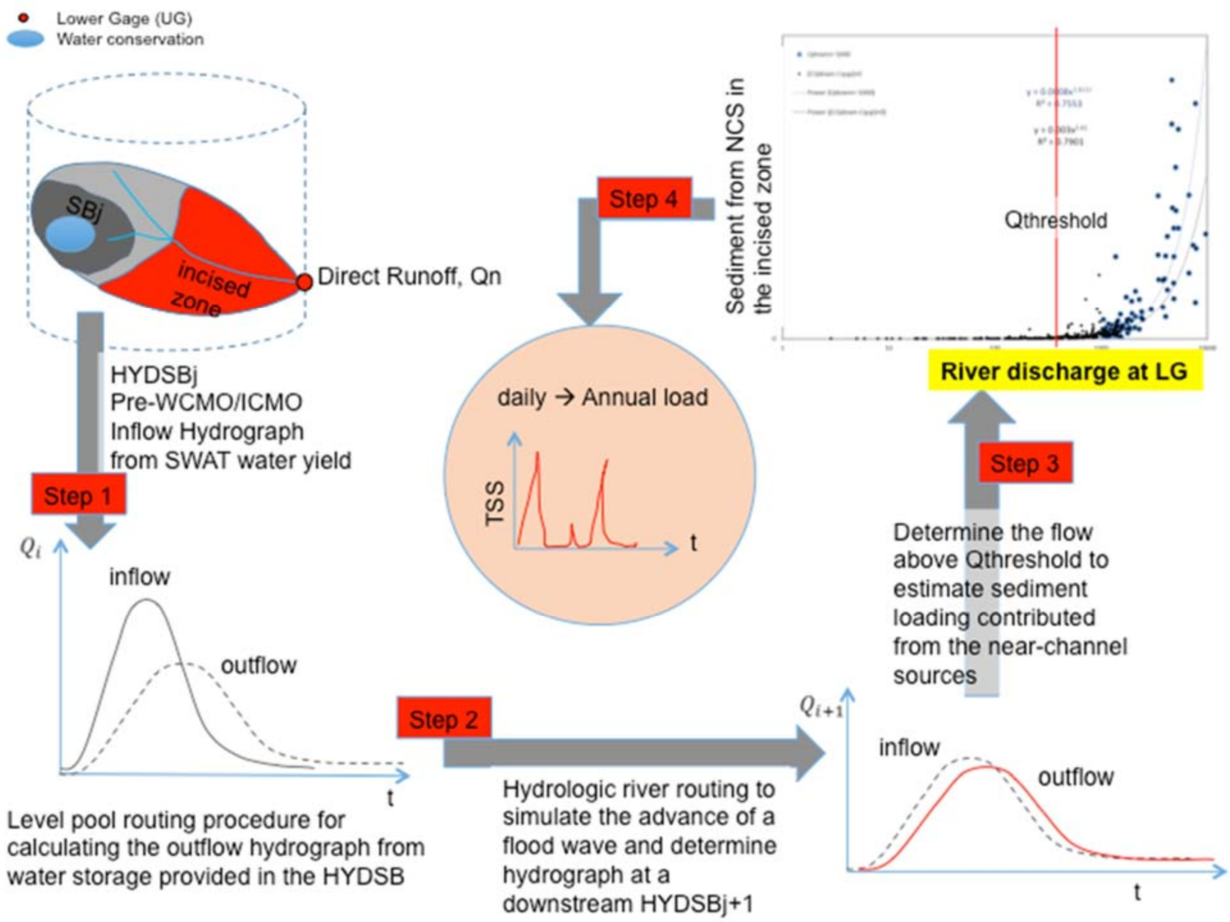

Figure 6.20: a schematic describing evaluation of water conservation management on peak flow reduction and consequent reduction in annual sediment loading from NCSs.

6.8.4 Sediment routing and evaluation of sediment conservation

Sediment loading is calculated at each SEDSB *j* with the effects of allocated MOs. Figure 6.21 illustrates the sediment loading algorithm and its sequence at each SEDSB: 1) Soil erosion rate (SE_j, Mg/yr) as a result of implementing TLMO is calculated. 2) Sediment delivery ratio on field (SDR_{fj}) for areas affected by AFMO, WCMO, and BFMO is calculated. NOMO is the field area unaffected by MOs. 3) Effects on sediment inputs from ravines (SI_{Rj}) and bluffs (SI_{Bj}) from RAMO and NCMO implementations are calculated, respectively. Sediment loading from streambanks (SI_{Sj}) is unaffected by MOs. Consequently, total sediment inputs from field, ravines, streambanks, and bluffs to stream (SI_j) is multiplied by the sediment delivery ratio in stream (SDR_{sj}) to calculate the sediment loading at watershed outlet from SEDSB j (SL_j).

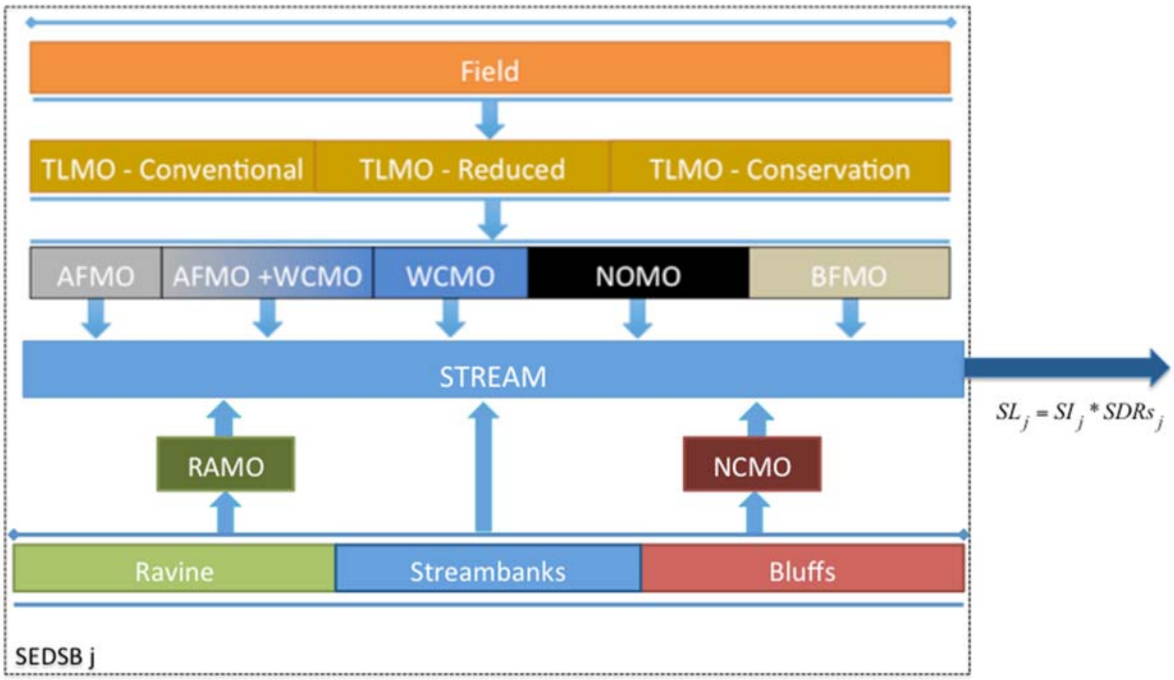

Figure 6.21: a schematic of sediment loading simulation in the MOSM. Sediment inputs (SI) consist of sediment loading from field, ravines, streambanks, and bluffs.

Total sediment loading without any MO implementation at the outlets of each of the Toposhed k is

$$\begin{aligned} SL_k &= \sum_{j}^{J_k} \left[SE_j \cdot SDR_{fj} + SI_{Rj} + SI_{Sj} + SI_{Bj}\right] SDR_{sj} \\ &= \sum_{j}^{J_k} \left[SI_{Fj} + SI_{Rj} + SI_{Sj} + SI_{Bj}\right] SDR_{sj} \\ &= \sum_{j}^{J_k} SI_j \cdot SDR_{sj} \end{aligned} \quad (6.18)$$

When MOs are implemented, different elements of [6.18] are modified to reflect the effectiveness of MOs. First, if TLMO is implemented in SEDSB j, SE_j will be reduced based on the proportions of conventional, reduced, and conservation tillage implemented in respect to the reference period tillage practice.

Second, if AFMO, WCMO, or BFMO are implemented in SEDSB j, then SDR_{fj} is reduced according to the effectiveness of different MOs for their contributing areas as illustrated in Figure 6.22. Note that the model considers overlapping contributing areas of AFMO and WCMO (A_{gw}), MOs that both get implemented in the further uplands in each SEDSB. In addition, as described in section 6.2, SDR_f values simulated in A_p (SDR_{fp}) is applied to BFMO that treat the areas adjacent to stream network, and SDR_f value simulated in A_f (SDR_{ff}) is applied to AFMO and WCMO.

Third, if RAMO is implemented, then the sediment input rates from the tips of ravines would be directly reduced by the effectiveness of the RAMO as illustrated in Figure 6.23. Similarly, if NCMO is implemented, then the sediment input rates from the bluffs would be directly reduced by the effectiveness of the NCMO.

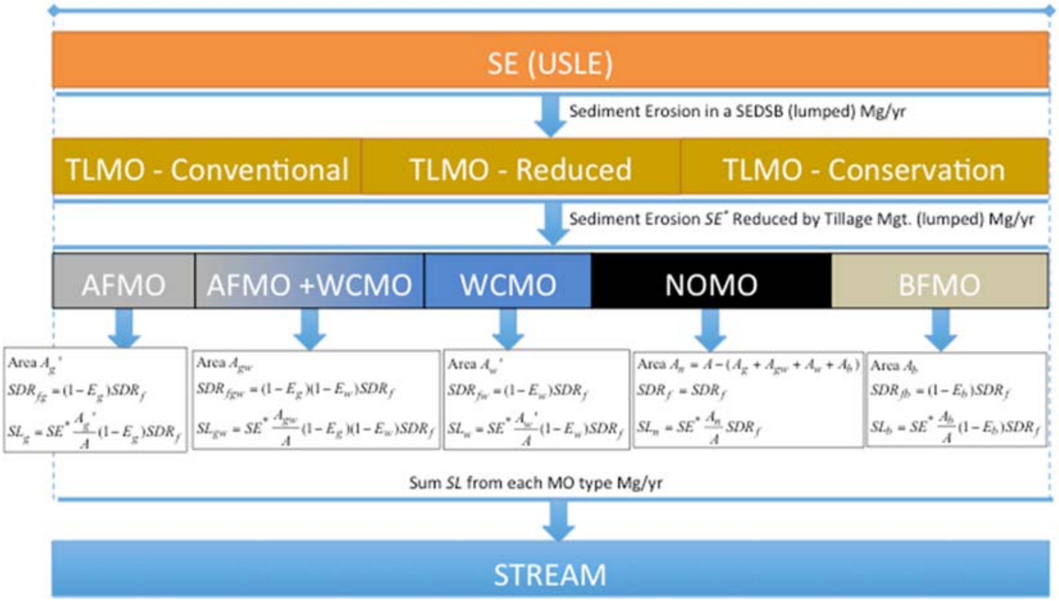

Figure 6.22: Illustration of MOs in the agricultural areas and their individual effects on sediment loading

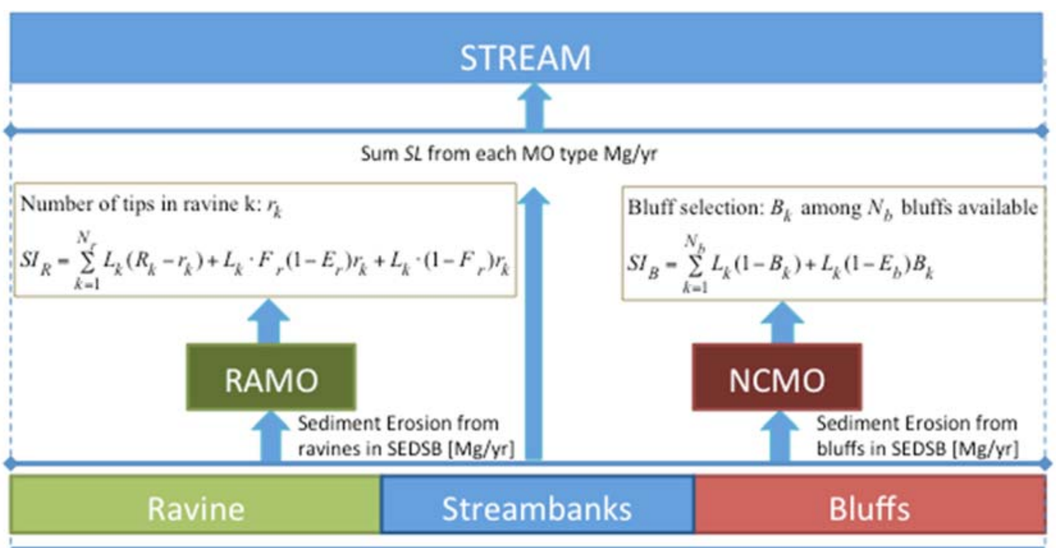

Figure 6.23: Illustration of NCS loading and evaluation of RAMO and NCMO with the sediment reduction algorithms

6.8.5 Outputs

The water routing algorithm evaluates the reduction in peak river discharge in the incised zone at the lower gage locations (See section 6.3, Figure 6.5 for the lower gages located below the incised zone). For example, Figure 6.24(a) shows the frequency of simulated flow classes above the Qthreshold at the Lower Maple gage. This figure compares the “no WCMO/ICMO” scenario versus the scenario implementing 2,431 acres of WCMOs in the zone 1. As a result of the peak flow reduction, sediment loading from streambanks and bluffs in the incised zone of the Maple is reduced by 21.7% as shown in Figure 6.24(b). This rate of sediment loading reduction is then applied to the rest of the Maple subwatershed in the sediment loading algorithm.

Sediment loading calculation is done stochastically in MOSM using the family of plausible solutions of SDR values generated by Topofilter. Specifically, as discussed in section 6.2, each SEDSB has a set of plausible SDR values on field near and far from the stream (SDR_{ff}, SDR_{fp}) and SDR values in stream (SDR_s), expressed as probability distributions. MOSM accesses these probability distribution parameters at each MC iteration to calculate sediment loading with and without MOs in the watershed.

Thus, the model outputs include mean, standard deviation, minimum, maximum, and 90th percentile of simulated SL values for all different SDR values generated within their probability distributions. For example, Figure 6.25 shows the annual sediment loading with 2,431 acres of WCMOs in the zone 1 and without MO implementation at the outlets of UM, MC, LC, and UL with 90th percentile error bars.

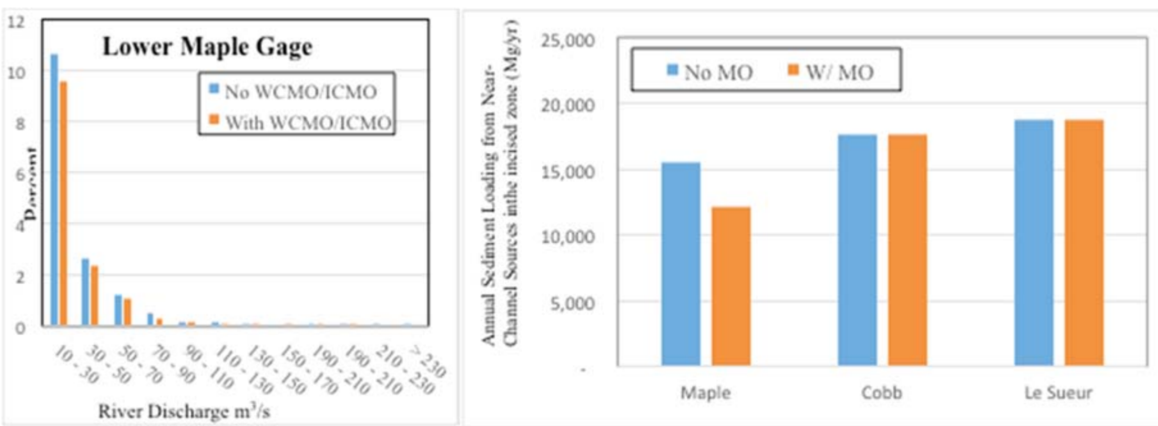

Figure 6.24: (a) Frequency distribution chart for flow classes above threshold discharge at the Lower Maple Gage (b) sediment loading reduction in the incised zones of the Maple, Cobb, and Le Sueur

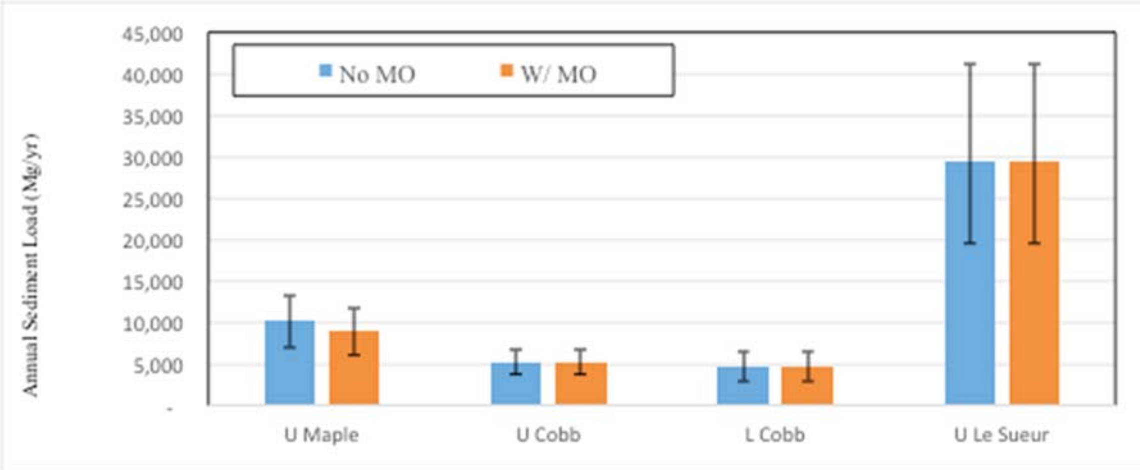

Figure 6.25 an example SL outputs at each watershed outlet, UM, MC, LC, and UL with 90th percentile error bars

6.9 Platform

MOSM operates on Microsoft Excel spreadsheet; thus, it is accessible to a wide range of users. The model comes with a user manual that provides an overview of the model, MOSM algorithms and spatial scales, input database, and instructions on the basic control inputs as well as detailed control input parameters for MO allocation, water routing, and sediment loading algorithms.

7 Application of Management Option Simulation Model

Operation of MOSM is illustrated here using application to the Le Sueur River Basin. MOSM is used to evaluate various MO scenarios where a MO scenario consists of MO portfolios (MOPs) to reduce either sediment loading or peak river discharge. Table 7.1 shows the default MO cost and effectiveness value used to simulate various MO scenarios.

Different MOP are evaluated in terms of annual sediment loading reduction and cost of MO implementation. MOs are allocated for the MOP scenarios using the default selection criteria, and the consequent annual costs are calculated using the default cost inputs. Also, SL reduction is calculated using the default MO effectiveness (Table 7.1). Tables 7.2 and 7.3 show the allocated MO extents for the scenario inputs of site-specific and hydrologic strategies, respectively.

Table 7.1: MO effectiveness and cost input table (green cells). Cost input consists of MO's installation cost ($/extent), maintenance cost ($/extent), and life span (year). TLMO effectiveness is calculated internally based on soil loss estimates, reference period tillage practice, and gage data. WCMO and ICMO's effectiveness on sediment loading reduction from near-channel sources are calculated internally through hydrologic routing algorithm; while WCMO also has effectiveness on capturing and storing sediment on agricultural field. Thus, effectiveness inputs are required for AFMO, BFMO, and WCMO on sediment delivery reduction (%); and for RAMO and NCMO on sediment erosion reduction (%).

MO efficiency	Installation	Ann. Maintenance	Life Span	Total
%	Cost	Cost	(yr)	Cost ($/yr)
Tillage Management (TLMO) EFFECTIVENESS & COST				
	Install. ($/ac)	Mntnc [$/(ac*yr)]	(yr)	Total ($/yr)
Conventional	26	8	1	6,461,562
Reduced	28	11	1	7,411,791
Conservation	14	6	1	3,800,919
Agricultural Field Management (AFMO) EFFECTIVENESS & COST				
Sed. Delivery	Install. ($/ac)	Mntnc [$/(ac*yr)]	Life Span	Cost ($/yr)
75 %	3,200	64	10	0
Buffer Strip Management (BFMO) EFFECTIVENESS & COST				
Sed. Delivery	Install. ($/ac)	Mntnc [$/(ac*yr)]	Life Span	Cost ($/yr)
100 %	1,000	45	10	0
Water Conservation Management (WCMO) COST				
Sed. Delivery	Install. ($/ac)	Mntnc [$/(ac*yr)]	Life Span	Cost ($/yr)
90 %	3,000	574	25	0
In-Channel Management (ICMO) COST				
	Install. ($/ft)	Mntnc [$/(ft*yr)]	Life Span	Total ($/yr)
	250	1	10	0
Ravine Management (RAMO) EFFECTIVENESS & COST				
Sed. Erosion	Install. ($/TIP)	Mntnc [$/(tip*yr)]	Life Span	Total ($/yr)
75 %	6,000	35	10	0
Near-Channel Source Management (NCMO) EFFECTIVENESS & COST				
Sed. Erosion	Install. ($/ft)	Mntnc [$/(ft*yr)]	Life Span	Total ($/yr)
70 %	200	1	5	0

Table 7.2: Summary of site-specific strategies with total extent selected, annual sediment loading (SL) reduction, annual cost, and unit cost of reducing a metric ton of sediment loading

Management Option Portfolio			Total extent selected			SL reduction	Annual Cost	Unit cost
Strategy	Scenario	Description	ac	ft	tips	Mg/yr	$/yr	$/Mg
Ag Field Management	T1AF1	TLMO: 33-33-33 (T1), AFMO10% all zones (AF1)	450	196,064		219	667,056	3,046
	T1AF2	T1, AFMO50% all zones (AF2)	2,167	943,994		1,008	3,211,682	3,186
	T1AF3	T1, AFMO100% all zones (AF3)	4,321	1,882,178		1,527	6,403,599	4,194
	T1AF1BF1	T1, AF1, BFMO10% all zone (BF1)	1,804	857,520		1,038	2,220,319	2,139
	T1AF1BF2	T1, AF1, BFMO50% all zone (BF2)	5,640	3,528,109		3,896	6,841,386	1,756
	T1AF1BF3	T1, AF1, BFMO100% all zone (BF3)	10,414	6,825,651		7,675	12,541,034	1,634
	T2AF1	TLMO: 25-25-50 (T2), AFMO10% all zones (AF1)	450	196,064		3,767	-900,823	-239
	T2AF2	T2, AFMO50% all zones (AF2)	2,167	943,994		4,468	1,643,803	368
	T2AF3	T2, AFMO100% all zones (AF3)	4,321	1,882,178		4,930	4,835,720	981
	T2AF1BF1	T2, AF1, BFMO10% all zone (BF1)	1,804	857,520		4,505	652,440	145
	T2AF2BF2	T2, AF2, BFMO50% all zone (BF2)	7,348	3,528,109		7,786	7,818,133	1,004
	T2AF3BF3	T2, AF3, BFMO100% all zone (BF3)	14,285	6,825,651		11,634	16,709,698	1,436
	T3AF1	TLMO: 0-50-50 (T3), AFMO10% all zones (AF1)	450	196,064		9,090	-188,151	-21
	T3AF2	T3, AFMO50% all zones (AF2)	2,167	943,994		9,658	2,356,475	244
	T3AF3	T3, AFMO100% all zones (AF3)	4,321	1,882,178		10,035	5,548,392	553
	T3AF1BF1	T3, AF1, BFMO10% all zone (BF1)	1,804	857,520		9,705	1,365,112	141
	T3AF2BF2	T3, AF2, BFMO50% all zone (BF2)	7,348	3,528,109		12,437	8,530,805	686
	T3AF3BF3	T3, AF3, BFMO100% all zone (BF3)	14,285	6,825,651		15,610	17,422,370	1,116
	T2AF1z3	T2, AFMO10% in zone 3 (AF1z3)	77	33,706		3,603	-1,453,202	-403
	T2AF2z3	T2, AFMO50% in zone 3 (AF2z3)	348	151,653		3,732	-1,051,921	-282
	T2AF3z3	T2, AFMO100% in zone 3 (AF3z3)	695	302,735		3,845	-537,904	-140
	T2AF1z3BF1z3	T2, AF1z3, BFMO10% zone 3 (BF1z3)	476	207,424		4,045	1,126,963	279
	T2AF2z3BF2z3	T2, AF2z3, BFMO50% zone 3 (BF2z3)	1,652	751,188		5,886	637,085	108
	T2AF3z3BF3z3	T2, AF3z3, BFMO100% zone 3 (BF3z3)	3,189	1,457,627		7,480	2,433,551	325
Stream Buffer only	T2BF1	T2, BFMO10% all zone	1,354	661,455		4,312	-14,616	-3
	T2BF2	T2, BFMO50% all zone	5,190	2,584,116		6,891	4,606,451	668
	T2BF3	T2, BFMO100% all zone	9,964	4,943,473		10,278	10,306,099	1,003
	T3BF1	T3, BFMO10% all zone	1,354	661,455		9,550	698,056	73
	T3BF2	T3, BFMO50% all zone	5,190	2,584,116		11,712	5,319,123	454
	T3BF3	T3, BFMO100% all zone	9,964	4,943,473		14,509	11,018,771	759
	T2BF1z3	T2, BFMO10% zone 3	399	173,718		4,015	-1,241,640	-309
	T2BF2z3	T2, BFMO50% zone 3	1,304	599,535		5,728	121,127	21
	T2BF3z3	T2, BFMO100% zone 3	2,494	1,154,892		7,209	1,403,576	195
NCS Management	T2RA1	T2, RAMO10% all zone (RA1)			80	6,092	-1,505,877	-247
	T2RA2	T2, RAMO50% all zone (RA2)			338	11,547	-1,305,920	-113
	T2RA3	T2, RAMO100% all zone (RA3)			617	14,534	-1,089,688	-75
	T2NC1	T2, NCMO10% all zone (NC1)		26,227		23,569	-258,697	-11
	T2NC2	T2, NCMO50% all zone (NC2)		128,120		48,534	4,177,097	86
	T2NC3	T2, NCMO100% all zone (NC3)		252,346		59,042	9,710,767	164

Table 7.3: Summary of hydrologic strategies with total extent selected, annual sediment loading (SL) reduction, annual cost, and unit cost of reducing a metric ton of sediment loading

Management Option Portfolio			Total extent selected			SL reduction	Annual Cost	Unit cost
Strategy	Scenario	Description	ac	ft	tips	Mg/yr	$/yr	$/Mg
Water conservation Management	T2WC1	T2, WCMO5% all zone (WC1)	3,681			17,817	3,354,872	188
	T2WC2	T2, WCMO10% all zone (WC2)	6,370			27,490	6,950,900	253
	T2WC3	T2, WCMO30% all zone (WC3)	18,380			65,954	23,013,279	349
	T2WC4	T2, WCMO 50% all zone (WC4)	30,549			97,088	39,287,634	405
	T2WC5	T2, WCMO100% all zone (WC5)	60,577			139,415	79,446,424	570
	T2WC1z1	T2, WCMO10% zone1 (WC1z1)	3,134			16,818	2,623,005	156
	T2WC2z1	T2, WCMO50% zone1 (WC2z1)	15,608			62,163	19,306,271	311
	T2WC3z1	T2, WCMO100% zone1 (WC3z1)	31,086			102,548	40,005,736	390
	T2WC1z2	T2, WCMO10% zone2 (WC1z2)	1,929			10,757	1,011,316	94
	T2WC2z2	T2, WCMO50% zone2 (WC2z2)	9,048			34,753	10,532,515	303
	T2WC3z2	T2, WCMO100% zone2 (WC3z2)	17,977			59,465	22,473,972	378
	T2WC1z3	T2, WCMO10% zone3 (WC1z3)	1,308			7,705	180,822	23
	T2WC2z3	T2, WCMO50% zone3 (WC2z3)	5,893			20,919	6,313,090	302
	T2WC3z3	T2, WCMO100% zone3 (WC3z3)	11,514			32,989	13,830,959	419
Water Conservation & NCS Management	T2WC1z1NC1	T2, WCMO10% zone1, NCMO10% all zone	3,134	29,291		34,914	3,932,187	113
	T2WC1z1NC2	T2, WCMO10% zone1, NCMO50% all zone	3,134	128,537		57,471	8,367,981	146
	T2WC1z1NC3	T2, WCMO10% zone1, NCMO100% all zone	3,134	252,346		66,969	13,901,651	208
	T2WC2z1NC1	T2, WCMO50% zone1, NCMO10% all zone	15,608	29,291		73,753	20,615,454	280
	T2WC2z1NC2	T2, WCMO50% zone1, NCMO50% all zone	15,608	128,537		88,087	25,051,247	284
	T2WC2z1NC3	T2, WCMO50% zone1, NCMO100% all zone	15,608	252,346		94,135	30,584,918	325
	T2WC3z1NC1	T2, WCMO100% zone1, NCMO10% all zone	31,086	29,291		108,373	41,314,918	381
	T2WC3z1NC2	T2, WCMO100% zone1, NCMO50% all zone	31,086	128,537		115,478	45,750,711	396
	T2WC3z1NC3	T2, WCMO100% zone1, NCMO100% all zone	31,086	252,346		118,486	51,284,382	433
	T2WC1z1NC1z3	T2, WCMO10% zone1, NCMO10%zone3 (NC1z3)	3,134	17,536		34,113	3,406,784	100
	T2WC1z1NC2z3	T2, WCMO10% zone1, NCMO50%zone3 (NC2z3)	3,134	780,445		54,510	6,111,225	112
	T2WC1z1NC3z3	T2, WCMO10% zone1, NCMO100% zone3 (NC3z3)	3,134	152,503		62,965	9,439,170	150
	T2WC2z1NC1z3	T2, WCMO50% zone1, NCMO10% zone3	15,608	17,536		73,270	20,090,050	274
	T2WC2z1NC2z3	T2, WCMO50% zone1, NCMO50% zone3	15,608	78,045		86,360	22,794,491	264
	T2WC2z1NC3z3	T2, WCMO50% zone1, NCMO100% zone3	15,608	152,503		91,797	26,122,436	285
	T2WC3z1NC1z3	T2, WCMO100% zone1, NCMO10%zone3	31,086	17,536		108,156	40,789,515	377
	T2WC3z1NC2z3	T2, WCMO100% zone1, NCMO50% zone3	31,086	77,192		114,758	43,493,956	379
	T2WC3z1NC3z3	T2, WCMO100% zone1, NCMO100% zone3	31,086	152,503		117,509	46,821,900	398

Figure 7.1 illustrates tradeoffs among various MO implementation scenarios ranging from site-specific strategies to hydrologic strategies. The tradeoff curve evaluates the MO scenarios based on two objectives 1) maximize annual sediment loading reduction shown in the x-axis and 2) minimize annual cost shown in the y-axis. Thus, the dominant solutions tend to populate the southeast quadrant in the plot.

The tradeoff plot illustrates that the site-specific strategy that focus on MOs on agricultural field have limits in their capacity to reduce sediment at 15,610 Mg/yr (i.e., with TLMO scenario that omit conventional tillage practice, and 100% of AFMO and 100% of BFMO sites implemented at all zones of the watershed). Generally, focusing on BFMO or mixture of AFMO and BFMO is more effective than focusing on AFMO alone. In addition, AFMO or BFMO implemented in zone 3 is more efficient than implementing these MOs in all zones because sediment generated in zone 3 has more likelihood to be transported to the watershed outlet.

Addressing the NCS is generally more effective and far-reaching than field sediment because, as demonstrated in the sediment budget, NCS is the largest sediment source. However, NCMO and RAMO's capacity to remove sediment is limited at 70,002 Mg/yr when 100% of these MO sites are implemented.

Water conservation strategy generally reduces more sediment loading from streambanks and bluffs through peak flow attenuation than the site-specific strategy, but it is more costly than addressing the bluffs directly with NCMO. Specifically, when 100% of WCMO sites are implemented in all zones, sediment-loading reduction is 139,415 Mg/yr. In general, implementing WCMO higher in the watershed, in zones 1 or 2, is more effective in reducing sediment compared to allocating them in all zones or in zone 3, as demonstrated Table 7.3. Figure 7.2 shows the unit costs of WCMO implemented in different zones as a function of sediment reduction. This figure indicates that, in general, implementing WCMO is zone 1 incurs less unit cost especially when more than about 10% of WCMO sites are implemented.

The number of feasible solutions may be reduced with constraints on the allowable budget for management policy and minimum sediment loading reduction requirement. For example, if a maximum cost constraint is imposed at $20 Million/year and minimum SL reduction constraint is set at 60,000 Mg/year (Figure 7.1 illustrates this feasible area with red square); then, four scenarios remain as feasible solutions (Table 7.4 lists these solutions). Among these solutions, T2RA3NC3 (TLMO implementation according to the T2 scenario plus RAMO and NCMO implemented at 100% in all zones) has the lowest cost per metric ton of sediment reduced; thus this solution dominates the other four solutions. However, the management scenario with mixture of water conservation and NCS management, T2WC1z1NC3z3 (TLMO implementation according to the T2 scenario plus 10% WCMO sites in zone 1 and 100% NCMO sites in zone 3), is just as desirable with a slightly lower cost. These feasible solutions may be evaluated in terms of tradeoff between sediment reduction and cost: scenario T2RA3NC3 can reduce additional 7,037 Mg/yr sediment with an additional cost of $749,788/yr compared to T2WC1z1NC3z3.

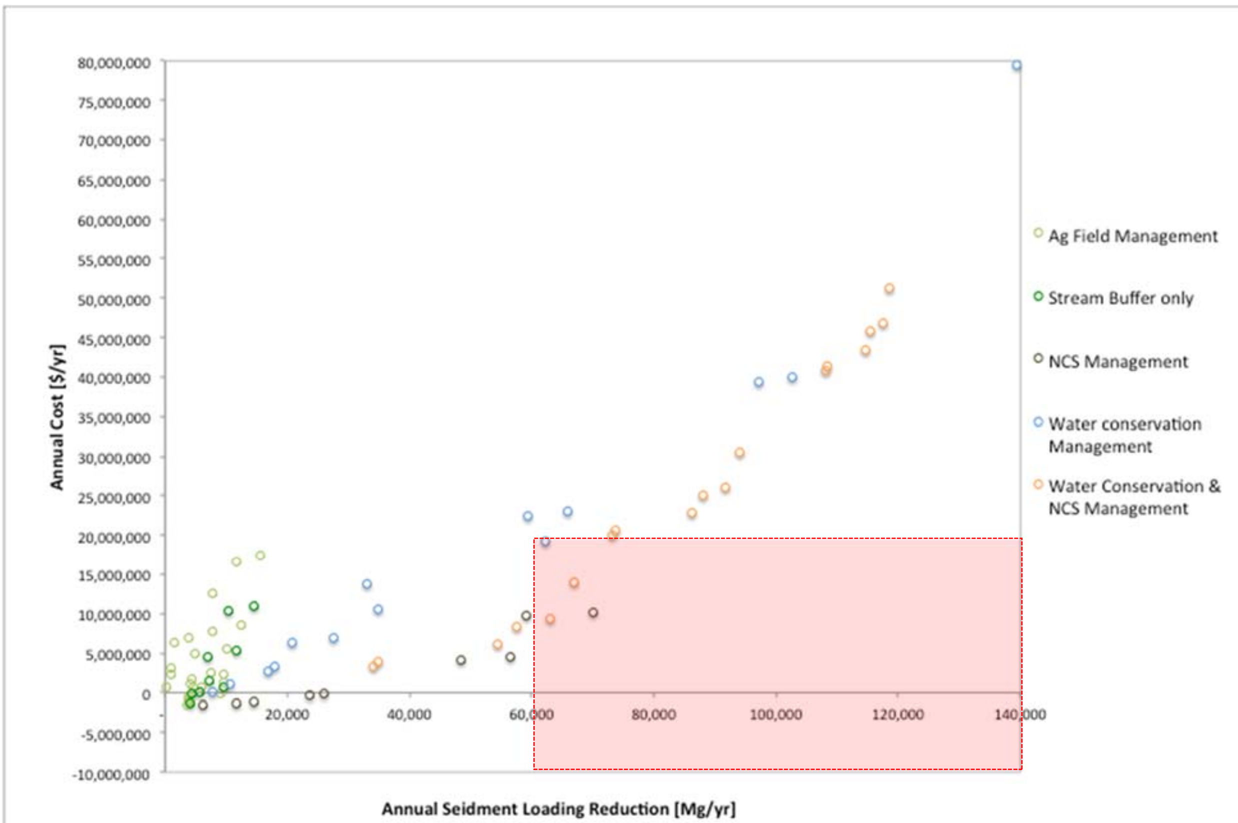

Figure 7.1: a tradeoff curve evaluating the objectives to 1) maximize annual sediment loading reduction in x-axis and 2) minimize annual cost of land acquisition, implementation, and maintenance on y-axis. The plot imposes a cost constraint at $20 Million/year and sediment loading reduction constraint at 60,000 Mg/yr where feasible solutions are populated in the red box.

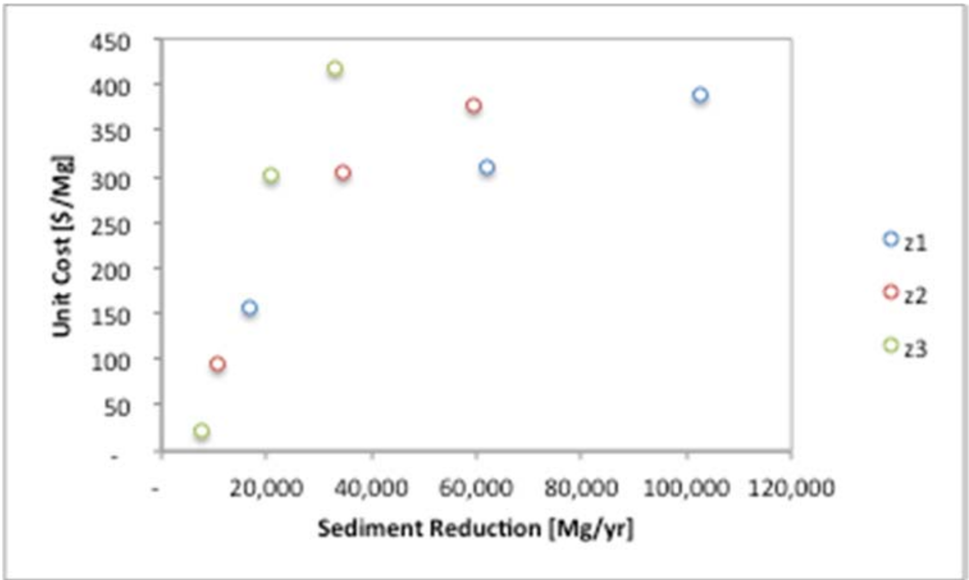

Figure 7.2: Comparison of WCMO effectiveness in zones 1, 2, and 3. Points indicate 10%, 50%, and 100% implementation with correspondingly increasing sediment reduction.

Table 7.4: list of feasible solutions with cost constraint at $20 Million/year and sediment reduction constraint at 60,000 Mg/year

Scenario	SL reduction [Mg/yr]	Annual Cost [$/yr]	Unit Cost [$/Mg]
T2WC1z1NC3z3	62,965	9,439,170	150
T2RA3NC3	70,002	10,188,958	146
T2WC1z1NC3	66,969	13,901,651	208
T2WC2z1	62,163	19,306,271	311

8 References Cited

Ambrosini, K. (2014). Analysis of Flap Gate Design and Implementations for Water Delivery Systems in California and Nevada. Accessed at http://digitalcommons.calpoly.edu/cgi/viewcontent.cgi?article=1125&context=braesp

Argonne National Laboratory. Wetlands Restoration/Constructed Wetlands: Technology Fact Sheet. Accessed at http://www.eeob.iastate.edu/classes/EEOB-590A/marshcourse/IV.4/IV.4h_Restoration_Constructed_Wetlands.pdf

Arora, K., Mickelson, S. K., Baker, J. L., Tierney, D. P., & Peters, C. J. (1996). Herbicide retention by vegetative buffer strips from runoff under natural rainfall. Transactions of the ASAE, 39(6), 2155-2162.

Arora, Kapil, Steven K. Mickelson, and James L. Baker. "Effectiveness of vegetated buffer strips in reducing pesticide transport in simulated runoff." Transactions of the ASAE 46.3 (2003): 635.

Beach, T., 1994. The fate of eroded soil: sediment sinks and sediment budgets of agrarian landscapes in southern Minnesota, 1851–1988. Annals of the Association of American Geographers 84, 5–28.

Belmont, P., 2011. Floodplain width adjustments in response to rapid base level fall and knickpoint migration. Geomorphology 128, 92–102.

Belmont, P., Gran, K.B., Schottler, S.P., Wilcock, P.R., Day, S.S., Jennings, C., Lauer, J.W., Viparelli, E., Willenbring, J.K., Engstrom, D.R., Parker, G., 2011. Large shift in source of fine sediment in the Upper Mississippi River. Environmental Science and Technology. 45, 8804–8810.

Belmont, P., Gran, K., Jennings, C.E., Wittkop, C., Day, S.S., 2011. Holocene landscape evolution and erosional processes in the Le Sueur River, central Minnesota. Field Guides 24, 439–455.

Belmont, P., Willenbring, J.K., Schottler, S.P., Marquard, J., Kumarasamy, K., Hemmis, J.M., 2014, Toward generalizable sediment fingerprinting with tracers that are conservative and nonconservative over sediment routing timescales. Journal of Soils and Sediments, v. 14 (8): 1479-1492.

Bevis, M., 2015, Sediment budgets indicate Pleistocene base level fall drives erosion in Minnesota's Greater Blue Earth River basin. M.S. Thesis submitted to the University of Minnesota, Duluth, MN. 96 p., http://hdl.handle.net/11299/170661.

Brown, C.B. 1943: Discussion of Sedimentation in reservoirs, by J. Witzig. Proceedings of the American Society of Civil Engineers 69,1493–1500.

Butcher, D.P., Claydon, J., Labadz, J.C., Pattinson, V.A., Potter, A.W.R. and White, P.1992, Reservoir sedimentation and colour problems in southern Pennine reservoirs. Journal of the Institute of Water and Environmental Management 6, 418–31.

Cho, S.J., in prep 2016, Development of an integrated environmental management simulation model to address non-point source sediment pollution from intensive agricultural watershed in Southern Minnesota. Ph.D. Thesis to be submitted to Johns Hopkins University.

Clayton, L., Moran, S.R., 1982. Chronology of late Wisconsinan glaciation in middle North America. Quaternary Science Reviews 1, 55–82.

Day, S.S., Gran, K.B., Belmont, P., Wawrzyniec, T., 2013. Measuring bluff erosion part 2: pairing aerial photographs and terrestrial laser scanning to create a watershed scale sediment budget. Earth Surface Processes and Landforms.

De Vente, J., Poesen, J., Arabkhedri, M., Verstraeten, G., 2007. The sediment delivery problem revisited. Progress in Physical Geography 31, 155–178.

Emmons & Olivier Resources, Inc. Minnesota River Valley Ravine Stabilization Charrette. February 2011. Accessed at https://www.scottcountymn.gov/Archive.aspx?ADID=326

Engstrom, D.R., Almendinger, J.E., Wolin, J.A., 2009. Historical changes in sediment and phosphorus loading to the upper Mississippi River: mass-balance reconstructions from the sediments of Lake Pepin. J Paleolimnol 41, 563–588.

Erskine, W., A. Keene, R. Bush, M. Cheetham, and A. Chalmers, 2012, Influence of riparian vegetation on channel widening and subsequent contraction on a sand-bed stream since European settlement: Widden Brook, Australia. Geomorphology, v. 147-148, pp. 102-114.

Fenton, M. M., Moran, S. R., Teller, J. T., & Clayton, L.,1983. Quaternary stratigraphy and history in the southern part of the Lake Agassiz basin. In *Glacial Lake Agassiz* (Vol. 26, pp. 49-74). St. John's Nfld.: Geological Association of Canada.

Ford, E, 2014, The effect of storm intensity and stream flow on sediment mobilization. Undergraduate Thesis submitted to Gustavus Adolphus College, 32 p

Foufoula - Georgiou, E., Takbiri, Z., Czuba, J. A., & Schwenk, J., 2015. The change of nature and the nature of change in agricultural landscapes: Hydrologic regime shifts modulate ecological transitions. Water Resources Research, 51(8), 6649-6671.

Fiener, P., and K. Auerswald. "Effectiveness of grassed waterways in reducing runoff and sediment delivery from agricultural watersheds." Journal of Environmental Quality 32.3 (2003): 927-936.

Fry, J., Xian, G., Jin, S., Dewitz, J., Homer, C., Yang, L., Barnes, C., Herold, N., and Wickham, J., 2011. Completion of the 2006 National Land Cover Database for the Conterminous United States, PE&RS, Vol. 77(9):858-864.

Galatowitsch, Susan M., and Arnold G. Van der Valk. Restoring prairie wetlands: an ecological approach. Iowa State University Press, 1994.

Gran, K.B., Belmont, P., Day, S.S., Jennings, C., Johnson, A., Perg, L., Wilcock, P.R., 2009. Geomorphic evolution of the Le Sueur River, Minnesota, USA, and implications for current sediment loading. Management and restoration of fluvial systems with broad historical changes and human impacts: Geological Society of America Special Paper 451, 119–130.

Gran, K., Belmont, P., Day, S., Jennings, C., Lauer, J.W., Viparelli, E., Wilcock, P., Parker, G., Azmera, L., Etcherling, C., 2011. An Integrated Sediment Budget for the Le Sueur River Basin.

Gran, K.B., Finnegan, N., Johnson, A.L., Belmont, P., Wittkop, C., Rittenour, T., 2013. Landscape evolution, valley excavation, and terrace development following abrupt postglacial base-level fall. Geological Society of America Bulletin B30772–1.

Gurnell, A., 2013, Plants as river systems engineers. Earth Surface Processes and Landforms, v. 39, pp. 4-25.

HEI (Houston Engineering Inc.), 2016, (PTMAPP): Theory and development documentation. http://ptmapp.rrbdin.org/files/04052016_PTMA_Theory_Report.pdf

Hupp, C.R. and A. Simon, 1991, Bank accretion and the development of vegetated depositional surfaces along modified alluvial channels. Geomorphology, v. 4, pp. 111-124.

Inter-fluve, Inc. SAND CREEK NEAR CHANNEL SEDIMENT REDUCTION: Feasibility Report October 2015. Accessed September 2016. https://www.scottcountymn.gov/DocumentCenter/Home/View/1802

Jennings, C.E., 2010. Draft Digital Reconnaissance Surficial Geology and Geomorphology of the Le Sueur River Watershed (Blue Earth, Waseca, Faribault, and Freeborn Counties in South-Central MN): Minnesota Geological Survey Open File Report 10–03. http://purl.umn.edu/98053

Jennings, C.E., Lusardi, B.A., and Gowan, A.S., 2012, Surficial Geology, Plate 3 *in* Runkel, A.C., Meyer, G.N., and Lusardi, B.A., Geologic Atlas of Blue Earth County, Minnesota [Part A]: Minnesota Geologic Survey County Atlas Series, Atlas C-26, 6 plates, Retrieved from the University of Minnesota Digital Conservancy, http://purl.umn.edu/116097.

Lauer, J.W., Parker, G., 2008. Net local removal of floodplain sediment by river meander migration. Geomorphology 96, 123–149.

Lenhart, C. F., 2008. The influence of watershed hydrology and stream geomorphology on turbidity, sediment and nutrients in tributaries of the Blue Earth River, Minnesota, USA. PhD Thesis. St. Paul, Minnesota: University of Minnesota–Twin Cities.

Lenhart, C.F., Brooks, K.N., Hetteley, D., Magner, J.A., 2009. Spatial and temporal variation in suspended sediment, organic matter, and turbidity in a Minnesota prairie river: implications for TMDLs. Environmental Monitoring and Assessment, doi: 10.1007/s10661-009-0957-y.

Lenhart, C.F., Peterson, H., and Nieber, J., 2011a, Increased streamflow in agricultural watersheds of the Midwest: Implications for management: Watershed Science Bulletin, Spring 2011, p. 25–31.

Lenhart, C.F., Titov, M.L., Ulrich, J.S., Nieber, J.L., and Suppes, B.J., 2013. The role of hydrologic alteration and riparian vegetation dynamics in channel evolution along the lower Minnesota River. Transactions of the ASABE, v.56, n.2, pp. 549-561.

Lenhart, C.F., Verry, E.S., Brooks, K.N., Magner, J.A., 2011b. Adjustment of prairie pothole streams to land-use, drainage and climate changes and consequences for turbidity impairment. River Research and Applications 28, 1609–1619.

Lewandowski, A., Everett, L., Lenhart, C., Terry, K., Origer, M., & Moore, R. (2015). Fields to Streams: Managing Water in Rural Landscapes. Part Two, Managing Sediment and Water.

Matsch, C.L., 1983. River Warren, the southern outlet to glacial Lake Agassiz. Glacial Lake Agassiz 26, 231–244.

McKay, L., Bondelid, T., Dewald, T., et al, 2013, National Hydrography Dataset Plus Version Two. http://www.horizon-systems.com/nhdplus/NHDPlusV2_home.php

Meyer, G.N., and Lively., 2012, Sand Distribution Model, Plate 4, *in* Runkel, A.C., Meyer, G.N., and Lusardi, B.A., Geologic Atlas of Blue Earth County, Minnesota [Part A]: Minnesota Geologic Survey County Atlas Series, Atlas C-26, 6 plates, 1:100,000 scale.

Midwest Plan Service. Conservation Tillage Systems and Management: Crop Residue Management with No-till, Ridge-till, Mulch-till, and Strip-till. Midwest Plan Service, Iowa State University, 2000.

Miller, T.P., J.R. Peterson, C.F. Lenhart, and Y.Nomura. 2012. The Agricultural BMP Handbook for Minnesota. Minnesota Department of Agriculture.

Minnesota Pollution Control Agency, Minnesota Department of Agriculture, Minnesota State University, Mankato Water Resources Center, and Metropolitan Council Environmental Services, 2009, State of the Minnesota River: Summary of surface water quality monitoring 2000-2008. 42 p.

Minnesota State University at Mankato, Water Resources Center (MNSU), 2012, Turbidity total maximum daily load study, Greater Blue Earth River Basin. MPCA report wq-iw7-29b, 241 p.

Mitchell, N., 2015. Achieving peak flow and sediment loading reduction through increased water storage in the Le Sueur Watershed, Minnesota: a modeling approach (Master of Science Thesis). University of Minnesota, Duluth.

Moncrief, John F., Samuel D. Evans, and Gyles W. Randall. "Description of the Minnesota River Basin and General Recommendations of Residue Management Systems for Sediment Control." (1997).

Novotny, E.V., Stefan, H.G., 2007. Stream flow in Minnesota: Indicator of climate change. Journal of Hydrology 334, 319–333.

Penn State University. "Economics of Conservation Tillage" Accessed May 2016. http://extension.psu.edu/plants/crops/soil-management/conservation-tillage/economics-of-conservation-tillage

Schottler, S. P., 2012. Intensified tile drainage evaluation. LCCMR Final Report B1-038 2009 http://www.lccmr.leg.mn/projects/2009/finals/2009_05d.pdf, accessed June 1, 2013.

Schottler, S.P., Engstrom, D.R., Blumentritt, D., 2010. Fingerprinting sources of sediment in large agricultural river systems. Report for MPCA.

Schottler, S.P., Ulrich, J., Belmont, P., Moore, R., Lauer, J., Engstrom, D.R., Almendinger, J.E., 2013. Twentieth century agricultural drainage creates more erosive rivers. Hydrological Processes 1–11.

Sekely, A.C., Mulla, D.J., and Bauer, D.W., 2002, Streambank slumping and its contribution to the phosphorus and suspended sediment loads of the Blue Earth River, Minnesota: Journal of Soil and Water Conservation, v. 57, p. 243–250.

Smolen, M. D., et al. "Annual Report: Status of Agricultural Nonpoint Source Projects." Biological and Agricultural Engineering Department, NC Agricultural Extension Service NC State University, Raleigh, NC (1989).

Steenberg, J., 2012, Bedrock Geology, Plate 2, *in* Runkel, A.C., Meyer, G.N., and Lusardi, B.A., Geologic Atlas of Blue Earth County, Minnesota [Part A]: Minnesota Geologic Survey County Atlas Series, Atlas C-26, 6 plates, 1:100,000 scale.

Teller, J. T., & Clayton, L. (1983). *Glacial Lake Agassiz* (Vol. 26). St. John's Nfld.: Geological Association of Canada.

Thoma, D.P., Gupta, S.C., Bauer, M.E., Kirchoff, C.E., 2005. Airborne laser scanning for riverbank erosion assessment. Remote Sensing of Environment 95, 493–501.

Tomer, M.D., Porter, S.A., James, D.E., Boomer, K.M.B., Kostel, J.A., McLellan, E., 2013. Combining precision conservation technologies into a flexible framework to facilitate agricultural watershed planning. Journal of Soil and Water Conservation, v. 68, n.5, p. 113A-120A. doi: 10.2489/jswc.68.5.113A.

Trimble, S.W., 1999. Decreased Rates of Alluvial Sediment Storage in the Coon Creek Basin, Wisconsin, 1975-93. Science 285, 1244–1246.

Turowski, J.M., 2012. Semi-alluvial Cannels and Sediment-Flux-Driven Bedrock Erosion In Church, M., Biron, P., and Roy, A. (*Eds*.), Gravel Bed Rivers: Processes, Tools, Environments. 580 pp. Hoboken, N.J.: Wiley-Blackwell.

Upham, W., 1895, The Glacial Lake Agassiz: U.S. Geological Survey Monograph 25, 658 p.

Uri, Noel D. "An evaluation of the economic benefits and costs of conservation tillage." Environmental Geology 39.3-4 (2000): 238-248.

USDA/NRCS. "Iowa Job Sheet: Contour Buffer Strips. Iowa Conservation Practice 332." (2011). Accessed September 2016. http://www.nrcs.usda.gov/Internet/FSE_DOCUMENTS/nrcs142p2_006620.pdf

US EPA. "Guidance Specifying Management Measures for Sources of Nonpoint Pollution in Coastal Waters." Document 840-B-92-002, January 1993. Accessed May 2016. https://www.epa.gov/sites/production/files/2015-09/documents/czara_chapter2_agriculture.pdf

Verstaeten, G., and Poesen, J., 2000, Estimating trap efficiency of small reservoirs and ponds: methods and implications for the assessment of sediment yield: Progress in Physical Geography, v. 24, p. 219–251.

Walling, D.E., 1983. The sediment delivery problem. Journal of Hydrology 65, 209–237.

Willenbring, J.K., and vonBlackenburg, F., 2010, Meteoric cosmogenic Beryllium-10 adsorbed to river sediment and soil: applications for Earth-surface dynamics. Earth Science Reviews, v. 98: 105-122.

Zhou, X., et al. "Cost-effectiveness and cost-benefit analysis of conservation management practices for sediment reduction in an Iowa agricultural watershed." Journal of soil and water conservation 64.5 (2009): 314-323.

9 Appendix 1. Ravine Monitoring 2013-2014

During the 2013 and 2014 monitoring seasons, four Sigma Hach auto-samplers were installed in three ravines that were previously monitored from 2008-2010 (Gran et al., 2011). Figure A.1 shows the locations of all ravines sampled over the course of the previous project. During 2013 and 2014, samplers were installed in RavU90, RavL90, Rav8, and Rav22S. Samples were collected during storm events and analyzed for total suspended solids (TSS) concentrations. Table A.1 shows general parameters for each ravine along with monitoring seasons and number of samples analyzed each year during 2013 and 2014.

Figure A.1: Locations of auto-samplers installed between 2008 and 2010. For this project, samplers were re-installed in Rav8, RavU90, and RavL90. (Image from Gran et al., 2011).

Table A.1: Ravine & Monitoring season information

	Rav U90	RavL90	Rav8	Rav22S
Drainage Area (ha)	274	400	436	235
Incised Ravine Area (ha)	4.7	31.2	47.1	3.6
Upland Area (ha)	270	369	389	231
Relief (m)	12	42	47	14
Dates sampler was deployed*	4/3/13-9/21/13	4/11/13-10/16/13	4/8/13-9/19/13	Dry all season
	4/23/14-7/23/14	4/27/14-7/23/14	5/7/14-7/25/14	4/27/14-6/29/14
# TSS samples analyzed in 2013	39	51	102	N/A
# TSS samples analyzed in 2014	73	125	52	68

*All samplers were off for periods of time within the monitoring season due to storm damage and equipment malfunction.

The ravine samplers were installed and run in 2013 and 2014 through a contract with Gustavus Adolphus College. Samplers were installed in April or May each year. During 2013, almost 200 water samples were collected and analyzed for TSS. In 2014, over 300 water samples were collected and analyzed for TSS. In both years, large storms ripped out some or all of the installed sampling equipment at every site, leading to periods of time in which no data were collected. Unfortunately, these equipment failures made calculation of monitoring season loads difficult. Instead, loads for individual storms were calculated from measured flow and TSS data where possible.

Flow data and TSS concentrations are shown for 2013 in Figure A.2. During 2013, an auto-sampler was installed in Rav22S, but there was no flow during the entire time the sampler was deployed. There were a series of two flood peaks on June 21nd and June 23rd in which most of the sediment was moved for the year from these ravines. Unfortunately, none of the 3 samplers were able to capture both peaks of the storm fully.

In 2014, there were several major events captured at one or more of the samplers. A full report on the sampling is given in Ford (2014). The loads from 2014 were dominated by a major event with over 8" of rain that started on June 16th with most of the rain falling on the night of June 17th – 18th. All of the samplers stopped working during the flood event. The ravines ran high for several days on end. Grab samples revealed TSS concentrations remained high for several days; high flows were able to continue eroding ravines for several days after the initial precipitation event had ended. Concentrations during the June 16-20th, 2014 event are given in Table A.2.

Table A.2: June 2014 storm TSS concentrations

TSS concentrations (mg/L)	RavL90	Rav8
6-17-14	920	N/A
6-18-14	2057	2340
6-19-14	1400	1750
6-20-14	120	420

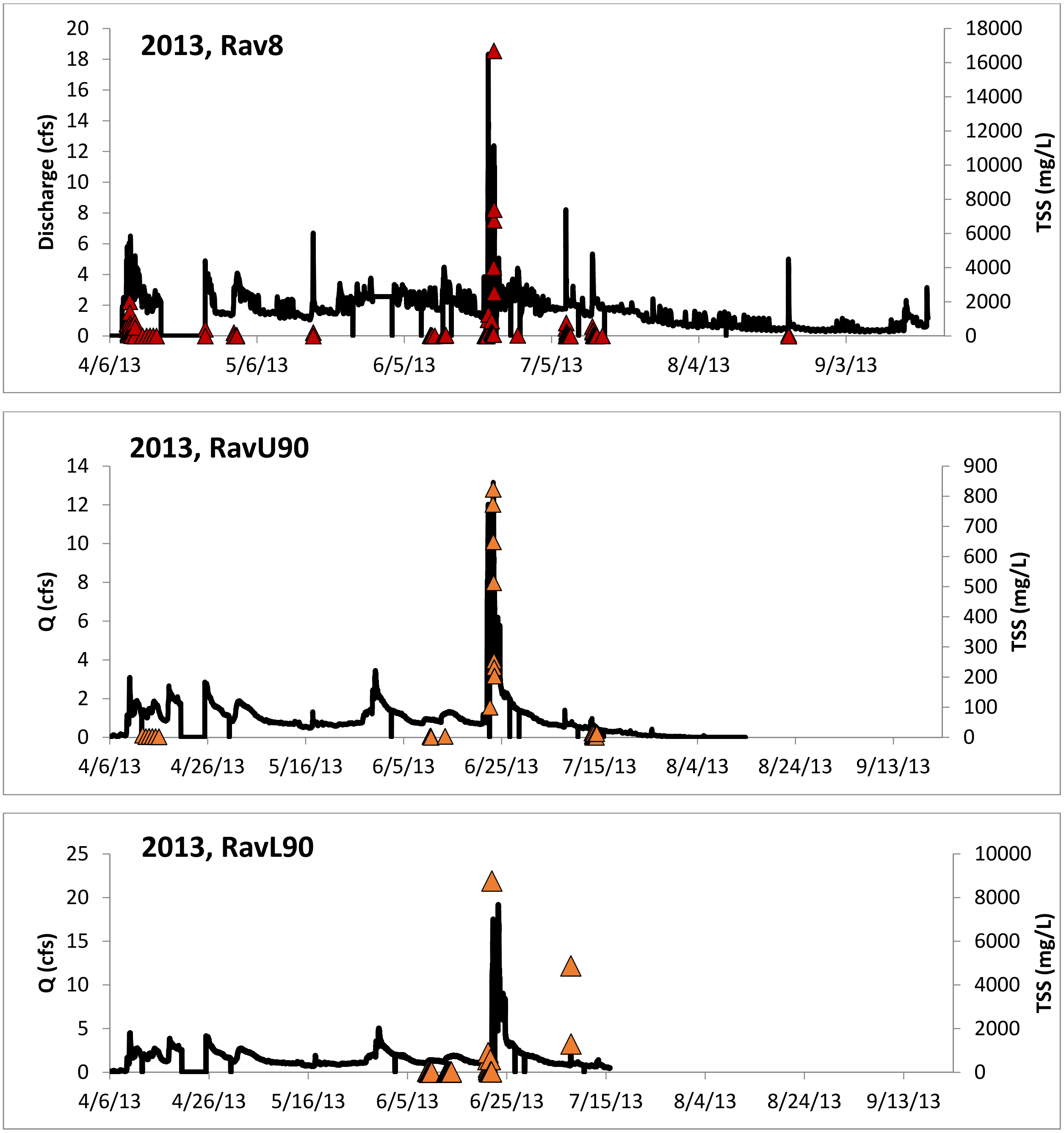

Figure A.2: 2013 data from the three ravines which had flowing water during the monitoring season: RavL90, RavU90, and Rav8. TSS concentrations are shown in red triangles, overlain onto the discharge record for the monitoring season.